Draft of Final Progress Report

Project Title: Supercritical Fluids Processing of Biomass to Chemicals and Fuels
Award Number: DE-FG36-06GO86014

Recipient: Iowa State University, University of Iowa
Project Location: Ames, IA; Nevada,

Reporting Period: May 31, 2006 – July 30, 2011
Date of Report: September 30, 2011
Written by: Norman K. Olson, Sipho C. Ndlela (Iowa Energy Center, Iowa State University), Gary Aurand (The University of Iowa, Iowa City)

Status:

Task A – Equipment Specification and Procurement

1. **Planned Activities**: This task involves procurement of a supercritical fluid reactor system and a supercritical fluid separation system.
    a. **Milestone A.ML.1 – Equipment Specification:** This milestone is complete.
    b. **Milestone A.ML.2 – Bids Published:** This milestone is complete.
    c. **Milestone A.ML.3 – Equipment Purchased and Installed:** This milestone is complete.

2. **Actual Accomplishments**:
    a. **Milestone A.ML.1 – Equipment Specification:** This milestone is complete.
    b. **Milestone A.ML.2 – Bids Published:** This milestone is complete.
    c. **Milestone A.ML.3 – Equipment Purchased and Installed:** This milestone is complete.

3. **Explanation of Variance**:
    a. **Milestone A.ML.1 – Equipment Specification:** See previous reports for explanations.
    b. **Milestone A.ML.2 – Bids Published:** See previous reports for explanations.
    c. **Milestone A.ML.3 – Equipment Purchased and Installed:** See previous reports for explanations.

4. **Plans for Next Quarter**:
    a. **Milestone A.ML.1 – Equipment Specification:** This milestone is complete.
    b. **Milestone A.ML.2 – Bids Published:** This milestone is complete.
    c. **Milestone A.ML.3 – Equipment Purchased and Installed:** This milestone is complete.

Task B - Supercritical Reaction Systems Research

1. **Planned Activities**:
    a. **Subtask B.1 – Liquid-Liquid Reactions:** Conduct experiments and analysis on cellulose reactions to sugars in supercritical and subcritical water. Continue experiments on catalyst-free esterification of fatty acids and triglyceride transesterification in supercritical alcohols.

b. **Subtask B.2 – Solid-Liquid Reactions:** Research and develop understanding of reaction routes in which cellulose and various biomass sources are converted into sugars and chemicals. Reaction conditions will be supercritical and/or subcritical temperatures of alcohols using a one-liter stainless steel high-pressure reactor and a continuous reactor. Products will be analyzed while simultaneously developing analytical methods using various equipment including NMR, GCMS, HPLC and LCMS.

2. Actual Accomplishments:

a. **Subtask B.1 – Liquid-Liquid Reactions:**

Recently completed effort under B.1 from previous reports

Report 15, July 30, 2010

Cellulose hydrolysis

As a result of research on cellulose hydrolysis in hydrothermal systems, a novel method was discovered for producing furfural from xylose and other 5-carbon sugars. The method uses inexpensive non-toxic substances (water, CO_2, and salt) to rapidly convert pentoses to furfural in high yields in a continuous process. An advantage of the method is that the furfural is easily separated into a form amenable to further processing into hydrocarbons in traditional packed bed catalytic reactors. The discovery may enable the manufacture of hydrocarbon gasoline from low-value biomass such as corncobs. A provisional patent application was filed by the University of Iowa Research Foundation: *Methods of Producing Furfural*; Aurand, G.A., Comer, C.M.; Filed May 14, 2010; U.S. Serial No. 61/334,654.

Fatty acid esterification

Linoleic acid was reacted with alcohols (methanol or ethanol) in equimolar amounts to produce alkyl esters (methyl linoleate or ethyl linoleate). No catalyst was added to the mixture. Experiments in the temperature range of 373K to 583K were performed in capillary batch reactors made with corrosion-resistant quartz tubes (2 mm i.d. × 6 mm o.d.).

Triglyceride - transesterification

Refined deodorized and bleached (RBD) soybean oil was tested under direct supercritical transesterification conditions using a one-liter batch reactor at varying molar ratios of 82 moles of methanol to oil. Temperature ranged from 300 to 350^{o}C, 27 to 107 MPa. In addition, the effect of adding a co-solvent and water towards completion of the transesterification reaction in forming methyl esters was evaluated. Post treatment techniques included an Amberlite BD 10 dry in removing free glycerine from crude biodiesel samples. Furthermore, esterification reactions on oleic acid were performed at 300 to 350^{o}C and at 8 methanol to oil molar ratio.

Report 16, October 30, 2010

Simultaneous supercritical (SC) trans/esterification reactions were further evaluated with waste restaurant grease (10% FFA) and crude corn oil (16% FFA) at 8 molar methanol to oil ratio and 300^{o}C. Results from this study were

compared to both oleic and soybean esterification studies in Report 15, July 30th, 2010. Having looked at direct SC trans/esterification of grease and corn oil, the next step was to look at hydrolyzing triglycerides in the oil followed by FFA esterification. To establish these hydrolysis experiments, RBD soybean oil was tested at 200 to 280°C and at oil to water ratios of 4:1 and 5:1.

Report 17, January 30, 2011

Under Task B1 in report 17, this section covered a process that was split into two parts. First was the oil hydrolysis step, followed by esterification reaction. Feedstocks studied were: soybean oil (0.01% FFA), waste restaurant grease (10% FFA) and crude corn oil (16% FFA) using a one liter high pressure reactor, at 300°C and mass ratios of 5:1 oil: water (O:W). Analysis of resulting samples from the hydrolysis step gave varying FFA values for each sample tested. For example, soybean increased to 80% FFA; whereas, restaurant grease changed to 73% FFA, and crude corn oil peaked at 84% FFA. Following the hydrolysis portion, the resulting high FFA products were then placed under direct SC-MeOH esterification to generate methyl esters at 300°C and 8 moles of methanol to oil.

Report 18, April 30, 2011

In this report, hydrolysis experiments using a batch reactor were extended to assess the effects of increasing the molar ratio of water above the previous values (i.e. 4:1 and 5:1). Values of 3.3:1 and 2:1 O:W ratio were used. For this case, temperature was maintained at 300°C for conditions at 2:1 and 3.3:1. Furthermore, a temperature effect on hydrolysis was evaluated from 325°C to 350°C, at constant 5:1 O:W ratio. Based on the analysis results, when increasing water vs. oil (O:W ratio) from 5:1 to 2:1, changes in the %FFA were from 12 to 25%. The trend was as follows: soybean oil from 80% (5:1, O:W) to 90% (2:1, O:W), restaurant grease from 73% (5:1, O:W) to 90% (2:1, O:W), and crude corn oil from 84% (5:1, O:W) to 90% (2:1, O:W). As noted, when using the batch reactor system and also due to thermodynamic factors, 100% recovery from trigylycerides to free fatty acids was not attained.

An attempt to study the temperature effect from 300 to 350° C at 5:1 O:W ratio was hampered by an increase in the product thermal degradation. This then complicated the sample analysis, which gave a wide range from 60 to 80% FFA. The issue of dark colored samples from the reactor was observed previously, which was due to thermal degradation of the oil during the reaction. An attempt to purge the reactor using helium prior to running the experiment did not resolve the problem due to extended heating periods. For instance, it took 8 hours to reach the target temperature, followed by over 12 hours of cooling the reactor to room temperature.

Cellulose hydrolysis

The main effort on this task involved developing computer code for cellulose depolymerization models. The model simulations being developed will be used to analyze experimental data to determine the mechanism(s) of cellulose hydrolysis in hydrothermal systems. This will be accomplished by comparing molecular weight distributions of cellulose samples before and after reaction to the changes in molecular weight distribution predicted by various depolymerization mechanisms. The models will be based on physically meaningful parameters, such as rate constants, which will be obtained by fitting

the simulations to the data. Ultimately the models will be used to predict optimum conditions for sugar production.

Prior to this work, cellulose was hydrolyzed under hydrothermal conditions to yield glucose and other fermentable sugars (e.g., fructose, cellobiose). The maximum glucose and total fermentable sugar yields were about 40% and 50%, respectively. In this process, glucose is an intermediate product that subsequently degrades into furanic compounds and low molecular weight organic acids, so simply increasing the reaction time leads to lower yields. The work herein described is aimed at understanding more completely the cellulose hydrolysis process and the associated side reactions.

Initial experiments were conducted using a tubular reactor. A simple schematic diagram of the apparatus is shown in Figure 1. Water or reactant solution was pumped by a Maximator® air driven high pressure liquid pump (PPSF111) through the tubular reactor inside an electric tube furnace (Themolyene, D79300). The reactor effluent was cooled by a heat exchanger, and sampled via the gas-liquid separator. The temperatures in the center of the tubular reactor and at the exit were measured by thermocouples, and the pressure of the system was measured by a pressure gauge between the pump and the reactor inlet. Figure 2 shows some representative results from the initial cellulose hydrolysis studies.

Since glucose may decompose under the cellulose hydrolysis conditions, experiments were conducted to study glucose decomposition in the tubular reactor. Initial experiments to determine the glucose disappearance as a function of reactor temperature resulted in a smooth curve except for a small "bump" in the residual glucose at about 290 °C. The bump initially was suspected to be a result of random experimental error. However, ten runs subsequently were conducted at each of twelve temperatures. The results showed very good reproducibility, and the bump remained. The curve in Figure 3 shows the mean values of remaining glucose at each reactor temperature with bars indicating the calculated standard error.

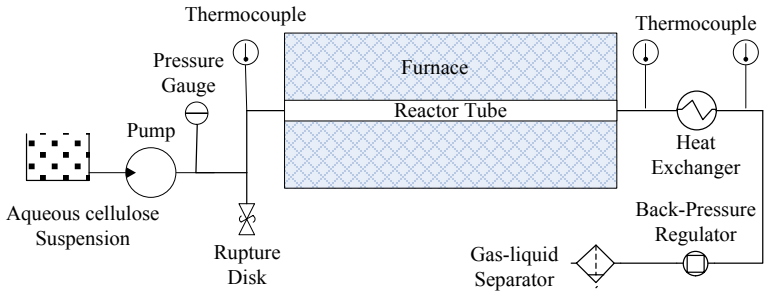

Figure 1. Schematic diagram of tubular reactor apparatus.

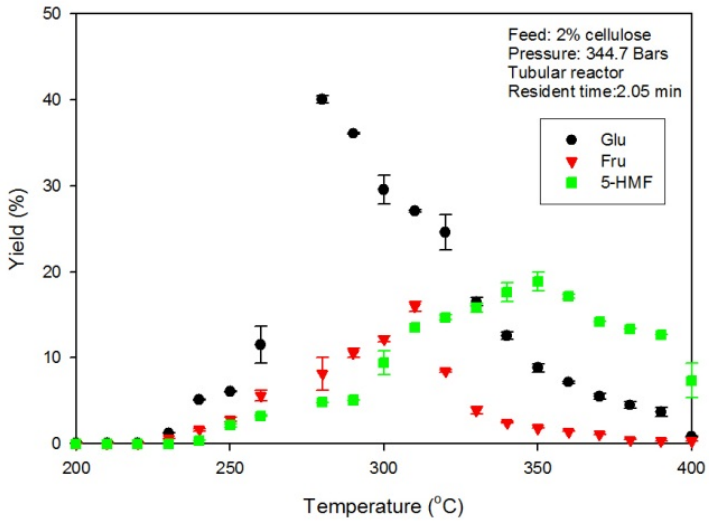

Figure 2. Cellulose reaction products at different reactor exit temperatures.

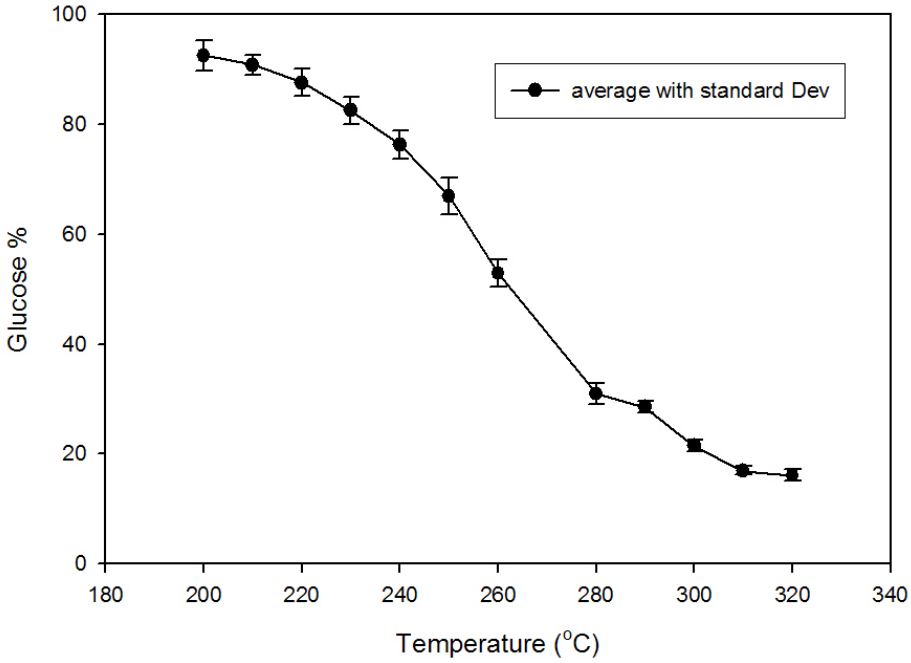

Figure 3. Glucose decomposition as a function of reactor temperature at constant pressure and flowrate.

A second apparatus, referred to as the microreactor, was employed to obtain kinetic parameters for glucose disappearance. Figure 4 is a schematic of the microreactor system. The microreactor vessel was a high-pressure, five-port manifold (High Pressure Equipment Company) with a reaction volume of 0.17 ml. The vessel was insulated with a wrapping of glass wool and aluminum foil. Supercritical water and a room-temperature aqueous solution containing the reactant were introduced into the reactor via separate ports as shown in the inset of Figure 4. To create the supercritical water stream, the water was pumped

through a length of tubing enclosed in a tube furnace. The temperature of the supercritical water and the flow rates of the two streams were adjusted to control the residence time and to yield the desired reaction temperature upon mixing. The center port was used for measuring the reaction temperature via a thermocouple probe. Room-temperature water was introduced through the downstream port at a flow rate sufficient to quench the reaction. The effluent from the reactor was cooled further upon passing through a double-pipe heat exchanger constructed in house. The product stream was depressurized via a back-pressure regulator downstream of the heat exchanger and collected for analysis. All reactions were conducted in subcritical water in the temperature range from 260 °C to 340 °C at a pressure of 27.6 MPa.

The results of the glucose decomposition experiments in the microreactor are displayed in the kinetics plots in Figures 5 and 6. Cellulose is presumed to break down into smaller cello-oligosaccharide intermediates during the conversion to glucose. Therefore, experiments were also performed to measure the decomposition kinetics of cellobiose, and cellotriose. For comparison to starch hydrolysis, malto-oligosaccharides were also studied. The measured kinetics parameters are listed in Table 1.

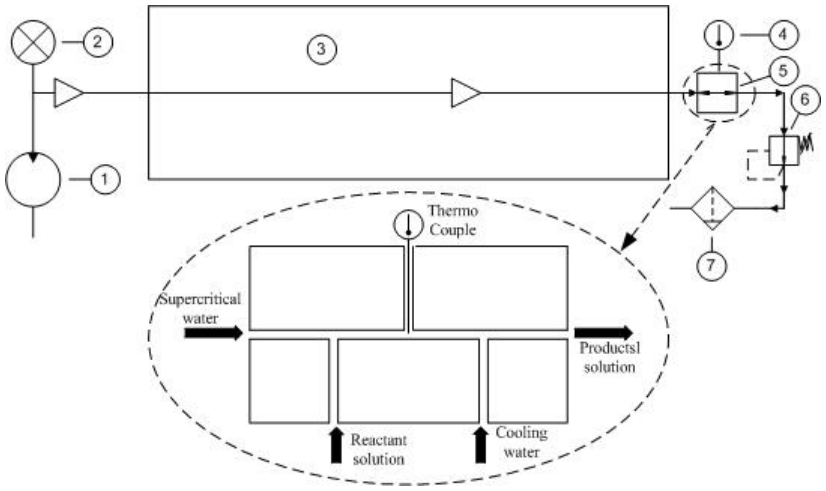

Figure 4. The schematic of the micro reactor: 1) pump, 2) pressure gauge, 3) electric tube furnace, 4) thermocouple, 5) microreactor, 6) backpressure regulator, 7) liquid-gas separator

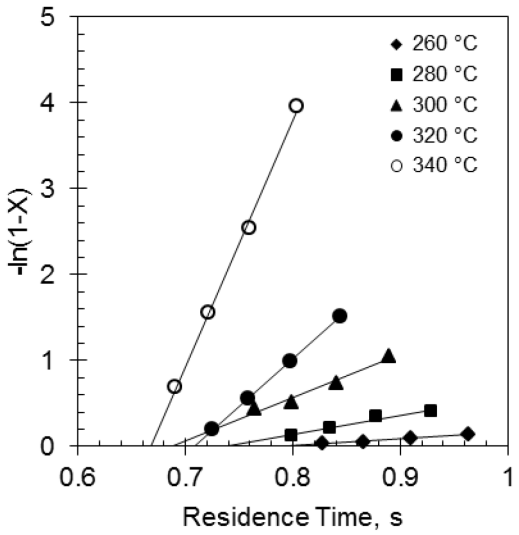

Figure 5. First-order rate plot for glucose disappearance in subcritical water.

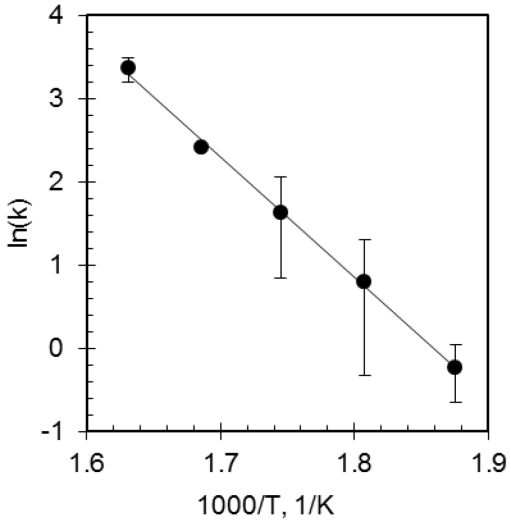

Figure 6. Arrhenius plot for glucose disappearance in subcritical water.

Table 1. Experimental kinetic parameters for the hydrothermal decomposition of monosaccharides, cello-oligosaccharides and malto-oligosaccharides. The reported error ranges are 95% confidence intervals.

Reactant	Activation Energy, kJ/mol	$Log_{10}A$, log s^{-1} (A=Arrhenius pre-exponential)
Glucose	120±10	11.6±0.9
Fructose	80±40	8±3
Cellobiose	80±5	8.4±0.5
Cellotriose	60±30	7±3
Maltose	90±20	10±2
Maltotriose	60±50	7±4
Maltotetraose	50±200	6±19

Mathematical models were developed for the reactors used in the hydrothermal conversion of cellulose to sugars. COMSOL Multiphysics finite element modeling software was used to model the temperature and flow patterns in the laboratory reactors. Accurate temperature- and pressure-dependent water properties were incorporated into the models via Matlab® code based on the IAWPS-97 water property formulations. The kinetic parameters obtained for glucose decomposition using the microreactor were incorporated into the reactor model for the large tubular reactor. The only fitted parameter in the model was a combined radiative/convective heat transfer coefficient between the furnace and reactor tube. This was previously adjusted to obtain a good fit between the calculated and experimental reactor exit temperatures based only on fluid transport properties, neglecting chemical reactions. This parameter was not adjusted when adding the independently obtained kinetic constants to incorporate the reactions. Figure 7 compares the results of the model simulation with the experimental data. There is excellent agreement between the simulation and the experimental results, which increases confidence in the model, the kinetic parameters obtained from the microreactor, and the original data from the tubular reactor. Even the bump in glucose yield described above is reflected in the simulation result, suggesting that it is not a statistical fluke, but is a real effect, likely due to a variation in fluid properties.

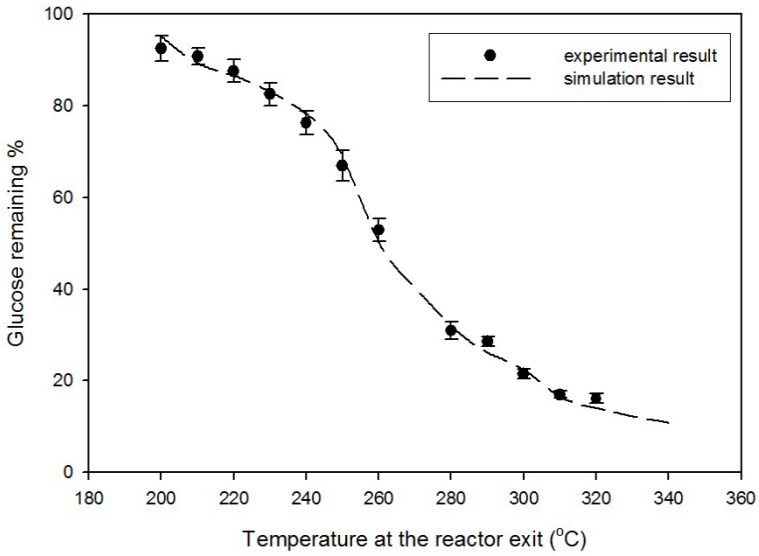

Figure 7. Simulation of glucose reaction at 10 g/min in the tubular reactor shows excellent agreement with experiment. Experimental error bars represent 95% confidence intervals.

Since the goal is to simulate glucose yields from cellulose, cellulose hydrolysis reactions need to be incorporated into the model. Methods for quantifying the degree of polymerization (DP) for partially hydrolyzed cellulose and starch were investigated. Determination of the DP is necessary for understanding the polysaccharide hydrolysis process in hydrothermal systems. An ASTM method for measuring the intrinsic viscosity of cellulose was adopted in evaluating the viscosity–average molecular weight (MW_v) and viscosity-based DP of cellulose obtained from Sigma-Aldrich. The testing involves the use of calibrated Cannon-Fenske viscometers of sizes 50 and 100 placed in a water bath operated at 25 °C. Cellulose, insoluble at room temperature in water, was dissolved in the ASTM recommended reagent, cupriethylenediamine hydroxide solution (CED). The reagent was prepared in our lab by reacting copper (II) hydroxide with ethylenediamine in a 1:2 molar ratio.

Viscosities were obtained for concentrations ranging from 0.1 to 1.7 g/dl. Based on these data, the intrinsic viscosity was determined, which in turn was used to calculate the viscosity-average molecular weight (MW_v) and the degree of polymerization (DP). Results indicated a MW_v of 37,000 and a DP of about 228. This average molecular weight is in conformity with the Sigma-Aldrich product specification which certifies the average molecular weight to be between 36,000 and 40,000.

Molecular weight measurements were then used to measure the rate of hydrothermal hydrolysis of cellulose in subcritical water. Cellulose particles (1 wt%) in water were reacted in the microreactor and molecular weight of the non-liquified residue was analyzed. A shrinking core kinetics model was used to describe the hydrolysis of cellulose on the particle surface. The experimental results are shown in the kinetics plots in Figures 8 and 9. The activation energy,

EA, and the frequency factor, *A*, evaluated based on the plot in Figure 9 are 100 ± 30 kJmol^{-1} and $10^{9\pm3}$ s^{-1}. The error values represent 95 % confidence intervals. Cellulose was also reacted in supercritical water in the microreactor. Under supercritical conditions, it is presumed that water penetrates the crystal structure of cellulose, making the glycosidic bonds more available for hydrolysis. In supercritical water, cellulose liquefaction proceeds very fast. For example, conversion of 36.8 % was obtained at 374 °C with a residence time of 0.142 s, and conversion of 89.5 % was obtained at 390 °C with a residence time of 0.154 s. In these experiments, remaining cellulose was analyzed gravimentrically, and first order kinetics were assumed. The kinetics results are displayed in Figures 10 and 11. The activation energy and pre-exponential factor obtained are 400 ± 100 kJmol^{-1} and $10^{30\pm11}$s^{-1} respectively. Reported errors are 95% confidence intervals.

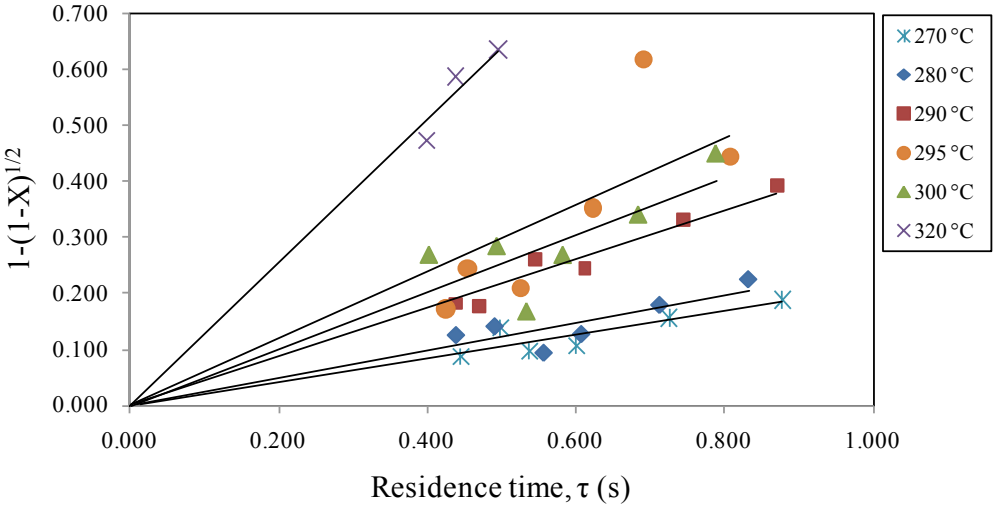

Figure 8. Rate plot for subcritical water cellulose hydrolysis based on a shrinking core kinetics model.

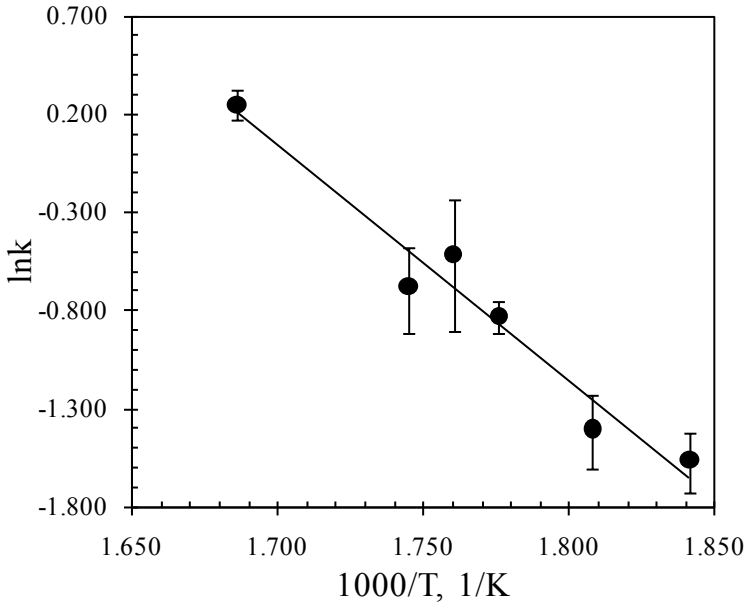

Figure 9. Arrhenius plot for the conversion of crystalline cellulose in subcritical water and at 5000 psi based on shrinking core model.

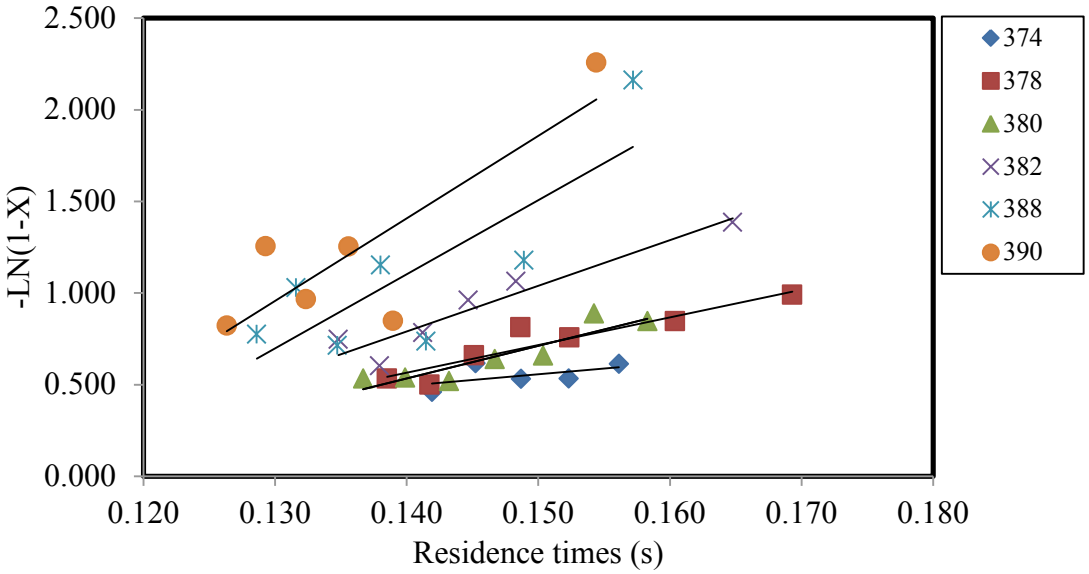

Figure 10. Rate plot for the liquefaction of cellulose in supercritical water.

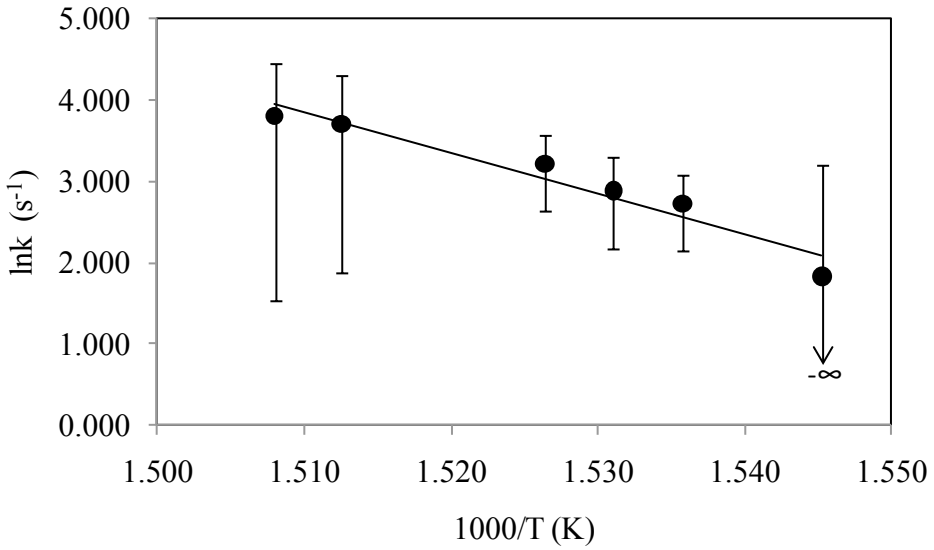

Figure 11. Arrhenius plot for the liquefaction of cellulose in supercritical water.

Oil esterification using a high pressure 1 liter batch reactor

SC-Methanol esterification of Corn and restaurant grease:

Simultaneous supercritical (SC) trans/esterification reactions were evaluated with waste restaurant grease (10% FFA) and crude corn oil (16% FFA) at 8 molar methanol to oil ratio and 300^{o}C. To establish these hydrolysis experiments, RBD soybean oil was tested at 200 to 350 ^{o}C and at oil to water ratios of 4:1 and 5:1. The next set of experiments include reaction of high free fatty acid (FFA) oils, for example corn oil (16 %FFA) and restaurant grease (10 %FFA). In Figure 12 below is an image of the crude samples prior to a reaction i.e. soybean oil, corn oil and restaurant grease from left to right. The crude soybean sample had 0.2 % FFA and thus 99.8 % triglyceride, whereas the corn oil and restaurant grease consisted of approximately 84% and 90% triglycerides respectively.

Figure 12. Image from left to right: RBD soy bean oil, crude corn oil, restaurant grease

In undertaking these experiments, two approaches were taken. First, the oils were subjected into direct SC-Methanol esterification at (8 Molar ratio, Moles of Methanol to Moles of Oil). Secondly, the oil samples were subjected under a hydrolysis reaction (Oil to Water weight ratio, O:W, 4:1 & 5:1), which was then followed by SC-Methanol esterification at (8 Molar ratio). Reactions discussed here were conducted at 300^{o}C using the high pressure batch reactor described in previous reports.

Direct SC-Methanol esterification:
As mentioned the first set of experiments were subjected under direct SC-Methanol esterification at 300^{o}C and 2500 psi. The reactor was heated over a period of 7 hours before attaining the target temperature after which it was maintained at 300^{o}C for 30 minutes before cooling it to room temperature. The sample was removed from the reactor and then placed in a separatory funnel overnight. Separation resulted into two phases as shown in the Figure 2 and 3 below, the top phase mostly methanol, but the bottom layer consisted mostly of crude biodiesel (methyl esters).

Analysis of samples from direct esterification reaction at 8 Molar ratio and 300^{o}C suggested that both FFA and triglyceride present initially in both corn oil and restaurant grease were converted into methyl esters. This was confirmed by titration and GC results as follows: Prior to the reaction, corn oil contained 16% FFA, but after reaction 0.66% FFA remained. GC analysis indicated that conversion rates of the starting triglycerides into methyl esters were above 90%.

Further analysis of the reaction products from the esterification of restaurant grease initially containing 10% FFA resulted to 1% FFA post reaction, whereas, % conversion of restaurant grease's triglyceride into methyl esters was about 85%. As observed in from the corn and restaurant grease reaction, simultaneous esterification/ transesterification of FFA and triglyceride under SC-Methanol is plausible although the % conversion rates were slightly lower in comparison to the previous oleic acid and soybean oil esterification results. At 300^{o}C both oleic acid and soybean oil conversion rates were above 94%. However, there were similarities with regards to the separation of samples post reaction into two distinct phases, without a glycerine layer. Typically three layer forms after separation for instance post a transesterification experiment under basic catalyst/ methanol reaction at 60^{o}C. The three separated layers would normally include the top methanol, middle crude biodiesel, and bottom glycerine layer. Nevertheless, at such high temperature under SC-Methanol conditions the glycerine phase is distributed between the two phases; presence of the glycerine in these phases was noticed when each of these phases was analyzed using a GC.

Oil hydrolysis followed by direct SC-Methanol esterification:
After assessing direct esterification/ transesterification under SC-methanol condition the next step was to evaluate another technique in improving conversion rates. This was achieved by a combination of both hydrolysis and esterification reaction. Refined soybean oil sample (0.2% FFA) was tested at 200 and 280^{o}C at O:W ratios 4:1 and 5:1 and later followed by methanol-esterification. After drying the samples analysis results suggested that about 80 % of the triglycerides were hydrolyzed to FFA (96%FFA). Following the hydrolysis experiments, the oil sample was esterified under SC-methanol conditions after which methyl esters were formed. Having shown success of the sequential hydrolysis followed by esterification, this technique was then extended to include a different RBD Soybean oil sample (0.01 %FFA), waste restaurant grease (10% FFA) and crude corn oil (16 %FFA). In each sample, the remainder was mostly triglycerides. An example of the hydrolysis experiments is indicated in Figure 13. Experiment parameters were run at ratio of Oil to Water of 5 to 1 (Oil: Water, 5:1) and 300^{o} C in a one liter high-pressure reactor. Resulting FFA varied, for instance soybean oil attained about 80% FFA, restaurant grease reached 73% FFA, and crude corn oil peaked at 84% FFA. Supplemental experiments that convert these oils to 100% FFA are being investigated by increasing oil: water ratio and also by varying the temperature to understand its role in impacting the extent of the hydrolysis reaction.

Furthermore, the resulting high FFA products were then placed under direct SC-MeOH esterification following separation of the water layer. Two problems were noticed in the past after hydrolysis of soybean oil: First, the sample turned darker due to thermal degradation, and secondly, an emulsion formed. In the current experimental setup, thermal degradation was minimized by first purging the sample under Helium for up to 2 hours, whereas emulsification was minimized by slowing down the stirrer rpm from 300 to 250 rpm and also by extending the settling period up to 10 hours.

Analysis of esterification samples are indicated in Figure 13. Based on these plots, it was speculated that the FFA values decreased as the esterification reaction progressed. Changes in FFA values were associated with formation of methyl esters, which was further supported by results from a GC analysis. Post reaction analysis results ranged from 4 to 2 % FFA.

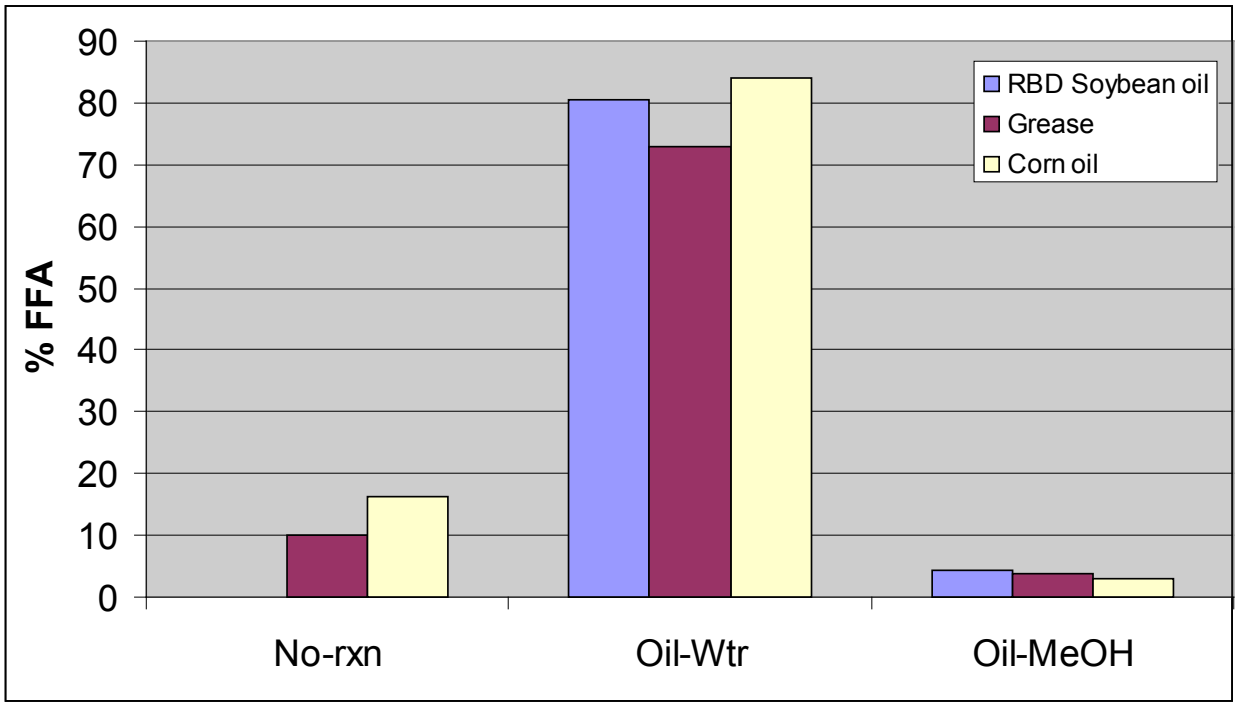

Figure 13. Oil Hydrolysis (Oil: Water; 5:1) 300ºC, followed by direct SC-MeOH esterification (8 Molar MeOH: Oil), 300ºC

In addition, a combination of this carryover coupled with water generated during the esterification reactions could be another contributing factor in slightly higher %FFA at the end of the reaction. To validate the effect of water under esterification, an approach was undertaken in which water was added during an esterification reaction. An example of this experiment was at Oil: Water, 1.8:1 and Oil: MeOH, 2.3:1. Results of this study are shown in Figure 14. Here the extent of the esterification reaction was hindered by a partial formation of free fatty acids to approximately 17% FFA. Despite presence of these free fatty acids, GC analysis did indicate that the remaining components were methyl esters. Following this

experiment consisting of methanol and water, direct SC-MeOH esterification of these oils resulted to lower %FFA as indicated in Figure 14. These were now much lower ranging to 0.5 to 0.8%FFA. Additional analysis of these samples showed that the amount of water from a sample taken after the hydrolysis (Oil: Water, 5:1) experiment in Figure 13 was much higher when compared to the Oil-MeOH-Water in Figure 14. Therefore, presence of water above 10% could have a negative impact during esterification. In cases where the feedstock consists of water exceeding 10%, the samples should be either flash evaporated or the esterification should be run in two consecutive steps.

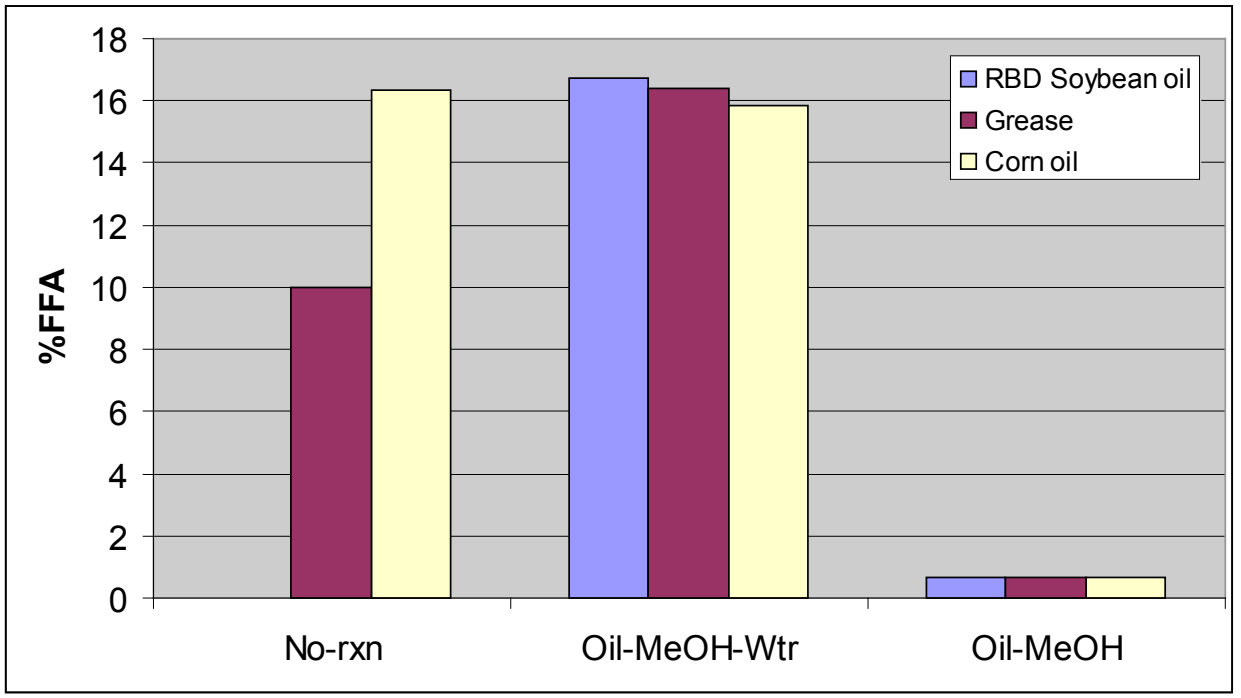

Figure 14. Water effect (Oil: Water, 1.8:1; Oil: MeOH, 2.3:1), during SC-MeOH esterification, followed by SC-MeOH esterification (8 Molar MeOH: Oil)

Using a batch reactor the effects of increasing the molar ratio of water above the previous values (i.e. 4:1 and 5:1). Values of 3.3:1 and 2:1 O:W ratio were used. For this case, temperature was maintained at 300^{o}C for conditions at 2:1 and 3.3:1. Furthermore, a temperature effect on hydrolysis was evaluated from 325^{o}C to 350^{o}C, at constant 5:1 O:W ratio. Based on the analysis results, when increasing water vs. oil (O:W ratio) from 5:1 to 2:1, changes in the %FFA were from 12 to 25%. The trend was as follows: soybean oil from 80% (5:1, O:W) to 90% (2:1, O:W), restaurant grease from 73% (5:1, O:W) to 90% (2:1, O:W), and crude corn oil from 84% (5:1, O:W) to 90% (2:1, O:W). When increasing the temperature from 300 to 350 ^{o}C, at 5:1, O:W the final %FFA ranged from 80 to 90%. As noted, when using the batch reactor system and also due to thermodynamic factors, 100% recovery from trigylycerides to free fatty acids was not attained in a single step.

Oil esterification using a high pressure flow reactor

Results from the high pressure batch reactor hydrolysis and esterification reactions from 200 to 350^{o}C suggested fatty and methyl esters were formed. At high temperatures, thermal degradation resulted such that it was difficult to analyze some samples accurately. To minimize such problems, a continuous flow reactor was then utilized for hydrolysis and esterification experiments. The advantage of such a system was better control of residence time anywhere from 5 to 30 minutes and also enhanced control features in controlling the system pressure and monitoring temperature ranges from 200 to 350^{o}C. Heating a batch reactor system from 25 to 350^{o}C took about 9 hours, whereas a flow reactor within a similar temperature range reaches the final temperature in 20 to 30 minutes. Raw materials are transferred into the reactor using two high pressure liquid pumps, through a preheater before entering the reactor. In addition, the final product flows continuously and is cooled using a shell and tube heat exchanger before collecting for analysis.

The first set of hydrolysis experiments subjected soybean oil to 200 and 300^{o}C, 10 minute residence times, O:W at 5:1, and 200 to 2300 psi. The system pressure was varied by setting the control valve to specific settings (200 to 2300 psi) during which reactor contents would not flow out until that pressure was achieved and then released. After releasing the product, another cycle followed by building system pressure and then resealed. The cycle continued until a new pressure setting was installed. Samples collected were then stored and analyzed. Images of samples collected are shown in Figure 15.

Two phases were formed at initially. For example, at 200 psi/200^{o}C and 200 psi/300^{o}C (i.e. the first set of images from L-R), the top oil layer and a bottom water layer resulted. An increase in pressure to 2300 psi showed a different trend. First an emulsion phase formed in both systems 200^{o}C and 300^{o}C at the bottom. Secondly, two phases formed at 200^{o}C, but the 300^{o}C system gave an emulsion at the top, oil in the middle, and water was at the bottom (second set of images from L-R).

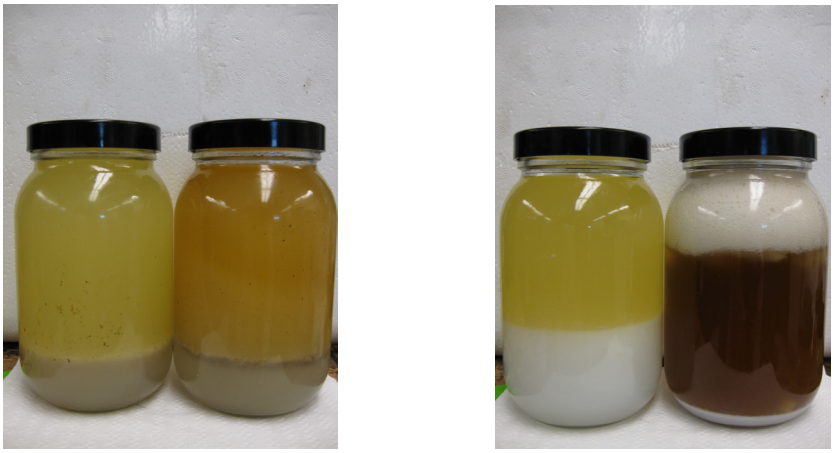

Figure 15. Pressure effect on the hydrolysis of triglycerides from soybean oil. Flow reactor at 10 minutes residence time. Images L to R, 200ºC/200psi, 300ºC/200psi, 200 ºC/2300psi, 300ºC/2300psi

These samples were then analyzed by measuring the product oil acid number in relation to the starting soybean oil. As depicted in Figure 16, %FFA remained very low for the condition at 200ºC, similar to batch reactor results, and at 10 minutes residence time. Based on these results, it can be speculated that pressure had no effect on hydrolyzing the oil at low temperatures and short residence times. On the other hand,experiments at 300ºC suggested no significant changes between 200 to 1500 psi, followed by a sharp increase in %FFA between 1500 to 2300 psi (i.e from 4 to 41% FFA). Additional testing with conditions up to 6000 psi, 300 to 350 ºC was completed and will become part of the final report. An overall summary of these tests using the continuous reactor system will be addressed in the upcoming final report.

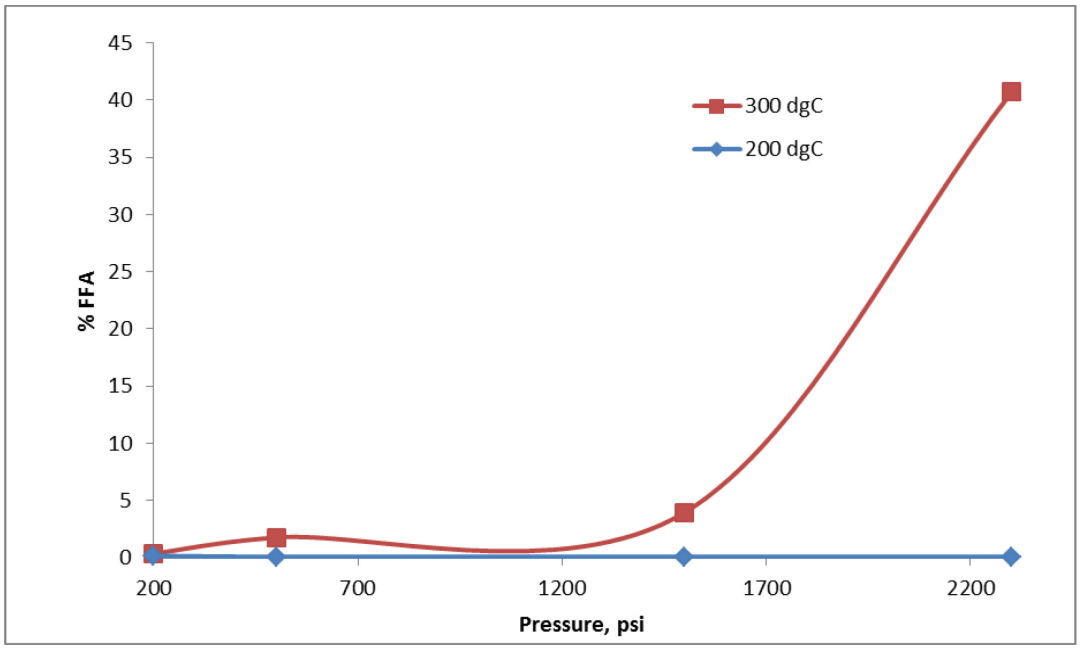

Figure 16. Pressure effect on the hydrolysis of triglycerides from soybean oil, flow reactor at 10 minutes residence time, 200 and 300°C

b. Subtask B.2 – Solid-Liquid Reactions: Continued experiments and analysis of cellulose and sugar reactions. Develop methods and analysis of samples using GCMS, LCMS and HPLC. Studied sugar hydrolysis reactions using a batch reactor and a flow reactor. Studied cellulose/methanol reactions under high pressure and temperature using a continuous flow reactor. Studied cellulose and corn stover hydrogenation experiments in methanol.

Recently completed tasks under B.2 from previous reports

Report 15, July 30, 2010
In this report the analysis techniques from Report 14 were extended to include LCMS and HPLC. During this period, work on task B.2 focused on developing methods for analyzing samples using the LCMS in the ISU chemistry department. The goals were to compare results obtained from GCMS analysis and figure out what other components are present from samples taken from reaction of cellulose and methanol at high temperatures. Several sugar standards were prepared including glucose, fructose, levoglucosan, galactose and maltose.

Report 16, October 30, 2010
Analysis of samples using LCMS and HPLC:
Progress on developing analytical techniques of products from cellulose – methanol reaction was hampered by various challenges. These included LCMS and HPLC column getting plugged and too much background noise on the spectra that overlaped with identified peaks. To minimize these issues, future samples would be passed through a guard column to trap contaminants. Also, numerous standards were prepared to accurately identify peaks. Although there

were challenges with the LCMS and HPLC, the GCMS and NMR continued to be very useful in identifying product samples.

Cellulose Methanol reaction using a continuous flow system:
In continuing to understand the reaction pathways for converting cellulose into sugars and chemicals, current experiments extended the previous batch reactor studies of cellulose and methanol reaction using a continuous reactor. Current reactor conditions were 250 and 300^{o}C and 500 to 5000 psi. The cellulose-methanol mixture was continuously passed through the system using a high pressure hydrocarbon pump through a pre-heater into a vertical tubular reactor. Residence times throughout this reactor system were maintained at 30 minutes.

Sugar hydrolysis using a high-pressure batch reactor:
A separate set of experiments studied hydrolysis of a pure sugar sample at 5 and 10 wt% solutions using a high-pressure batch reactor at 200^{o}C and 30 minutes residence time. Information obtained from the analysis of a product sample will be useful in identifying the composition and mechanism of simple sugars in relation to cellulose hydrolysis routes.

DOE Report 17, January 30, 2011
Hydrogenation studies:
This report went over preliminary hydrogenation studies on corn stover – methanol reactions at 300^{o}C to 3500 psi, in which hydrogen was added at 600 psig at room temperature prior to the reaction. Product samples were analyzed using a GCMS and results were compared to conditions at 300^{o}C for corn stover without H_2. Preliminary assessment of product samples suggested that H_2 addition impacted the extent of the reaction by yielding a different product composition when compared to the case in the absence of H_2.

Sugar/Cellulose hydrolysis using a batch and flow reactor:
This study covered sugar-water and cellulose-water reactions using a batch reactor at 200 to 300^{o}C. A follow up of this study was run using a flow reactor at 200^{o}C, from 500 psi to 5000 psi and then analyzed with a GCMS. An attempt to analyze these samples using an HPLC ran into numerous problems after which sample analysis was put on hold.

DOE Report 18, April 30, 2011
In this current report, the concentration for sugar (sucrose)-water vs. sugar-methanol reactions at 200^{o}C was increased from 1 to 5% and then studied using a high pressure batch reactor. The significance of this study was to assess a kinetic pathway with a less complex molecule when compared to cellulose which is more difficult to break down under mild conditions. Samples were then analyzed using a GCMS and an HPLC system. A summary of these analyses suggested that experiments for the sugar-methanol system resulted in a mixture of sugars, esters, furans and organic acids, whereas, products generated from the sugar-water reaction consisted mostly of furan derivatives. Also, an HPLC analysis of a 1% sugar-water system confirmed the presence of D-glucose, D-fructose and levoglucosan from hydrolyzing sucrose.

Thermal decomposition of cellulose under subcritical and supercritical conditions using methanol:

To optimize cellulose conversion into chemicals it is important to understand how it decomposes under reaction conditions such as temperature and pressure. The effect of varying temperature on cellulose decomposition was first tested by heating the samples to high temperatures under inert conditions using a thermogravimetric analyzer (TGA). In the second test, both temperature and pressure effects were monitored at sub/supercritical conditions of methanol and MeOH/CO_2 mixture, using a high pressure batch reactor. The critical pressure of methanol at 240°C is 1138 psi and that of CO_2 at 31°C is 1072 psi so reactions were conducted at temperatures ranging from 200 to 350°C. The first part of this section will assess the temperature and pressure on cellulose decomposition during the reaction and then compare to the TGA inert conditions.

Using a TGA instrument, cellulose was first heated under nitrogen at non-isothermal conditions from 50 to 900°C as shown in Figure 17, which consists of a thermogravimetric curve (TG) and its derivative curve (DTG). The TG/DTG curves trace cellulose weight changes that may be related to chemical or physical variations. From the derivative curve, two noticeable weight losses are apparent, the first at about 80°C and the second at 305°C. Since the first weight change took place at a lower temperature, it can be deduced that it is associated with the loss of physisorbed water on the surface of the cellulose. This weight loss amounted to about 4 wt%.

The second weight change may be associated with structural changes in the cellulose that resulted in a weight loss of about 20 wt%. Although the starting cellulose was white in color, a visual inspection of the sample at the end of the process at 900°C showed a black powder.

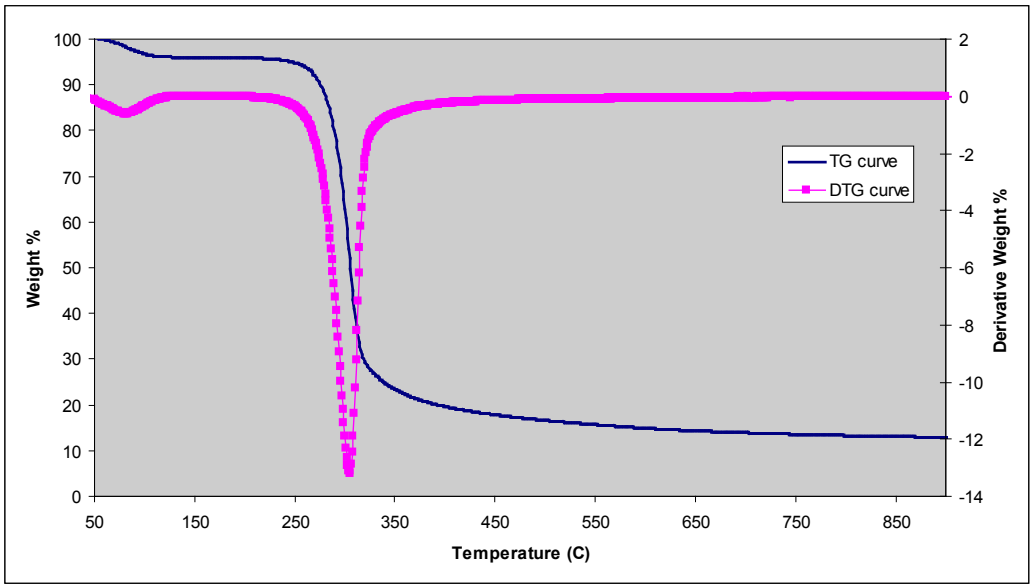

Figure 17: TGA curve of cellulose from 50 – 900°C under inert conditions

After evaluating the non-isothermal conditions, another set of experiments was conducted at isothermal conditions (i.e. 200, 250, 300 and 400°C) as shown in Figure 18. These experiments confirmed the weight losses shown in Figure 3 at specific temperatures over time. At each temperature, the initial weight loss of 4 wt% was observed within 0 – 5 minutes. At 200°C it is clear that there are no further significant weight changes, thus suggesting that cellulose does not necessarily decompose under these conditions. The final sample color after the 200°C reaction was grayish-white. At 250°C a slow weight loss occurred throughout the experiment to about 38 wt% and the final sample was observed to be light grey in color. The last two sets at 300 and 400°C had the largest weight changes and were most similar to the non-isothermal weight loss.

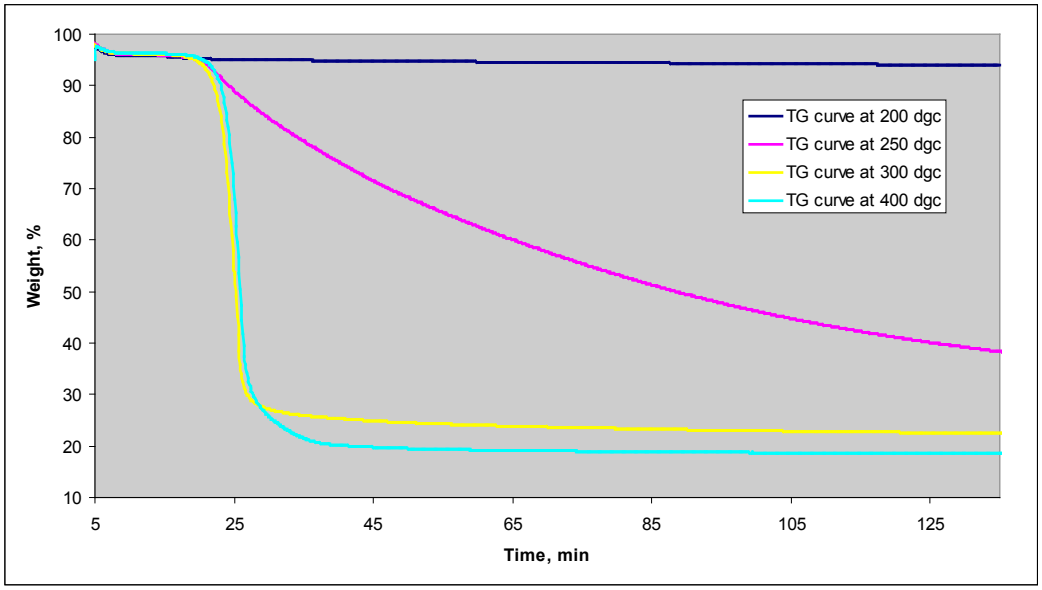

Figure 18: TGA curves at inert, isothermal conditions

The TGA data was good for tracing the thermal decomposition of cellulose under inert conditions, but it was still not clear whether these weight changes implied possible structural changes. To understand if any structural changes took place during TGA conditions, samples were further analyzed using a Scanning Electron Microscopy (SEM) for imaging and an SEM X-ray spectrometer that measured and compared the elemental analysis for each condition. Figure 5 (Reference cellulose), Figure 19 to 24 (TGA: 200 to 900°C) are SEM images that show the cellulose particles (mixture of 10 to 30 micron particle sizes) and their corresponding morphology at each temperature. There were no significant changes to the particle morphology at these conditions, which suggests that cellulose may be thermally resistant at inert conditions. Further tests using an SEM X-ray spectrometer suggested that there was a loss of oxygen when moving from low to high temperatures as shown in Figure 25-26. The SEM X-ray graph contradicts observations from the SEM that showed no particle morphology changes, but it is consistent with observations from the TGA trends above 300°C.

SEM images:

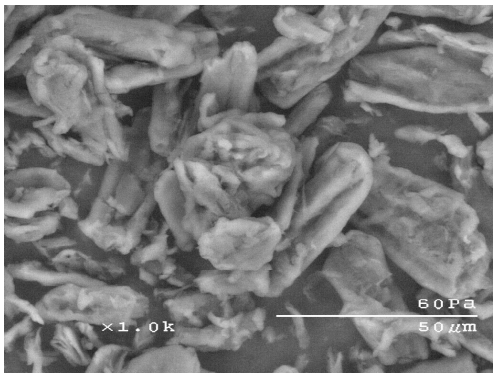

Figure 19. Cellulose reference

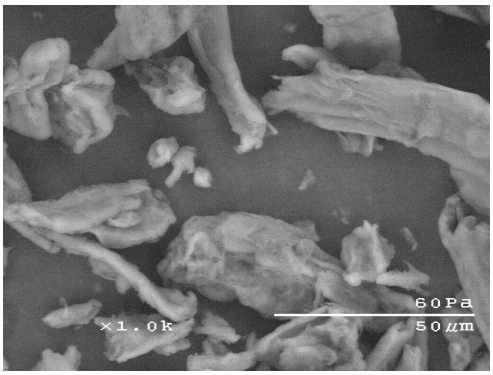

Fig.20 Cellulose after TGA at 200 °C

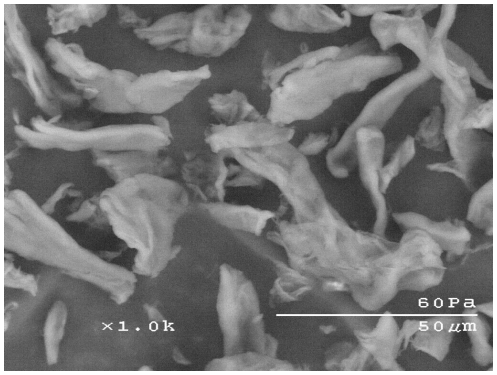

Figure 21. Cellulose after TGA at 250 °C

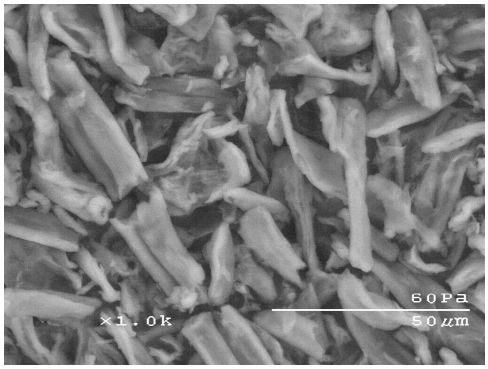

Figure 22 Cellulose after TGA at 300 °C

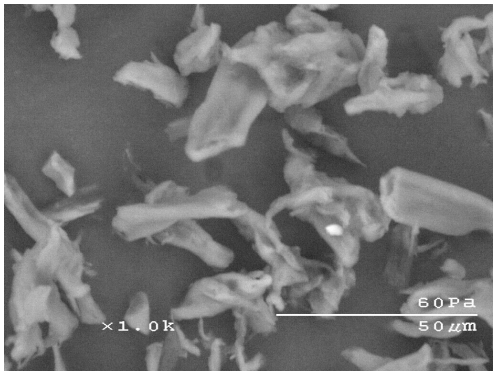

Figure 23 Cellulose after TGA at 400 °C

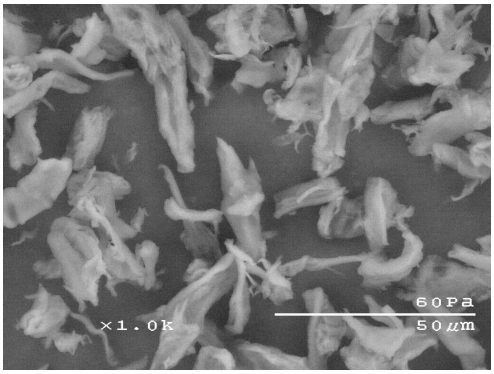

Fig.24 Cellulose after TGA at 900 °C

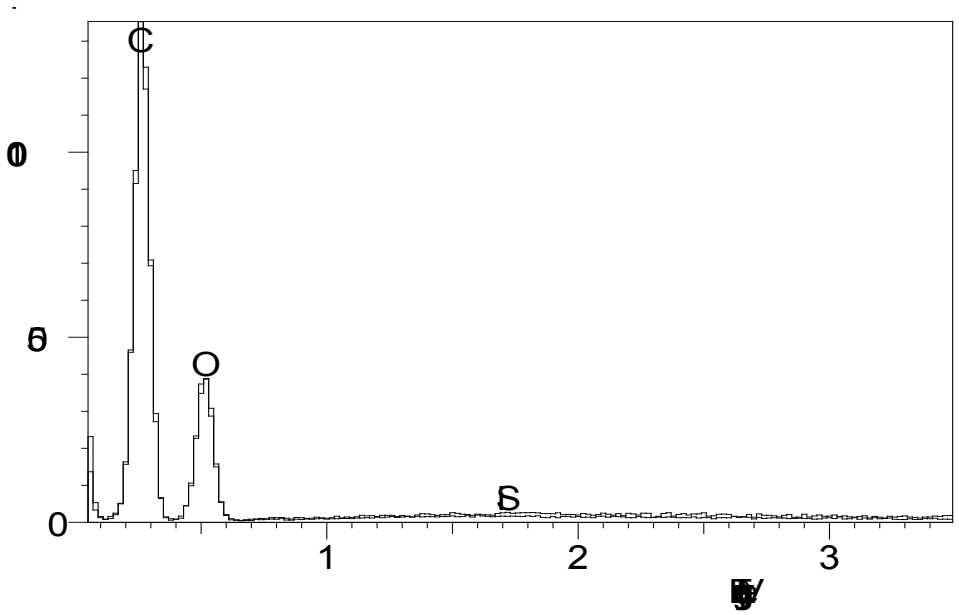

Figure 25: Data from SEM-Xray spectrometry 20 kx; Full line TGA represent conditions 200°C, dashed line is the reference cellulose
Note: at 200°C there was no loss of oxygen.

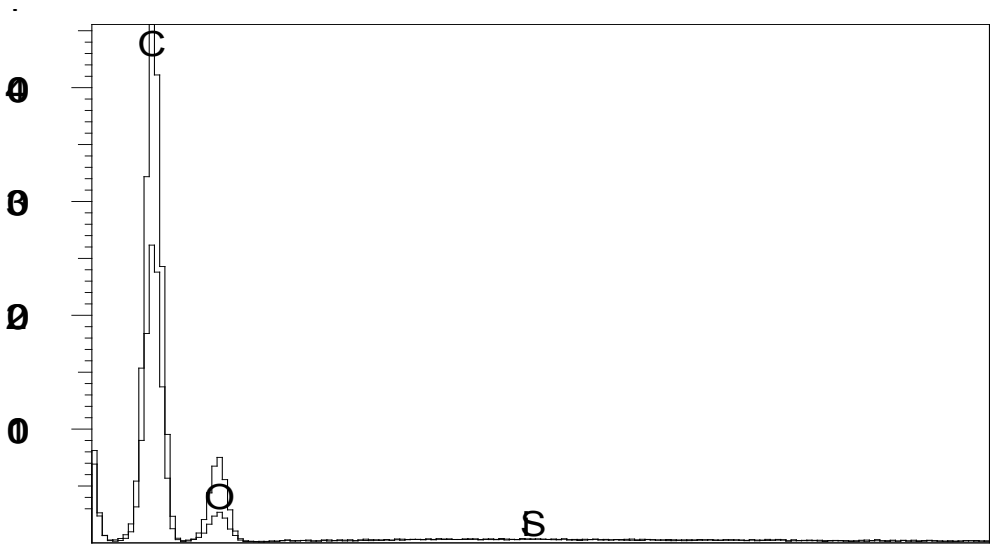

Figure 26: Data from SEM-Xray spectrometry 20kx; Full line TGA at 400°C and 900 °C, dashed line reference cellulose. Note: at 400°C and 900 °C, oxygen was lost

Results from TGA, SEM and SEM X-ray spectroscopy were complimentary tools in assessing the thermal decomposition of cellulose. The next step was to use

information gained from these studies to explain cellulose decomposition behaviors under subcritical and supercritical methanol and CO_2 conditions. A high pressure batch reactor was set up and 10 grams of cellulose and 360 grams of methanol were placed in it. The system was then heated for 4 to 6 hours to a specific temperature (i.e. 200, 300, 325 and 350°C). Some experiments were carried out using only methanol and others in the presence of both methanol and CO_2. For the latter case, CO_2 was pumped in at 12ml/min to a specific pressure.

The batch reactor was heated to a specific temperature and then maintained constant and stirred for an hour before cooling by removing insulation and blowing a fan while stirring for another 8 hours. At the end of the reaction, the batch reactor was vented to remove gases and then opened to collect the contents. The solvent and solids were separated by using a centrifuge. The solvent was further separated using a rotary vaporizer to recover methanol. The remaining liquid sample was then taken for further analysis using an NMR, GCMS and HPLC.

After the solids (unreacted cellulose) were separated from the solvent, they were dried under inert conditions and the final weight and color noted. At the end of the 200 to 300°C reactions, a light grey sample was recovered with the smallest conversions i.e. high amounts of unreacted cellulose as shown in Figure 27 and 28. Solids recovered from the 325 and 350°C reactions were dark grey to black in color. Shown in Figures 27 and 28 are the % conversion of cellulose and the amount of remaining residue after the reaction. Based on this data the change in cellulose in the presence of a solvent was proportional to the temperature increase. At 350°C under supercritical MeOH conditions with or without CO_2, cellulose was converted 99 wt% in comparison to the starting materials. The preferred conditions for these reactions would be at a temperature below 350°C. Observation of the solvent and solid products from reactions above 300°C showed a much darker brown solvent and black color remaining solids when compared to results at lower temperatures. Whereas, at temperatures below 300 °C the resulting solvent was light brown with solids light grey in color.

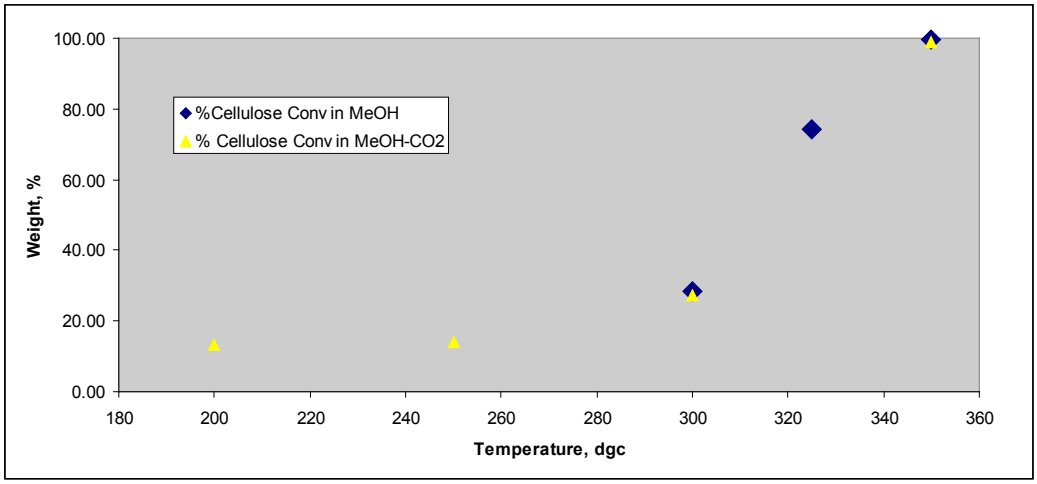

Figure 27: Analysis of cellulose at sub and supercritical conditions in methanol

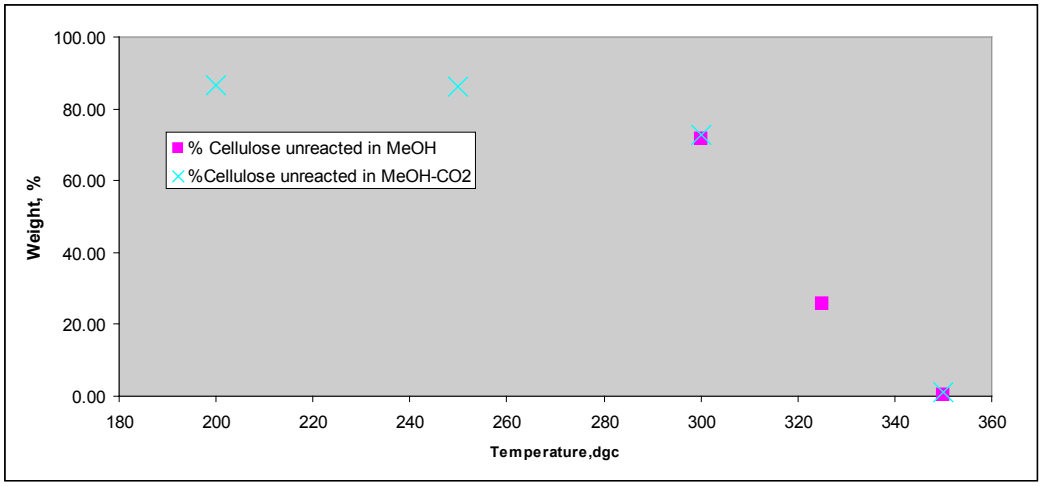

Figure 28: Analysis of cellulose sub and supercritical conditions in methanol

Based on the studies described above, temperature played a major role during thermal decomposition of cellulose using either a TGA or batch reactor system. In either system, low temperatures did not seem to change the cellulose to a large extent. Since lower temperatures are preferable, future studies will also include water to make use of it superior supercritical properties to optimize cellulose conversions at lower temperatures.

Batch Reactor setup and testing:

Figure 29 is an image of a one liter high pressure batch reactor at BECON mainly used to conduct research discussed in this report. The reaction setup begins by first inspecting the reactor to make sure it is in good working condition. After inspection, it is loaded with a measured amount of cellulose followed by methanol. It is then closed and pressure tested for leaks. In the absence of leaks, the experiment is started. For the purposes of this report, the reactor was heated non-isothermally to 350^{o}C and pressurized to 3600psi (26 MPa) for 1 hour after which the heater was shut down and a fan started to cool the reactor externally.

Batch reactor parts:

1. One liter reactor
2. Pressure gauges (digital and Astra gauge)
3. Heat control unit for main reactor and pre-heater
4. Solvent pump
5. Modular mixer speed control
6. CO_2 pump

Figure 29. High pressure batch reactor system

The total cycle for heating (6 hours), steady state condition (1 hour), and cooling the reactor took a total period of up to 24 hours. Additional, conditions were tested that are not the focus of this report including running the experiments at various temperatures from 200 to 350^{o}C, using various mixing rates (mass transfer effect), and measuring the impact of pressure on cellulose reactions with alcohols using CO_2.

At the end of the experiment the product sample (which is the main crude sample (Cr)) was removed and prepared for analysis. The Cr sample was taken to the laboratory to recover methanol using vacuum rotary vapor equipment and the resulting sample obtained will be called rotavap sample (RTVPCrude) in this report.

Following methanol removal, all samples were taken for extensive analysis conducted using a GCMS system consisting of an Agilent GC model 6890 integrated with a micromass GCT. The analytical part for GC used a DB5 column (L: 30 m, Di: 250 µm,Thickness 0.25 µm). The carrier gas was Helium 1 ml/min, initial temperature at 100^{o}C for 2 minutes, heating rate at 15^{o}C/min to 310^{o}C. For the Micromass system (MS) the conditions were: electron energy at 70 eV, source temperature of 100^{o}C using an electron ionization source. Additional ionization sources later used in this study included methane (CH_4) and an ammonia (NH_3) chemical ionization source. Molecular weight (m/z) measurements were taken from 35 to 1000. Sample analyzed with a GCMS were prepared by taking about 10 to 50 mg of RTVPcrude sample and diluted with methanol using a 25 ml flask. Using an auto sampler, about 1 micro liter liquid sample was injected into the GC.

Cellulose and Corn stover reaction behavior in methanol effect at 300 ^{o}C

As noted above the focus was only monitored the transition of cellulose during reactions in the presence of a solvent. The following section now includes analysis of the liquid portion post reaction. Evaluated was the composition for reaction products from Methanol-Cellulose interaction at low and high temperatures. The liquid product was analyzed using an NMR, GCMS and HPLC. The first part addressed experimental analysis for a cellulose sample in methanol at 300^{o}C and 2500 psi followed by comparisons of results from corn stover experiments. Using a GCMS analyser a liquid RTVPcrude sample was injected as prepared above. The analysis methods included an Ei, Ci-CH_4, and a Ci-NH_3 sources. A GC trace of these results is shown in Figure 30 below. Several peaks corresponding to specific compounds were present.

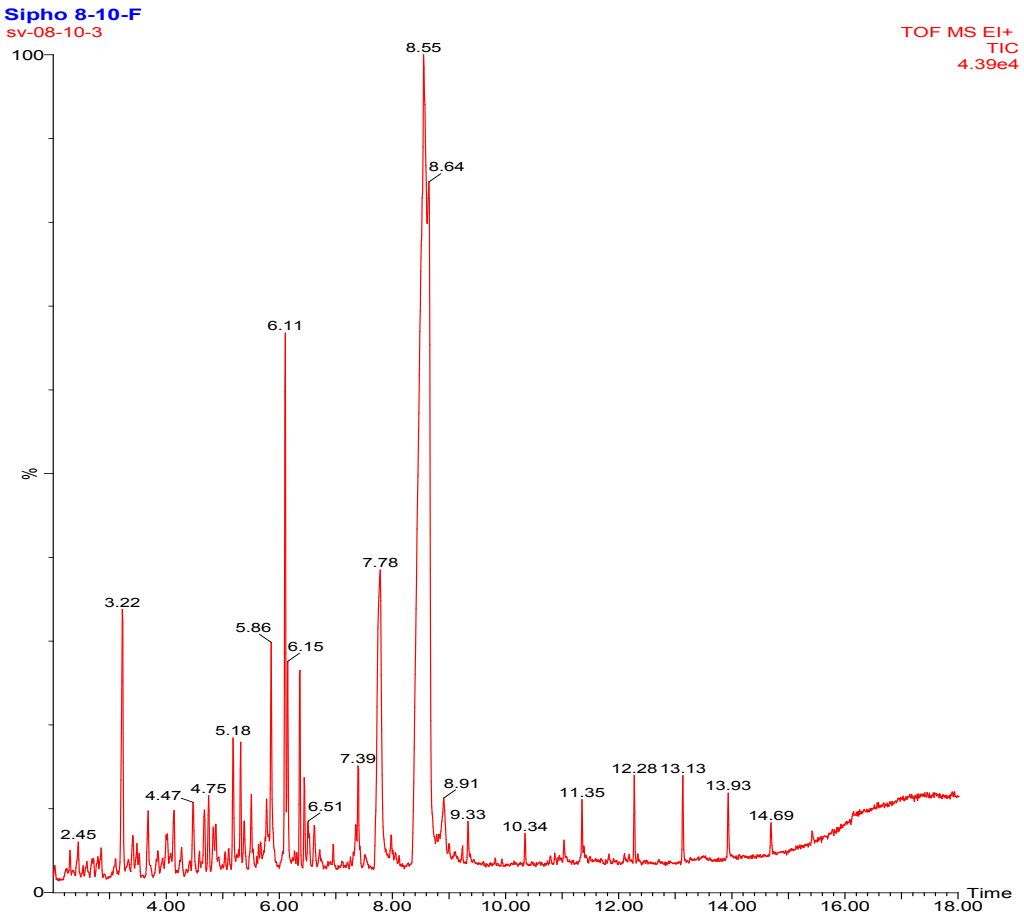

Figure 30. GC trace from analysis of RTVPcrude sample after high presure reaction at 300°C, 2500 psi in a cellulose/methanol mixture.

In Figure 30 the largest peak is at 8.55 followed by a another another peak at 8.64 shoulder. There are a few intermediate peaks including these at 3.22, 6.11, and 7.78. In addition to these various other peaks appear to overlap in the scan range. Since there are numerous peaks here initial assesment of components in the sample mostly focused on major and intermediate peaks. For example, Figure 31 show a chromatogram associated with a GC peak at 3.22. The corresponding molecular weight (m/z) at this peak was m/z: 112 followed by m/z:69. Futher assesment of these peaks using a gcms data library suggested that a peak at 3.22 could be associated with three two other m/z data includind 154 and 174. All these m/z 112, 154 and 172 at peak 3.22 were further checked against data obtained using the Ei and Ci methods. A mixture of m/z data may be suggesting that the peak is not pure due to poor peak separation. Therefore, future scans need to be improved by running the GCMS at longer time scan that will allow clear peak separation. Compounds associated with these m/z data are listed in Table 2 below. At m/z 112 the corresponding compounds suggested by the library had these chemical formular was $C_6H_8O_2$, C_8H_{16}, $C_7H_{12}O$ and the corresponding compound name in order from left to right were 2-hydroxy-3-methyl-2-cyclopenten-1-one, 1,4-dimethylcyclohexane, 3 methylcyclohexanone.

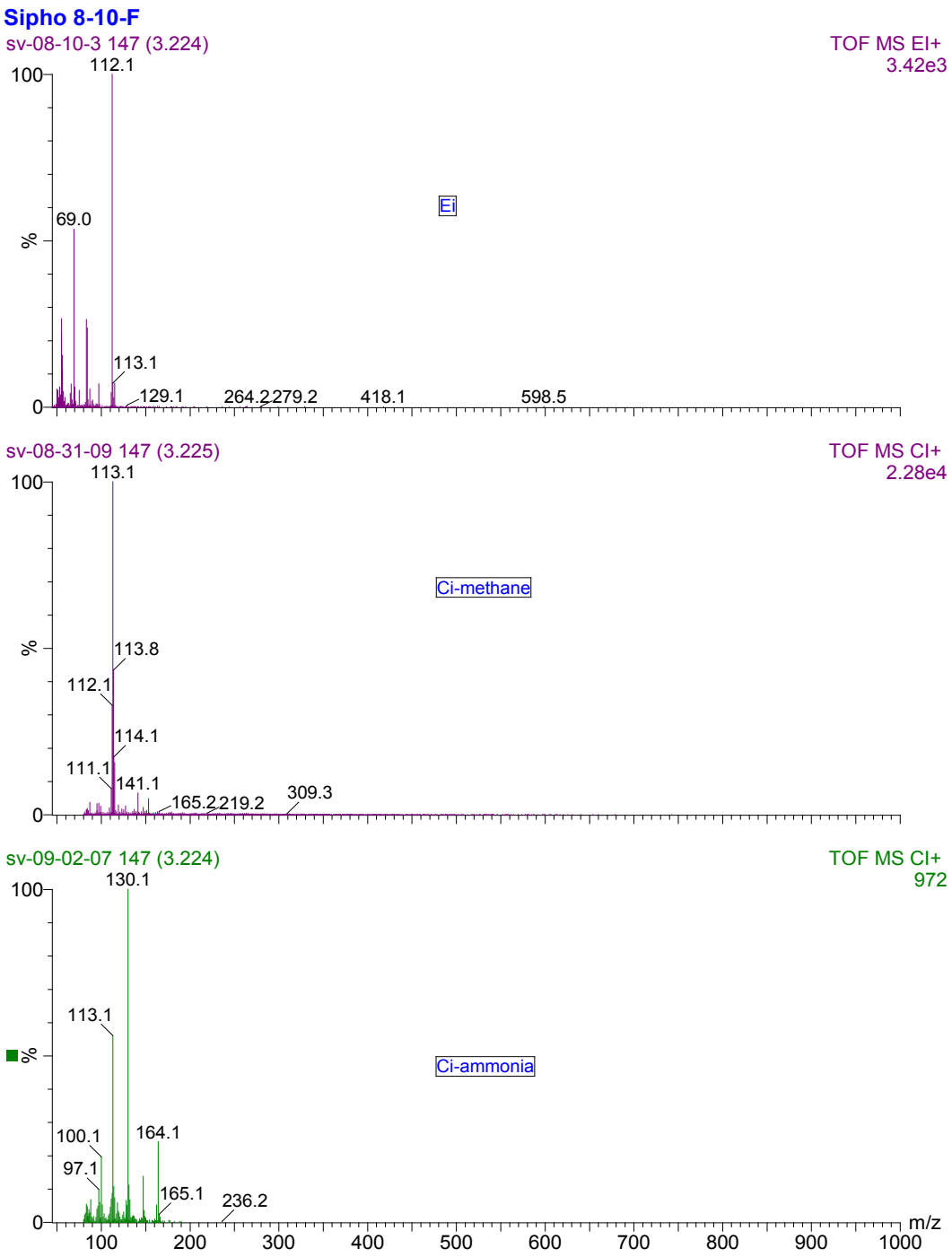

Figure 31. Mass Spectroscope of 3.224 GC peak showing m/z data using an Ei, Ci-CH_4, and Ci-NH_3 from RTVPcrude sample after high presure reaction at 300°C using cellulose and methanol

Based on results in Table 1 m/z 154 and 172, were identified as 5-methyl-2-1 Cyclohexanone and Acetic acid respectively. Further work is still underway to improve resolution and reduce peak overlapping. In addition selected pure standards of these compounds will be purchased and then analyzed using the GCMS at similar conditions. Despite these challenges resulting from overlapping

peaks, results in Table 2 were still useful in identifying a range of compounds formed during a reaction of cellulose with methanol. Compounds present from this experiment mostly consisted of organic acids, various organic compounds, sugars, and compounds formed from silicone grease contamination.

Analysis of GC peak from 3.22 to 7.783, and 9.33 (m/z range: 112 to 170) suggested a range of components including organic acids such as acetic, hexanoic and heptanoic acids and others. Sugars appeared in this range 7.783 to 8.55 in which some peal overlap took place. Sugars noticed here included D-allose, D-Galactose and these overlap with levoglucosan. At higher GC peak range from 10.342 to 14.693 compounds with silicon are present that is $C_{16}H_{30}O_4Si_3$, $C_{16}H_{48}O_8Si_8$. These silicon based compounds were suspected to have come from a interaction of cellulose/ methanol with silicone grease which is used when sealing the reactor.

Table 2 GCMS data for Cellulose/Methanol reaction at 300°C, 2500 psi

GC peaks from EI, CH4-CI, and NH3-CI data	Compound m/z based on EI and CI data	Compound Structural Formula	Corresponding Compound from GCMS database
3.224	112	$C_6H_8O_2$, C_8H_{16}, $C_7H_{12}O$	(2-hydroxy-3-methyl-2-cyclopenten-1-one, 1,4-dimethylcyclohexane, 3 methylcyclohexanone)
3.224	154	$C_{10}H_{18}O$	5-methyl-2-1 Cyclohexanone
3.224	172	$C_{10}H_{20}O_2$	Acetic acid
5.183	126	$C_6H_6O_7$	5-hydroxymethyl-2-furancarboxaldehyde
5.858	116	$C_6H_{12}O_2$	Hexanoic acid
5.858	164	$C_6H_{12}O_5$	Methyl-a-D arabinopyranoside, a'methyl xyloside, 2-deoxy-d-glucose
6.108	176	$C_7H_{12}O_5$	Methyl (3R)-trans-3-hydroxy-5-hydroxtethyltetra-hydrofuran-3-carboxylate
6.149	164	$C_6H_{12}O_5$	a'-Methyl xyloside, Methyl-a'-D-arabinopyranoside
7.783	130	$C_7H_{14}O_2$	Heptanoic acid
7.783	162	$C_6H_{10}O_5$	Levoglucosan
7.783	180	$C_8H_{14}O_6$	D-Allose
8.55	164	$C_6H_{12}O_5$	a'-D-Ribopyranoside, methyl
8.55	180	$C_6H_{12}O_6$	D-Galactose
8.55	194	$C_7H_{14}O_6$	Methyl a'-d-galactopyranoside
9.333	186	$C_{11}H_{22}O_2$	Decanoic acid, methyl ester
9.333	186	$C_9H_{18}O_2$ Si	3-hydroxy-3-(trimethylsilyl)cyclohexanone

9.333	186	$C_8H_{10}O_5$	Dimethylester of (2-oxopropylidene) malonic acid
10.342 - 14.693	370 – 592	$C_{16}H_{30}O_4Si_3$, $C_{16}H_{48}O_8Si_8$	Benzoic acid, 2,6-bis[(trimethylsilyl)oxy]-trimethyl ester; Cyclooactasiloxane, hexadecamethyl-

GCMS analysis of Corn Stover reactions in methanol at 300°C

In this section experimental analysis focused on a corn stover sample in methanol at 300°C and 2500 psi. The analysis was conducted using a GCMS by injecting a liquid RTVPcrude sample and analyzed using Ei, Ci-CH_4, and Ci-NH_3 sources. A GC trace of these results is shown in Figure 32 below consisting of analysis from both a corn stover and cellulose experiment.

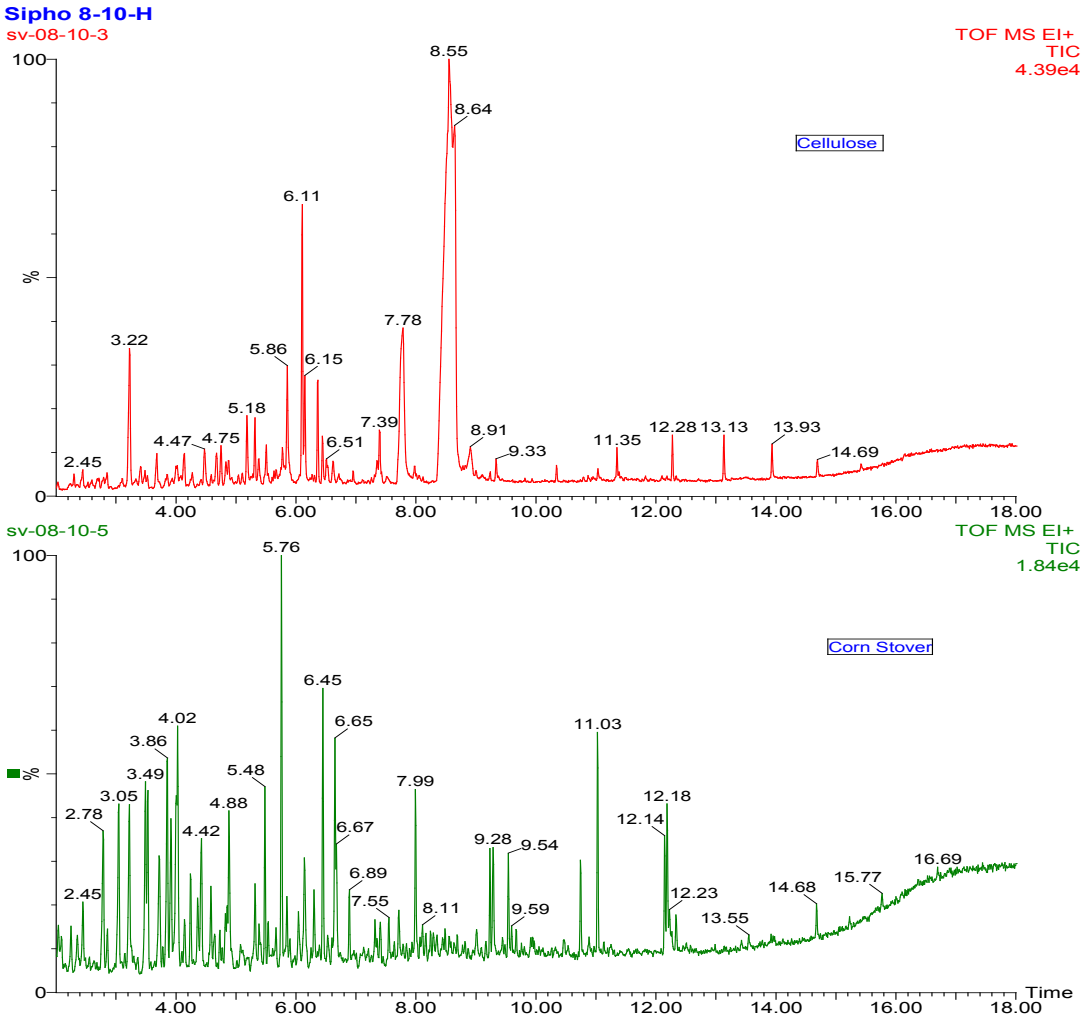

Figure 32. GC trace from analysis of RTVPcrude sample after high presure reaction at 300°C using cellulose and corn stover in methanol

Both traces in Figure 32 have multiple peaks present. A major peak for the cellulose sample is at 8.55 whereas 5.76 for the corn stover. In the case of corn stover a number of intermediate peaks were in the range 2 to 5.48 whereas for the cellulose sample an intermediate peak in this range existed at 3.22. In both cases smaller peaks existed starting at 13 to the end of the run. To simplify the analysis below,major peaks and intermediate peaks were evaluated to assess compounds present in these samples. A comparison of the two systems will be drawn from results in Table 2 and Table 3.

Table 3 GCMS data for Corn Stover/Methanol reaction at 300°C, 2500 psi

GC peaks from EI, CH4-CI, and NH3-CI data	Compound m/z based on EI and CI data	Compound Structural Formula	Corresponding Compound from GCMS database
2.783	116	$C_6H_{12}O_2$	Pentanoic acid methyl ester, Butanoic acid 2-methyl-methyl ester
2.783	116	$C_7H_{16}O$	Hexane, 3-methoxy; Ether, sec-butyl isopropyl
2.783	118	$C_5H_{10}O_3$	Methyl 4-hydroxybutanoate
2.783	130	$C_7H_{14}O_2$	Hexanoic acid, methyl ester; Pentanoic acid, 4-methyl-,methyl ester
2.783	130	$C_8H_{18}O$	Hexane, 3-methoxy-3-methyl; 3-Pentanol, 2,3,4-trimethyl
4.024	132	$C_6H_{12}O_3$	2,5 Dimethoxytetrahydrofuran; Furan; Butanoic acid, 4 methoxy-, methyl ester
4.024	132	$C_5H_8O_4$	Propanedioic acid, dimethyl ester
4.024	158	$C_{10}H_{22}O$	Pentane, 2,2,4,4-tetramethyl-3-methoxy-
4.024	158	$C_9H_{18}O_2$	Pentanoic acid, 2-ethyl-2-methyl-methyl ester, Hexanoic acid 2-ethyl-methyl ester
4.024	160	$C_7H_{12}O_4$	Butanedioic acid, methyl -dimethyl ester
5.758	152	$C_9H_{12}O_2$	Phenol, Benzene
6.45	154	c: $C_8H_{10}O_3$	Phenol, 2,6-dimethoxy
6.45	196	$C_{10}H_{12}O_4$	Phenol, 2,6-dimethoxy
7.991	182	$C_{10}H_{14}O_3$	Benzene, 1,2,3-trimethoxy-5-methyl
7.991	182	$C_9H_{10}O_4$	Benzoic acid, 3,4-dimethoxy-
9.233	210	$C_{11}H_{14}O_4$	Ethanone, 1-(3,4,5-trithoxyphenyl)
9.233	227	$C_{10}H_{13}O_5N$	3,4,5-Trimethoxybenzohydroxamic acid
9.283	192	$C_{11}H_{12}O_3$	2-Propenoic acid, 3-(4-methoxyphenyl)-, methyl ester, (E)-
9.283	210	$C_{11}H_{14}O_4$	5-(2'-hydroxy-5'methoxyphenyl) tetrahydrofuran-2-ol
9.283	210	$C_{11}H_{14}O_4$	5-(2'-hydroxy-5'methoxyphenyl) tetrahydrofuran-2-ol

10.742	222	$C_{12}H_{14}O_4$	2-Propenoic acid, 3-(4-methoxyphenyl)-, methyl ester
11.025	270	$C_{17}H_{34}O_2$	Hexadecanoic acid, methyl ester
11.025	270	$C_{17}H_{34}O_2$	Pentadecanoic acid, 14-methyl-, methyl
12.142	294	$C_{19}H_{34}O_2$	Octadeca-9,12-dienoic acid methyl ester
12.184	296	$C_{19}H_{36}O_2$	9-Octadecanoic acid, methyl ester
14.676	354	$C_{23}H_{46}O_2$	Docosanoic acid, methyl ester

Data in Table 3 suggested that there are numerous compounds present in the corn stover sample mostly consisting of organic acids and various organic compounds. In this instance sugars were not identified. Evaluation of corn stover at peak 2.783 gave m/z values 116, 118 and 130. The corresponding samples at this peak were organic acids. At 4.024 peak, esters were identified whereas the following peak at 6.45 suggested that phenols/ benzene were present. Additional analysis at 9.233 suggested that ethanone was noticed. The structure of ethanone and corresponding m/z spectra is shown in Figure 33. The final peak range looked at ranged from 10.742 to 11.025, with corresponding m/z data from 222 to 270. At this range the corn stover reaction mostly yielded various methyl esters. When comparing the results between corn stover and cellulose organic acids, methyl esters were common in both systems. Phenols and benzene are present in corn stover, but not in the cellulose analysis. However, the cellulose reaction systems had sugars in addition to organic acids.

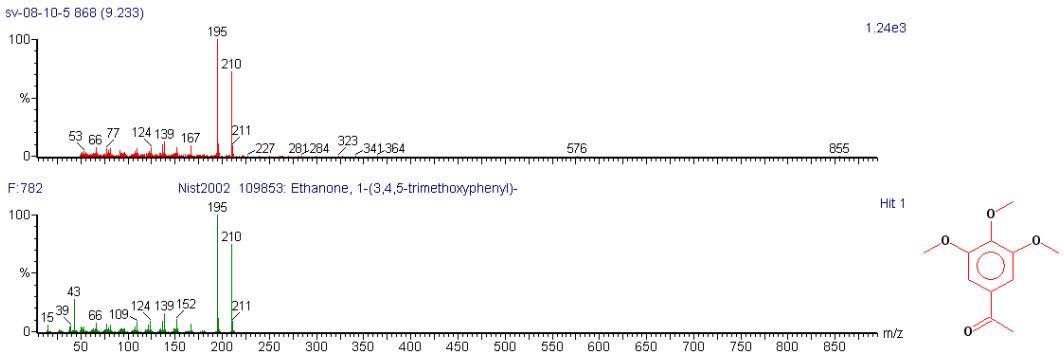

Figure 33. Mass Spectroscope at 9.233 GC peak shows m/z data using an Ei, Ci-CH_4, and Ci-NH_3 from RTVPcrude sample after high presure reaction at 300^{o}C using corn and methanol

The results discussed here compared the chemical composition for methanol-cellulose/ corn stover reactions. Next GCMS evaluated a cellulose-methanol reaction 350^{o}C. Two methods were attempted i.e. analysis of the volatile fraction of the sample, and analysis of the liquid fraction from the RTVP sample.

Sample analysis using GCMS

1. Analysis of volatiles from RTVP crude sample. The sample was transferred into a GC vial and heated in an oven for about 20 minutes to 70^{o}C. This sample was immediately removed from the oven and then

placed on the GC auto sampler tray. The GC syringe sampled the vapor space and injected a gas sample into the GC column.

2. About 10 mg of RTVPcrude sample was weighed and diluted with methanol using a 25 ml flask. Using an auto sampler, about 1 microliter liquid sample was injected into the GC.
3. 10 mg of liquid crude sample was diluted with 25 ml methanol and 1 microliter injected into the GC.

Analysis of volatile compounds by injecting a 1 microliter gas sample

Figures 35 and 36 are GC and MS graphs showing the analysis of a sample after a high pressure reaction with cellulose in the presence of methanol. In Figure 35, each peak on the GC trace corresponds to a specific compound with a molecular weight (m/z) on the mass spectroscopy data file. Initially the sample passes through a GC column (DB5) prior to entering the Micromass portion of the instrument. The data in Figure 36 was obtained by running the instrument in an electron ionization (EI) mode. At the 3.724 GC peak, the corresponding MS m/z values range from 40 to 61. A search and match database was used to account for compounds associated with each m/z value.

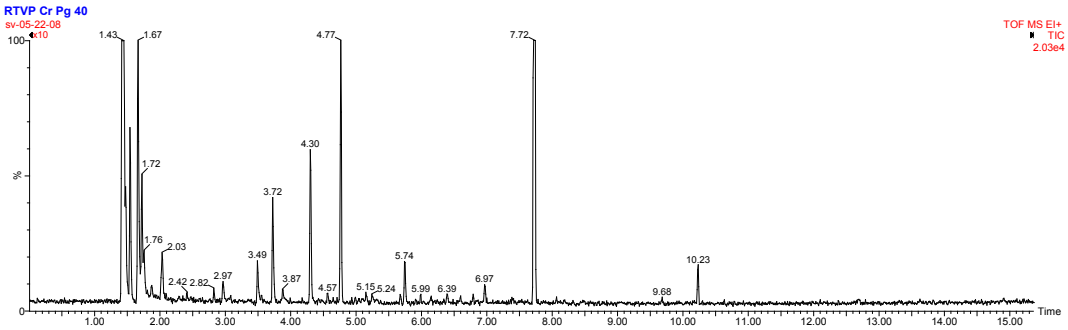

Figure 35. GC graph from vapor analysis of RTVPcrude sample after high presure reaction at 350^{o}C using cellulose and methanol

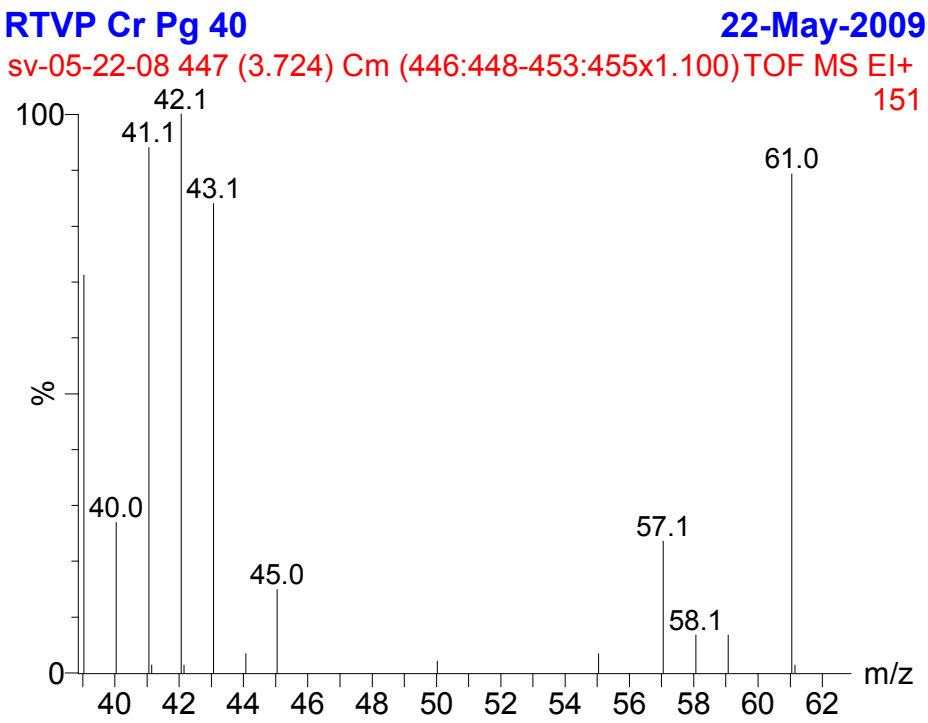

Figure 36. Mass Spectroscope of 3.724 GC peak showing m/z data using an electron ionization source, from vapor analysis of RTVPcrude sample after high presure reaction at 350°C using cellulose and methanol

Analysis results of the gas sample suggested that the crude sample contained volatile compounds with molecular weights ranging from m/z 58 to 59. This m/z data is associated with acetic acid [C_2H_5ON], 2-methyl-isobutane (propane [C_4H_{10}]), and acetone (2-propanone [C_3H_6O]). These compounds correspond to GC peaks from 1.432 to 1.666, but peaks from 1.666 to 10.23 could not be easily identified. Molecular weights of the unidentified compounds ranged from 100 to 250 m/z. After analyzing the volatile compounds, the liquid portion of the RTVPcrude sample was analyzed to identify the non-volatile compounds with molecular weights above 100 m/z.

Analysis of liquid RTVPcrude sample

Figures 37 and 38 are GC and MS analyses of liquid RTVPcrude sample. A liquid sample was injected into the GCMS and probed with an electron ionization source (EI). Analysis of this sample resulted to several compounds with molecular weights ranging from m/z 45 to 300.

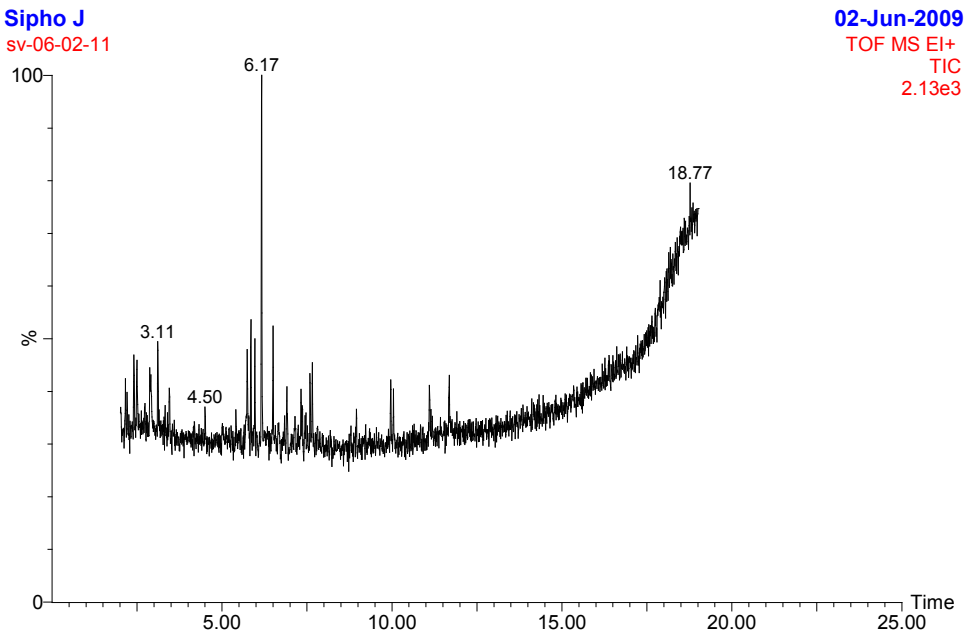

Figure 37. GC graph from analysis of a RTVPcrude liquid sample after a high presure reaction at 350ºC using cellulose and methanol

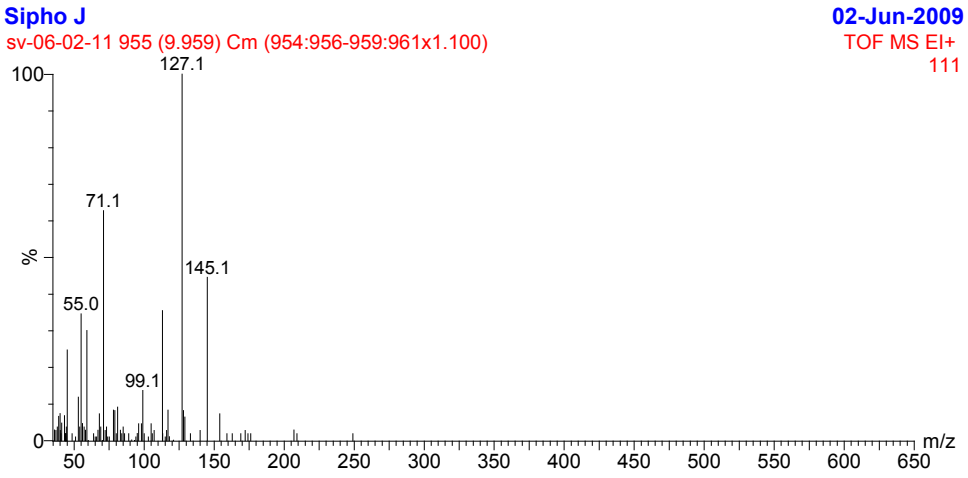

Figure 38. MS data from 9.959 GC peak using an electron ionization source and RTVPcrude liquid sample after a high presure reaction at 350ºC using cellulose and methanol

At GC peak 3.108 and MS m/z 86, two sets of compunds were identified. One with the molecular formula $C_5H_{10}O$ was associated with 3-methyl-tetrahydrofuran, 1-propene, and butanal. The other molecular formula C_6H_{14} corresponded to methylpentane and hexane. More analysis is being performed to identify the correct compund corresponding to m/z 86. The m/z value was obtained from an EI source so the next evaluation will use a methane and ammonia chemical ionization source. This information will also be compared to NMR data that is currently being collected.

At GC peaks 5.850 - 6.501, the MS data at m/z 120 suggested the presense of C_9H_{12}: 1,2,3-tris(methylene)-cyclohexane or 1,2,3-trimethylbenzene. Large m/z values were identified as the GC peak values increased. This is consistent with the following peaks: GC 9.959, m/z 160 [$C_7H_{12}O_4$]: tetrahydro-2,5-dimethoxyfuran carboxaldehyde, and GC 11.101 - 11.685, m/z 162 [$C_6H_{10}O_5$]: levoglucosan to m/z 208 [$C_8H_{16}O_6$]: ethyl a-d-glucopyranoside.

Analysis of liquid crude sample (Cr) using GCMS

Table 4 shows results from the liquid crude sample (Cr) injected into the GCMS. This sample was taken from the reactor and analyzed before recovering the methanol using vacuum rotary vaporization. The sample was tested using an electron ionization source, methane, and ammonia chemical ionization (CI) source (CH_4-CI, NH_3-CI).

Table 4. GCMS data from liquid crude sample after high pressure reaction at 350°C using methanol and cellulose.

GC peaks from EI, CH4-CI, and NH3-CI data	Compound m/z based on EI and CI data	Compound Structural Formula	Corresponding Compound from GCMS database
2.592	90	$C_3H_6O_3$	acetic acid, hydroxymethyl ester, methyl gylcolate and/or carbonic acid, dimethyl ester
2.967	104	$C_4H_8O_3$	propanoic acid, 2-hydroxymethyl ester
3.534	N/A	N/A	N/A
4.584	N/A	N/A	N/A
6.893	126	$C_7H_{10}O_2$	1,3-cyclopentanedione
7.443	156	$C_{11}H_{24}$	Undecane
7.668	126	$C_7H_{10}O_2$	2-cyclopenten-1-one
7.743	160	$C_8H_{16}O_3$	Butanoic acid
8.868	176	$C_7H_{12}O_5$	3-acetoxy-3-hydroxy-2-methylpropionic acid, dimethyl 2-(hydroxymethyl)-2-methylmalonate
9.035	a: 114 b: 130 c: 190	a: $C_7H_{14}O$ b: $C_7H_{14}O_2$ c: $C_8H_{14}O_5$	a: 1-methylcyclohexanol b: butanoic acid c: butanedioic acid
9.627	176	$C_7H_{12}O_5$	methyl (3R)-trans-3-hydroxy-5-hydroxtethyltetra-
10.052	a: 156 b: 176 c: 204	a: $C_9H_{16}O_2$ b: $C_7H_{12}O_5$ c: $C_9H_{16}O_5$	a: 2-hexanal-propylene glycol acetal b: methyl (3R)-trans-3-hydroxy-5-hydroxtethyltetra- c: dimethyl 2-methoxyhexane-1,6 dioate
10.127	158	$C_7H_{10}O_4$	butanedioic acid, dimethyl ester
11.21	162	$C_6H_{10}O_5$	1,6-anhydro-a-D-glucopyranose (levoglucosan)
11.21	194	$C_7H_{14}O_6$	(alpha)a-D-galactopyranoside, methyl a-d-galactopyronoside

Based on the information in Table 1, there are numerous compounds present in this sample mostly consisting of organic acids and other organic compounds. Molecular weight (m/z) measurements were taken from 45 to 1000. This excluded peaks that could be associated with methanol. Note that the crude sample consisted of about 80 wt% methanol and about 20 wt% crude products.

The data highlighted in yellow shows the peak range 3.5 to 5.0. In this range, no compounds could be identified except those containing silicon including $C_6H_{16}Si$ and $C_5H_{14}OSi$. These silicon based compounds were suspected to have come from silicon grease which is used when sealing the reactor. Each peak corresponded to a single m/z data set, but a few (highlighted in green) suggested multiple compounds associated with a single peak. At the moment, more analysis is being performed to verify if these compounds can be confirmed using other analytical techniques including NMR, LCMS and HPLC.

Distillation using a Kugel Rohr:

Following the experiment the product sample (which is the main crude sample (Cr)) was removed and prepared for analysis. The Cr sample was taken to the laboratory to recover methanol using vacuum rotary vapor equipment and the resulting sample obtained will be called rotavap sample (RTVPCrude) in this report. The RTVPCrude sample was then fractionated under vacuum distillation using a Kugel Rohr. Figure 39 shows an image of three samples, from left to right, RTVCrude, crude, and a methanol sample after rotary-vaporization. The RTVCrude sample was then distilled using a Kugel Rohr system at 0.02 mmHg and 88^{o}C.

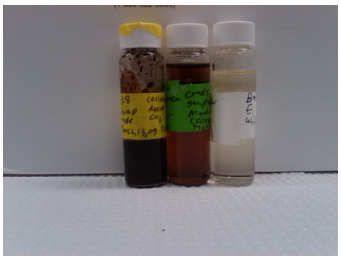

Figure 39. Product sample from SCF methanol with cellulose at 300^{o}C

Figure 40 shows an image of the side and top views of the Kugel Rohr system. As seen from the top view, the sample was placed in the first heating container (pot) at 88^{o}C with two temperature probes T1(air), and T2 (pot wall). Beside the pot are the collection flasks, CA (32^{o}C), cooled on the outside with ice water, and CB (-40^{o}C), cooled in 50 % mixture of liquid nitrogen/ 2propanol. Attached at the end were the rotating Kugel Rohr unit and a vacuum tube. This system was run for about 35 minutes, after which the samples in CA and CB became clear in color.

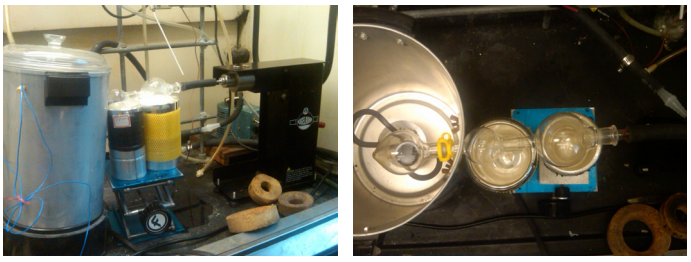

Figure 40. Side and top views of distillation setup at 88^{o}C and 0.02 mmHg

Based on the data in Table 5, approximately 52 wt% of sample was distilled from the original sample. However, the amount collected in CA was about 10% and CB about 1%. The biggest challenge at the start of the experiment was making sure that the vacuum pump was well controlled and lowered slowly to 0.02 mmHg. Unfortunately, excessive vacuum was applied at the beginning, resulting in the loss of some of the RTVPCrude sample that was in the pot heating zone. This may have contributed to some of the material that was lost prior to steady-state distillation conditions. Therefore, a large amount of the original sample is unaccounted for, based on a mass balance. More experiments are underway to improve the procedure. This may include using a different distillation setup.

Table 5. Mass balance for RTVCrude at 300^{o}C distilled sample

Description	Flask gross weight, gr	Flask Tare weight, gr	Net sample weight, gr	% Distilled, % Collected & %Lost
RTVPCrude before distillation (Pot)	26.9244	24.8181	2.11	
RTVPCrude after Distillation (Pot)	25.9194	24.8181	1.10	52.29
CA	22.9587	22.7566	0.20	9.60
CB	46.023	46.003	0.02	0.95
Black residue cleaned from CA and CB flask mouths	22.9228	22.75666	0.17	7.89
Total				70.72
Mass balance initial sample			2.11	
Mass balance (CA, CB, residue)			1.49	
Lost sample or unaccounted			0.62	29.28

During the distillation experiments, temperature and vacuum pressure was monitored as shown in Table 6 below. The steady state conditions were at 88^{o}C and 0.02 mmHg.

Table 6. Temperature profile for RTVPCrude 300°C sample using the Kugel Rohr system

% Variac Setting	Time, min	T1 (pot air), °C	T2 (pot wall), °C	CA (ice bath), °C	CB (Liquid N2 and 2-propanol), °C
0	0	25	25	0	-40
25	5	35	36	0	-40
25	10	46	46	0	-40
30	15	50	47	0	-40
40	25	77	73	0	-40
40	30	83	88	0	-40
35	35	82	88	0	-41

Analysis conditions using a GCMS:
The main analysis technique used was a GCMS. Samples were taken for extensive analysis using a GCMS system consisting of an Agilent GC model 6890 integrated with a micromass GCT. The analytical part for GC used a DB5 column (L: 30 m, Di: 250 µm, Thickness 0.25 µm). The carrier gas was Helium at 1 ml/min, initial temperature at 100°C for 2 minutes, heating rate at 15°C/min to 310°C. For the Micromass system (MS) the conditions were: electron energy at 70 eV, source temperature of 100°C using an electron ionization ion source (Ei). Additional ionization sources later used in this study included methane (CH_4) and an ammonia (NH_3) chemical ionization source. Molecular weight (m/z) measurements were taken from 45 to 1000. This excluded peaks associated with methanol since all samples were diluted in methanol. Sample analyzed with a GCMS were prepared by taking about 10 mg of RTVPcrude sample and diluted with methanol using a 25 ml flask. Using an auto sampler, about 1 micro liter liquid sample was injected into the GC.

GCMS analysis of product samples from cellulose reactions:
The first part for Task B2 will address experimental analysis for a cellulose sample in methanol at 300°C and 2500 psi and the second part of the report will then draw comparisons of results between cellulose reactions to those of the distilled using a Kugel Rorh (preliminary data). Using a GCMS analyser a liquid RTVPcrude sample was injected as prepared above. The analysis methods included an Ei, Ci-CH_4, and a Ci-NH_3 sources. A GC trace of these results is shown in Figure 41 below. Several peaks corresponding to specific compounds were present.

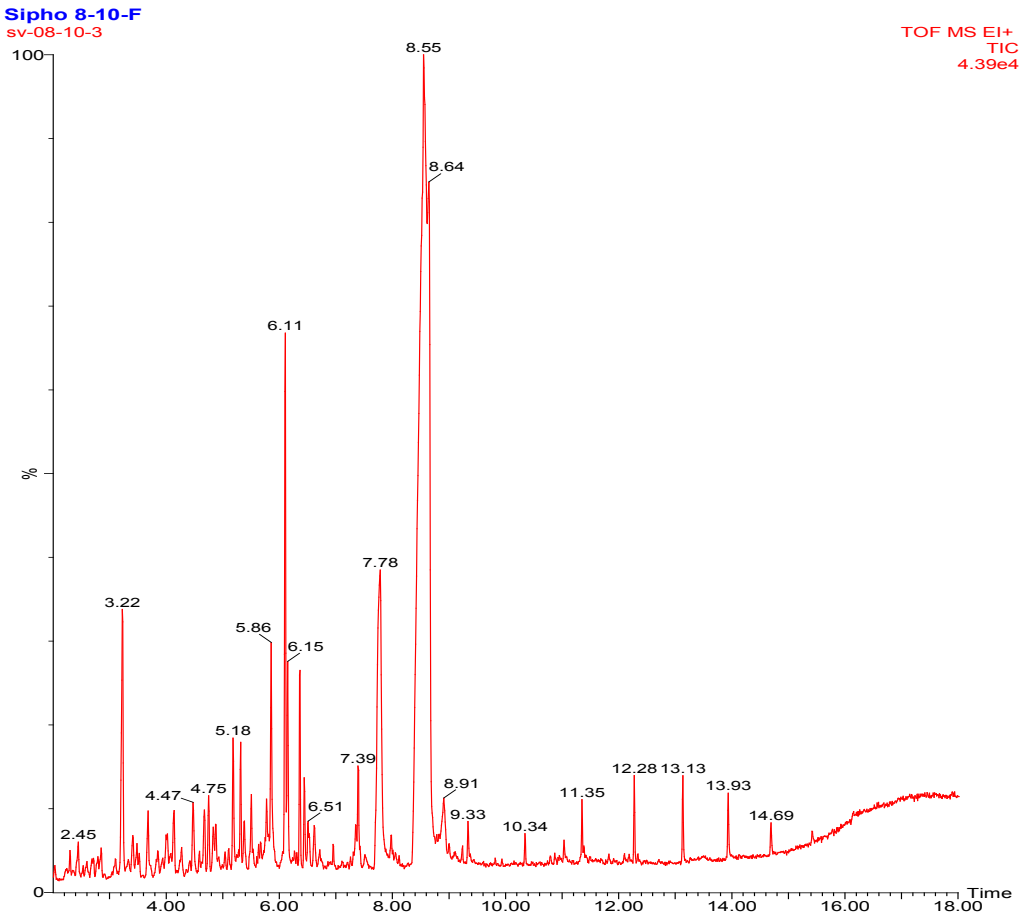

Figure 41. GC trace from analysis of RTVPcrude sample after high presure reaction at 300°C, 2500 psi in a cellulose/methanol mixture.

In Figure 41 the largest peak is at 8.55 followed by a another another peak at 8.64 shoulder. There are a few intermediate peaks including these at 3.22, 6.11, and 7.78. In addition to these various other peaks appear to overlap in the scan range. Since there are numerous peaks here initial assesment of components in the sample mostly focused on major and intermediate peaks. For example, Figure 42 show a chromatogram associated with a GC peak at 3.22. The corresponding molecular weight (m/z) at this peak was m/z: 112 followed by m/z:69. Futher assesment of these peaks using a gcms data library suggested that a peak at 3.22 could be associated with three two other m/z data includind 154 and 174. All these m/z 112, 154 and 172 at peak 3.22 were further checked against data obtained using the Ei and Ci methods. A mixture of m/z data may be suggesting that the peak is not pure due to poor peak separation. Therefore, future scans need to be improved by running the GCMS at longer time scan that will allow clear peak separation. Compounds associated with these m/z data are listed in Table 1 below. At m/z 112 the corresponding compounds suggested by the library had these chemical formular was $C_6H_8O_2$, C_8H_{16}, $C_7H_{12}O$ and the corresponding compound name in order from left to right were 2-hydroxy-3-methyl-2-cyclopenten-1-one, 1,4-dimethylcyclohexane, 3 methylcyclohexanone.

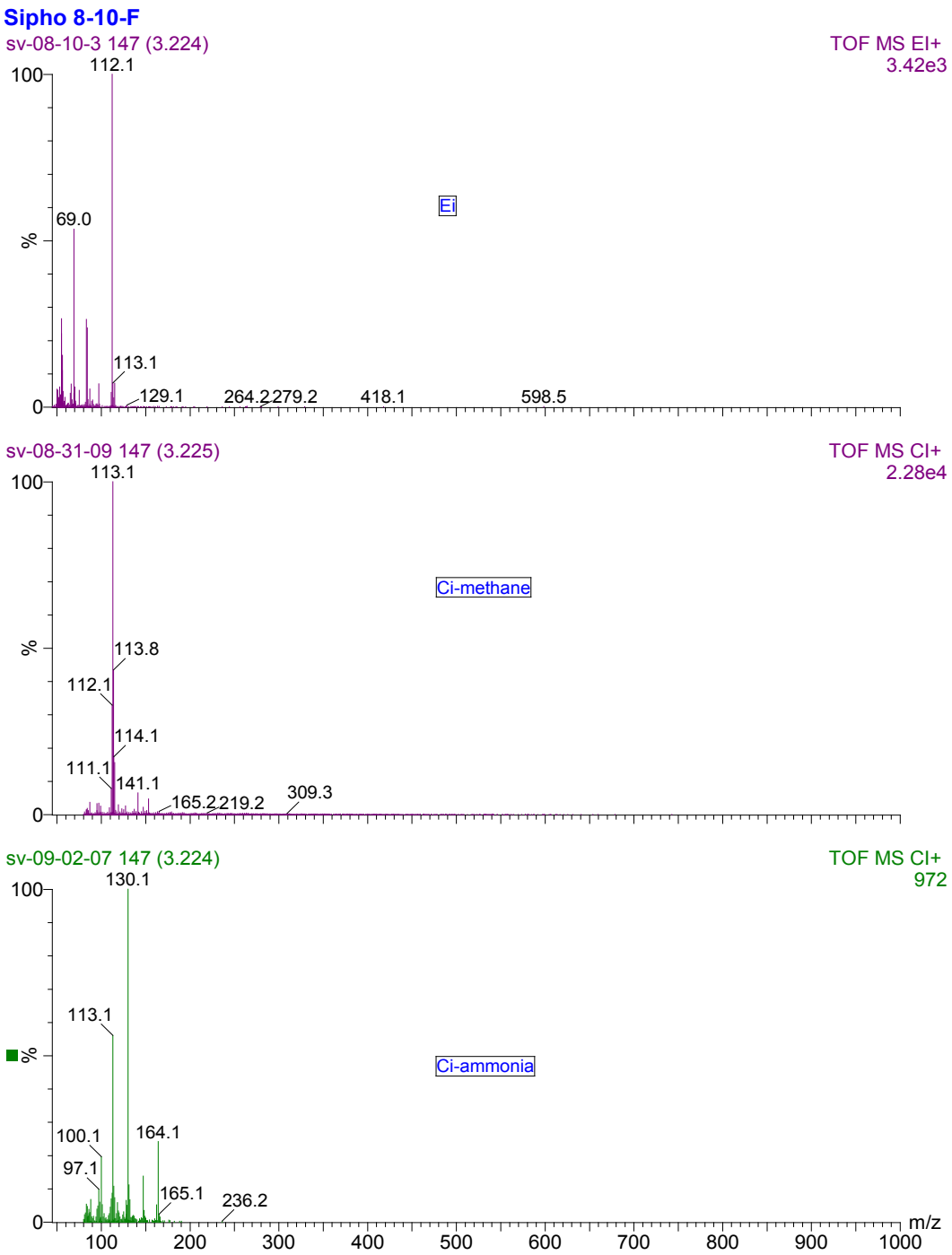

Figure 42. Mass Spectroscope of 3.224 GC peak showing m/z data using an Ei, Ci-CH_4, and Ci-NH_3 from RTVPcrude sample after high presure reaction at 300°C using cellulose and methanol

Based on results in Table 4 m/z 154 and 172, were identified as 5-methyl-2-1 Cyclohexanone and Acetic acid respectively. Further work is still underway to improve resolution and reduce peak overlapping. In addition selected pure standards of these compounds will be purchased and then analyzed using the GCMS at similar conditions. Despite these challenges resulting from overlapping

peaks, results in Table 5 were still useful in identifying a range of compounds formed during a reaction of cellulose with methanol. Compounds present from this experiment mostly consisted of organic acids, various organic compounds, sugars, and compounds formed from silicone grease contamination.

Analysis of GC peak from 3.22 to 7.783, and 9.33 (m/z range: 112 to 170) suggested a range of components including organic acids such as acetic, hexanoic and heptanoic acids and others. Sugars appeared in this range 7.783 to 8.55 in which some peal overlap took place. Sugars noticed here included D-allose, D-Galactose and these overlap with levoglucosan. At higher GC peak range from 10.342 to 14.693 compounds with silicon are present that is $C_{16}H_{30}O_4Si_3$, $C_{16}H_{48}O_8Si_8$. These silicon based compounds were suspected to have come from a reaction of cellulose/ methanol with silicone grease which is used when sealing the reactor

Table 5. GCMS data for Cellulose/Methanol reaction at 300°C, 2500 psi

GC peaks from EI, CH4-CI, and NH3-CI data	Compound m/z based on EI and CI data	Compound Structural Formula	Corresponding Compound from GCMS database
3.224	112	$C_6H_8O_2$, C_8H_{16}, $C_7H_{12}O$	(2-hydroxy-3-methyl-2-cyclopenten-1-one, 1,4-dimethylcyclohexane, 3 methylcyclohexanone)
3.224	154	$C_{10}H_{18}O$	5-methyl-2-1 Cyclohexanone
3.224	172	$C_{10}H_{20}O_2$	Acetic acid
5.183	126	$C_6H_6O_7$	5-hydroxymethyl-2-furancarboxaldehyde
5.858	116	$C_6H_{12}O_2$	Hexanoic acid
5.858	164	$C_6H_{12}O_5$	Methyl-a-D arabinopyranoside, a'methyl xyloside, 2-deoxy-d-glucose
6.108	176	$C_7H_{12}O_5$	Methyl (3R)-trans-3-hydroxy-5-hydroxtethyltetra-hydrofuran-3-carboxylate
6.149	164	$C_6H_{12}O_5$	a'-Methyl xyloside, Methyl-a'-D-arabinopyranoside
7.783	130	$C_7H_{14}O_2$	Heptanoic acid
7.783	162	$C_6H_{10}O_5$	Levoglucosan
7.783	180	$C_8H_{14}O_6$	D-Allose
8.55	164	$C_6H_{12}O_5$	a'-D-Ribopyranoside, methyl
8.55	180	$C_6H_{12}O_6$	D-Galactose
8.55	194	$C_7H_{14}O_6$	Methyl a'-d-galactopyranoside
9.333	186	$C_{11}H_{22}O_2$	Decanoic acid, methyl ester

9.333	186	$C_9H_{18}O_2Si$	3-hydroxy-3-(trimethylsilyl)cyclohexanone
9.333	186	$C_8H_{10}O_5$	Dimethylester of (2-oxopropylidene) malonic acid
10.342 - 14.693	370 – 592	$C_{16}H_{30}O_4Si_3$, $C_{16}H_{48}O_8Si_8$	Benzoic acid, 2,6-bis[(trimethylsilyl)oxy]-trimethyl ester; Cyclooactasiloxane, hexadecamethyl-

GCMS analysis of a distilled RTVPCr CA using a Kugel Rohr

In this section experimental analysis focused on samples that were distilled using a Kugel Rorh based on conditions in Table 6 and Table 7 above. GCMS information of the original sample before distillation is in Figure 41, 42 and Table 5. The GCMS conditions for the distilled samples CA, CB and Crude sample were modified by increasing sample residence time in the column as shown in Figure 43 below. The analysis was conducted using a GCMS by injecting a liquid sample and analyzed using Ei, Ci-CH_4, and Ci-NH_3 sources. Analyis of this data in Table 8 was analyzed using the NIST 2008 library.

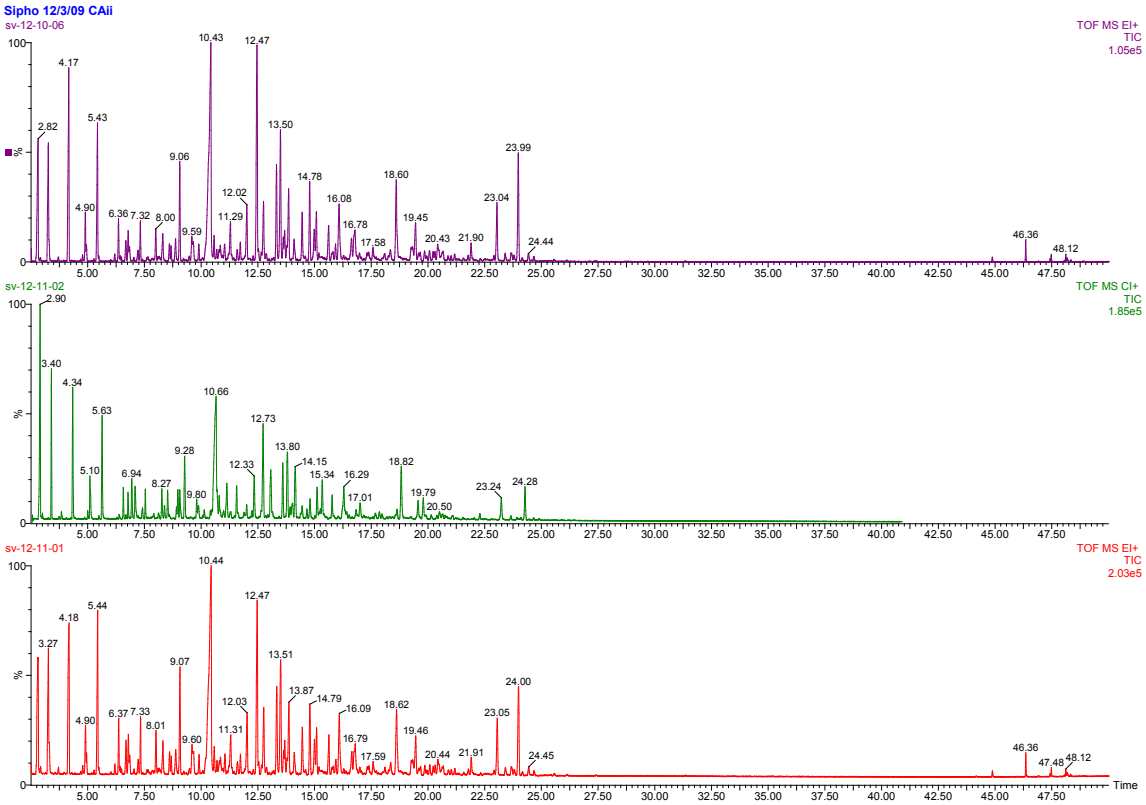

Figure 43. GC trace from analysis of distilled RTVPcrude CA, Ci-NH3 and Ci-CH4 (top to bottom) sample after high presure reaction at 300°C using cellulose

Table 8. GCMS data for distilled RTVPCr CA at 300°C, 2500 psi

peak	Cmpnd1	%prob1	Cmpnd2	%prob2
2.791	acetic acid, hydroxy-, methyl ester (C3H6O3)	96.4	Carbonic Acid, dimethyl ester (C3H6O3)	2.37
2.792	acetic acid, hydroxy-, methyl ester (C3H6O3)	94.9	Carbonic Acid, dimethyl ester (C3H6O3)	3.37
2.8	acetic acid, hydroxy-, methyl ester (C3H6O3)	95.2	1-Nitro-2-propanol(C3H7NO3)	1.82
3.258	propanoic acid, 2hydroxy-,methly ester, +/- (C4H8O3)	85.9	R-(-)-1,2-propanediol(C3H8O2)	7.73
3.259	propanoic acid, 2hydroxy-,methly ester, +/- (C4H8O3)	81	Isopropyl Alcohol (C3H8O)	5.37
3.267	propanoic acid, 2hydroxy-,methly ester, +/- (C4H8O3)	71.6	R-(-)-1,2-propanediol (C3H8O2)	15.1
4.141	Glycolaldehyde dimethyl acetal (C4H10O3)	83.2	Silanol, trimethyl (C3H10OSi)	4.74
4.142	Glycolaldehyde dimethyl acetal (C4H10O3)	88.8	Silanol, trimethyl (C3H10OSi)	2.3
4.176	Glycolaldehyde dimethyl acetal (C4H10O3)	85	Ethanol, 2,2'oxybis	7.26
5.275	Ethane, 1,1,2-Trimethoxy- (C5H12O3)	64.3	Propane, 2,2',2''-[methylidynetris(oxy)]tris(10H22O3)	17.2
5.284	N/A	N/A	N/A	N/A
5.284	N/A	N/A	N/A	N/A
5.408	2-Furanmethanol (C5H6O2)	52	3-Furanmethanol(C5H6O2)	41.9
5.417	2-Furanmethanol (C5H6O2)	51.5	3-Furanmethanol(C5H6O2)	35.3

Cellulose-Corn Stover Hydrogenation:

Figure 44 below is a plot taken in which cellulose and corn stover were placed under SC-MeOH reaction at 300°C. Concluding remarks from this study suggested that products from a cellulose reaction at 300°C analyzed by GCMS consisted of a mixture of organic acids, sugars, and several other components. Examples of organic acids included acetic, hexanoic, heptanoic and malonic acids, whereas sugars were levoglucosan, D-Allose, and D-Galactose. However, a different chemistry was obtained from product samples in corn stover-methanol reaction at 300°C. Based on the GCMS analysis the following components were suggested: ketones, aromatic hydrocarbons, and methyl esters. As evidenced by these results, reactions at high pressure are plausible although they were accompanied by a complex product composition, and an unreacted residue of cellulose and lignin.

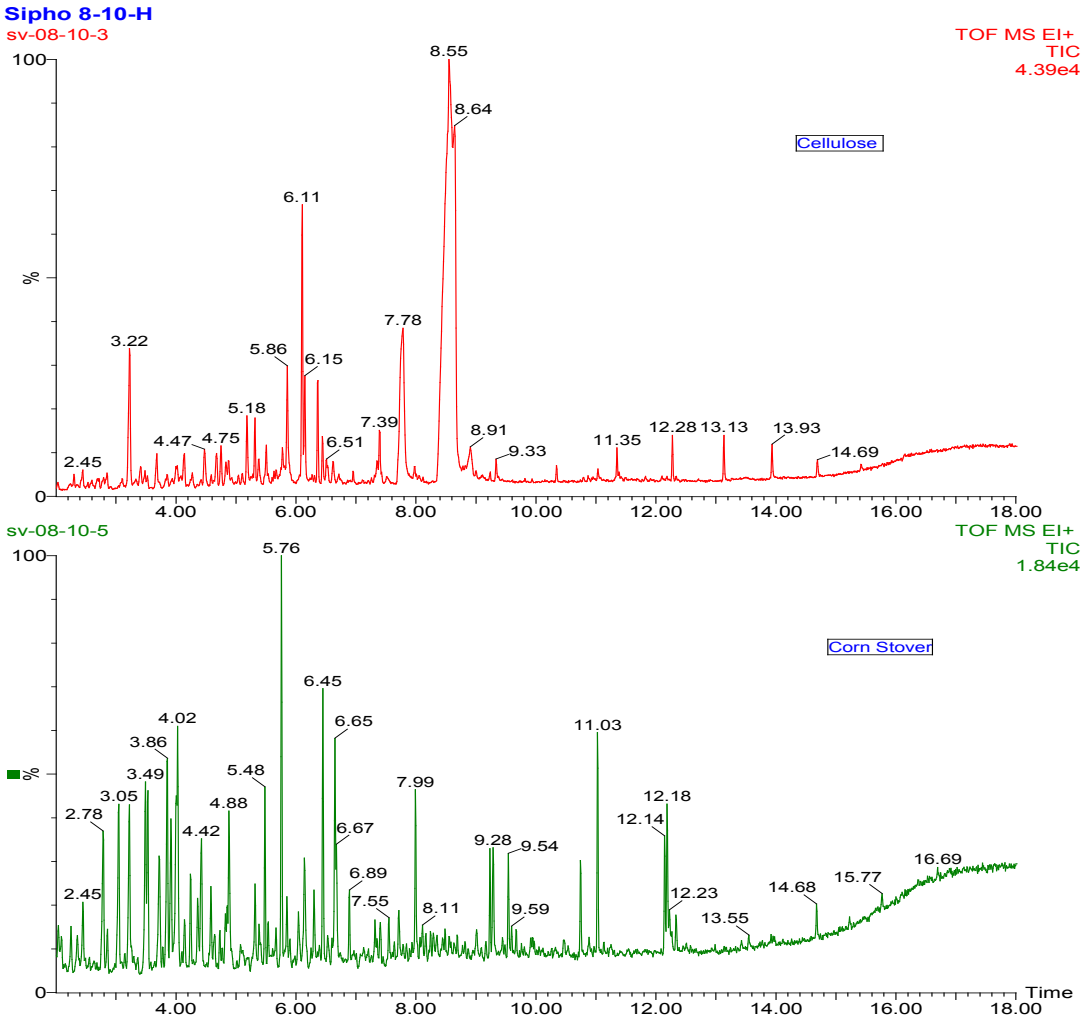

Figure 44. GC trace from analysis of RTVPcrude sample after high presure reaction at 300°C using cellulose and corn stover in methanol

Having looked at the previous reaction results, the next phase added hydrogen to increase selectivity towards phenols and aromatic compounds, which also minimized some of the

side reaction occurring during reaction. In these experiments, additional compounds do form due to thermal degradation. So by hydrogenating, the reaction pathway could be impacted to eliminate products from side reactions and thermally induced reactions. Typical hydrogenation reaction at low temperature and at low reaction pressure require solid catalysts (e.g. Nickel and Platinum) to initiate and catalyze the reaction. Under supercritical conditions solvent properties change to favour acidic catalytic effects, such that at 300°C and high pressure above 3000 psi reaction pressure hydrogenation could have an impact the reaction pathway without a catalyst. The reaction was performed in a stainless steel high pressure one liter reactor by first adding hydrogen at room temperature following purging the system with Helium. Initial hydrogen system pressure ranged from 100 to 600 psig. Product samples obtained from the experiments were then centrifuged and rotavaped prior to analyzing with a GCMS. Both cellulose and corn stover were studied; however, current analysis will discuss results from the corn stover experiments. Figure 45 below is a GCMS plot indicating possible components from a corn stover-Methanol-H_2 reaction at 300°C.

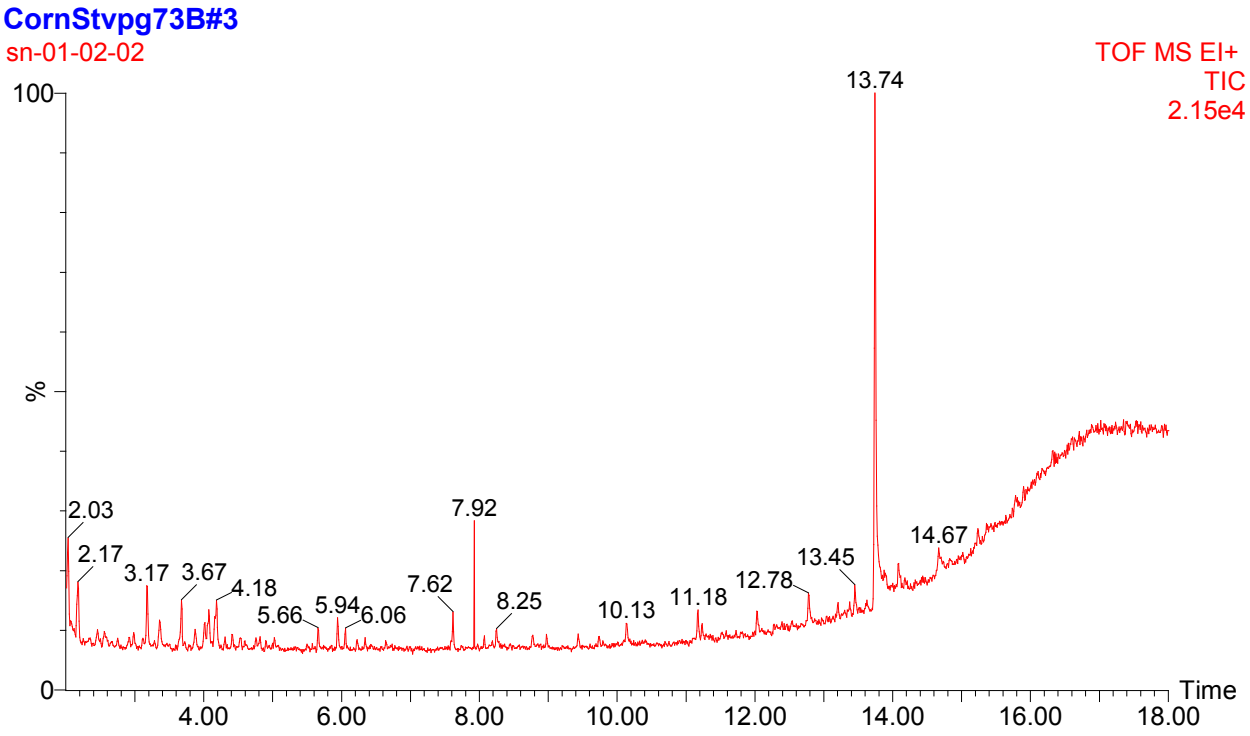

Figure 45. GC trace from analysis product sampler from a corn stover-MeOH-hydrogenation experiment at 300°C, initial H_2 pressure at 600 psig

Data obtained in Figure 44 - 45 were collected using the same scanning range and ramp program. When comparing sample corn stover results in each Figure 4, it has two major components at 7.92 and 13.74 peaks. On the other hand, the corn stover sample on Figure 44 suggested multiple major components. Preliminary analysis of the major peaks in Figure 45 suggested that 13.74 was associated with following compounds, 4,4'-Dimethoxy-2,2'-dimethylbiphenyl (Figure 46), Benzaldehyde, 4-methoxy-3-(4-methylphenoxy) and Benzo [1,2-b:5,4-b'] difuran-4, 8-dione, 5-methyl—2-(1-methyethyl). Whereas, for the peak at 7.92 the

library suggested that this was methlythelene chloride, possibly from contamination in the syringe or during sample preparation. Analysis of some of the minor peaks such as at 5.95 suggested presence of phenol-4-ethyl-2-methoxy- and Benzene-1,4-dimethoxy-2-methyl. At peak 2.032, the suggested compound was butanoic acid- 2-hydroxy-methyl ester. Furthermore, analysis at peak 1.774 suggested that these compounds: benzene 1-methoxy-2-(methoxymethyl) and tetramethyl silicate. The tetramethyl silicate may have resulted from the contamination from reactor high pressure sealing material.

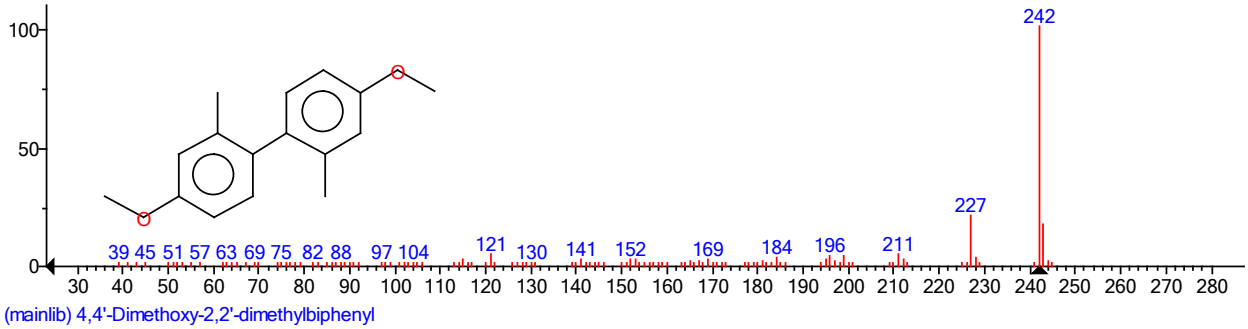

Figure 46. An example of a component at peak 13.74 suggested using a GCMS Nist 2008 library from a Corn Stover-MeOH-H_2 reaction at 300 ºC

Effect of sulfolate during a cellulose-methanol reaction:

The extent of a reaction for a biomass feedstock during a high temperature and pressure reaction can be influenced by cosolvents. This was observed from previous reports for the CO_2-methanol, water-methanol, CO_2-methanol-water experiments on cellulose and corn stover. Analyses of these systems with cosolvents as opposed to reactions with only methanol suggested CO_2 alone did not yield any significant changes. However, a combined system with CO_2-methanol-water yielded slightly higher sugar components when the sample was analyzed compared to the methanol only system. Despite the use of these cosolvents, thermal decomposition was still noticeable. To minimize these concerns, several cosolvents were tested, including sulfolane.

Several studies in other laboratories have shown that under a variety of conditions, sulfolane can increase yields of levoglucosan, while suppressing side reactions due to thermal decomposition. As discussed in previous reports, levogluosan forms in addition to other components during the methanol-cellulose reaction. Since sulfolane can reduce side reactions, and impact the levoglucosan yields, it was tested during a methanol-cellulose-sulfolane experiment at 300ºC. The product sample was then prepared for GCMS analysis. Results for this analysis are shown in Figure 47. As a comparison, the baseline study with methanol only was included.

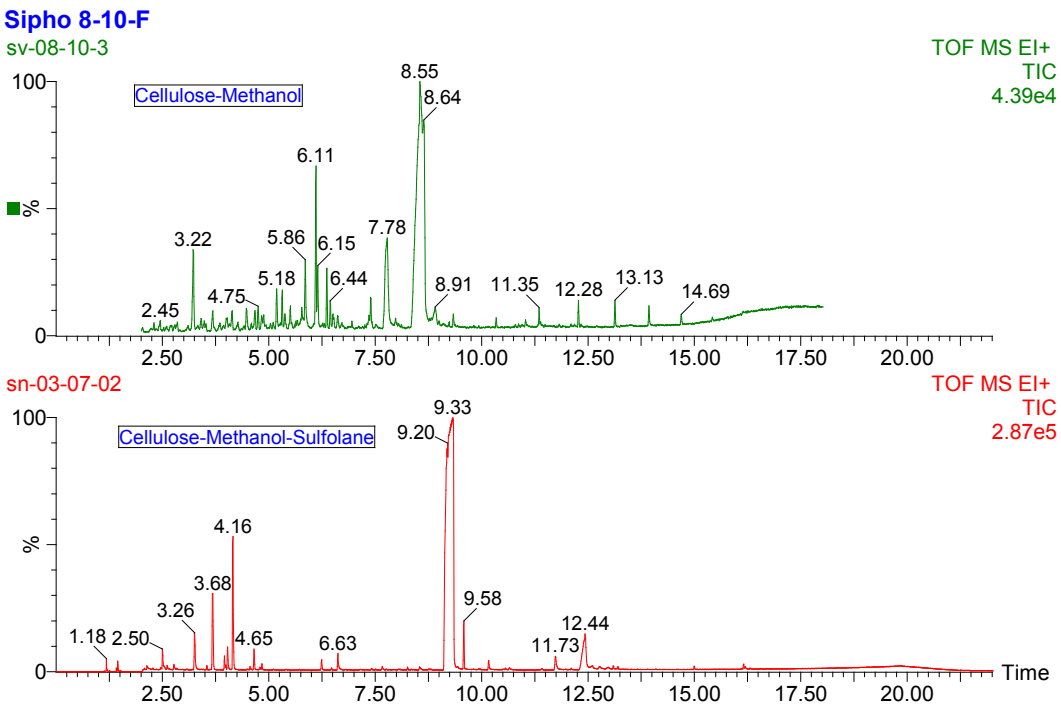

Figure 47. GCMS Chromatogram for Cellulose/MeOH vs. Cellulose/MeOH /Sulfolane at 300°C

There are several major and minor peaks in each plot associated with specific compounds suggested in Table 9. For the methanol only system the major peak was 8.55 associated with a'-D-Ribopyranoside, methyl; whereas, the 9.33 for the second system was associated with sulfolane. Levoglucosan was at 7.78 for methanol only system, but at 11.73 for the case with sulfolane. Data in Figure 47 and Table 9 showed that the system with sulfolane had fewer peaks. This was more visible for the peak range 5 to 7.5. Around peak 6, both systems gave furan derivatives. In addition, both systems consisted of other sugar components including D-Allose and D-Galactose. In the presence of sulfolane, pentanoic acid was suggested. Although acetic acid, hexanoic acid, malonic acid and heptanoic acid were not observed, these were suggested in the methanol only system. Common in both systems was a variety of organic acid methyl esters.

Since effect of sulfolane was noticeable in Figure 47 and Table 9, similar experiments were extended to include corn stover-methanol-sulfolane, water-sulfolane-methanol (cellulose & cornstover), and sugar-methanol-sulfolane. Analysis of those systems is continuing, but will form part of the final report.

Table 9. GCMS Chromatogram for Cellulose/MeOH vs. Cellulose/MeOH /Sulfolane at 300°C (continued on next page)

Cellulose-MeOH 300C				Cellulose-MeOH-Sulfolane 300C			
GC peaks from EI, CH4-CI, and NH3-CI data	**Compound m/z based on EI and CI data**	**Compound Structural Formula**	**Corresponding Compound from GCMS database**	**GC peaks from EI, CH4-CI, and NH3-CI data**	**Compound m/z based on EI and CI data**	**Compound Structural Formula**	**Corresponding Compound from GCMS database**
3.224	112	$C_6H_8O_2$, C_8H_{16}, $C_7H_{12}O$	(2-hydroxy-3-methyl-2-cyclopenten-1-one, 1,4-dimethylcyclohexane, 3 methylcyclohexanone)	2.5; 2.916	72; 154	C_4H_8O;$C_8H_{10}OS$	Propanal, 2-Methyl-,Benzene, [methylsulfinyl)methyl]
3.224	154	$C_{10}H_{18}O$	5-methyl-2-1 Cyclohexanone	3.259	104; 76	$C_4H_8O_3$; $C_3H_8O_2$	Propanoic acid, hydroxy-methy; ester, (+-); 1,2-propanediol (propylene glycol)
3.224	172	$C_{10}H_{20}O_2$	Acetic acid	3.684	92	C_7H_8	Toluene
5.183	126	$C_6H_6O_7$	5-hydroxymethyl-2-furancarboxaldehyde	4	118	$C_6H_{14}O_2$	2,2-dimethoxybutane
5.858	116	$C_6H_{12}O_2$	Hexanoic acid	4.034	106	$C_4H_{10}O_3$	Glycolaldehyde dimethyl acetal
5.858	164	$C_6H_{12}O_5$	Methyl-a-D arabinopyranoside, a'methyl xyloside, 2-deoxy-d-glucose	4.159	120	$C_5H_{12}O_3$	Ethane, 1,1,2-trimethoxy-
6.108	176	$C_7H_{12}O_5$	Methyl (3R)-trans-3-hydroxy-5-hydroxtethyltetra-hydrofuran-3-carboxylate	6.242	142	$C_7H_{10}O_3$	2-Furanethanol, Beta-methoxy-(S)-
6.149	164	$C_6H_{12}O_5$	a'-Methyl xyloside, Methyl-a'-D-arabinopyranoside	6.626	130	$C_6H_{10}O_3$	Pentanoic acid, (Methyl levulinate)

Table 1 (continued). GCMS Chromatogram for Cellulose/MeOH vs. Cellulose/MeOH /Sulfolane at 300°C

Cellulose-MeOH 300C				Cellulose-MeOH-Sulfolane 300C			
GC peaks from EI, CH4-CI, and NH3-CI data	**Compound m/z based on EI and CI data**	**Compound Structural Formula**	**Corresponding Compound from GCMS database**	**GC peaks from EI, CH4-CI, and NH3-CI data**	**Compound m/z based on EI and CI data**	**Compound Structural Formula**	**Corresponding Compound from GCMS database**
7.783	130	$C_7H_{14}O_2$	Heptanoic acid	9.326	120	$C_4H_8O_2S$	Sulfolane(2,3,4,5-tetrahydrothiophene-1,1-dioxide
7.783	162	$C_6H_{10}O_5$	Levoglucosan	9.58	156	$C_6H_4O_3S$	Thiophene-2-carboxylic acid, 5-formyl-
7.783	180	$C_8H_{14}O_6$	D-Allose	10.17	160	$C_6H_8O_3S$	2(5H)-Furanone,4-(mercaptomethyl)-3-methoxy-
8.55	164	$C_6H_{12}O_5$	a'-D-Ribopyranoside, methyl	11.73	180; 162	$C_6H_{12}O_6$;$C_6H_{10}O_5$	D-Allose; Levoglucosan
8.55	180	$C_6H_{12}O_6$	D-Galactose	11.82;.13.15	370 – 592	$C_{16}H_{30}O_4Si_3$, $C_{16}H_{48}O_8Si_8$	Benzoic acid, 2,6-bis[(trimethylsilyl)oxy]-trimethyl ester; Cyclooactasiloxane, hexadecamethyl-
8.55	194	$C_7H_{14}O_6$	Methyl a'-d-galactopyranoside	12.435	194	$C_{11}H_{22}O_2$	alpha-D-Glucopyranoside, methyl (or Beta-D Glucopyranoside)
9.333	186	$C_{11}H_{22}O_2$	Decanoic acid, methyl ester	12.427	194	$C_7H_{14}O_6$	alpha-D-Glucopyranoside, methyl (or Beta-D Glucopyranoside)
9.333	186	$C_9H_{18}O_2Si$	3-hydroxy-3-(trimethylsilyl)cyclohexanone	11.82;.13.15,17.211	370 – 592	$C_{16}H_{30}O_4Si_3$, $C_{16}H_{48}O_8Si_8$	Benzoic acid, 2,6-bis[(trimethylsilyl)oxy]-trimethyl ester; Cyclooactasiloxane, hexadecamethyl-
9.333	186	$C_8H_{10}O_5$	Dimethylester of (2-oxopropylidene) malonic acid	14.994	270	$C_{17}H_{34}O_2$	Hexadecanoic acid, methyl ester (Palmitic acid, methyl ester)
10.342 - 14.693	370 – 592	$C_{16}H_{30}O_4Si_3$, $C_{16}H_{48}O_8Si_8$	Benzoic acid, 2,6-bis[(trimethylsilyl)oxy]-trimethyl ester; Cyclooactasiloxane, hexadecamethyl-	16.31,16.152	298; 296	$C_{19}H_{36}O_2$; $C_{19}H_{36}O_2$	Heptadecanoic acid, 10 methyl-, methyl ester;11-Octadecenoic acid, methyl ester, (oleic acid, methyl ester or 9-Octadecenoic acid, methyl ester),

3. **Explanation of Variance**: This part of the overall effort is now finished according to planned schedule. All milestones completed.

4. **Plans for Next Quarter**: None. Project has reached termination per Grant Agreement.

Task C - Supercritical Extraction/Separation Systems Research

1. **Planned Activities**:
   The oil extraction study using a batch reactor system was completed during the previous reports and a manuscript is being prepared for submission to the Journal of the American Oil Chemists' Society (JAOCS). A plan is underway to transfer all knowledge gained from the batch and have been incorporated into the experimental plan for oil/protein extraction using a continuous reactor. Currently in this report, the goal was to set up and develop separation techniques using thin layer chromatography (TLC)followed by separating using flash chromatography. Samples separated included products from sugar/water reactions at 200^{o}C, methanol-cellulose and corn stover-methanol reactions. Future studies will eventually include separation methods using membranes.

2. **Actual Accomplishments**:

   Recently completed effort under Task C from previous reports

   Report 14, April 30, 2010
   This report focused on separating product samples from cellulose-methanol reactions at high pressures. The separation was performed using vacuum distillation Kugel Rohr equipment. Separated samples were then analyzed by NMR and GCMS.
   In addition, further development of the experimental plans of oil and protein extraction experiments from soybean flakes and extruded soybeans using a central composite design method were continued, followed by preliminary qualitative and statistical quantitative analysis.

   Report 15, July 30, 2010
   Data presentation of the preliminary data findings from subcritical oil/protein extraction of soybeans at May 2010 AOCS conference. This was followed by further assessment of the statistical data for each system of extruded flakes and soybean flakes. The study addressed continuing challenges with the ANOVA and surface models.

   Report 16, October 30, 2010
   Final data assessment, statistical parameter corrections and surface model re-evaluation completed. Also, we began a manuscript that is being prepared for submission to the Journal of the American Chemical Society. In addition, we initiated developing future experimental plans for oil/protein extraction from soybeans for the flow reactor.

   DOE Report 17, January 30, 2011
   Report 17 under Task C introduced the use of thin layer chromatograph plates (TLC) in assessing separation of polar vs. non-polar compounds from our product mixture by silica column flash chromatography techniques. The TLC method was tested on three samples taken from a batch reactor which included: a corn stover-methanol reaction in hydrogen at 300^{o}C, a 5% sugar-methanol reaction at 200^{o}C, and a 5% sugar-water

reaction at 200°C. All these samples had reacted in a one liter high pressure batch reactor. Various TLC solvents were tested at different polar concentrations with reference to silica plates, i.e. a 10% acetic acid in ethyl acetate, 20% acetic acid in ethyl acetate, 80% ethyl acetate in hexane, 50% ethyl acetate in hexane, and 20% ethyl acetate in hexane.

DOE Report, 18 January 30, 2011

This report under Task C focused on the analysis of 5% sugar-water solution samples first separated by TLC method and then through silica column flash chromatography. Separation through the column seemed to minimize some of the peaks by trapping less polar compounds in relation to silica based on the chosen solvent. On the other hand a less complicated chromatogram was obtained after the separation step.

Paper submitted for review to the "Journal of the American Oil Chemists' Society"

Aqueous Extraction of Oil and Protein from Soybeans with Subcritical Water

by

S.C. Ndlela[1], J.M.L.N. de Moura[2,3], N. K. Olson[1], and L.A. Johnson[*2,3]

[1]Iowa Energy Center-BECON
Nevada, IA 502011

[2]Center for Crops Utilization Research
Iowa State University
Ames, IA 50011-1061

[3]Department of Food Science and Human Nutrition
Iowa State University
Ames, IA 50011-1061

* To whom correspondence should be addressed at:
Center for Crops Utilization Research
1041 Food Sciences Building
Iowa State University
Ames, IA 50011-1061
Phone: 515-294-0160
Fax: 515-294-6261
E-mail: ljohson@iastate.edu

Abstract

Aqueous extraction using subcritical water is an environmentally friendly alternative to extracting oil and protein from oilseeds with flammable organic solvents. The effects of solids-to-liquid ratio (1:3.3 to 1:11.7), temperature (66 to 234 °C), and extraction time (13 to 47 min) were evaluated on the extraction of oil and protein from soybean flakes and from extruded soybeans flakes with subcritical water. A central composite design (23) with three center points and six axial points was used. Subcritical water extractions were carried out in a 1-L high-pressure stainless-steel batch reactor with constant stirring (300 rpm) at 5 to 560 psi. In general, oil extraction was greater for extruded soybean flakes than with soybean flakes. Most complete oil extraction for extruded soybean flakes was achieved at around 150 °C and was not affected by solids-to-liquid ratio, while oil extraction from soybean flakes was most complete at 66 °C and low solids-to-liquid ratio (1:11.7). Protein extraction yields from flakes were generally greater than from extruded flakes. Protein extraction yields from extruded flakes increased as temperature increased and solids-to-liquid ratio decreased, while greater protein extraction yields from soybean flakes were achieved when using low temperatures and low solids-to-liquid ratio.

Key-words: Subcritical water, oil extraction, protein extraction, flaking, soybeans, extraction

Introduction

Increasing worldwide soybean production is being driven by growing demand for high quality protein to feed livestock (primarily swine and poultry) and for vegetable oils to supply food and fuel sectors [1]. Countercurrent hexane extraction has long been used to extract most of soybean oil [2]; however, increasing environmental regulations and safety concerns regarding hexane use in oilseed-crushing units [3] are driving extensive research toward environmentally friendly extraction technologies [4].

Among emerging technologies to extract oil and protein from oilseeds, enzyme-assisted aqueous extraction processing (EAEP) has been considered to be an environmentally friendly process in which oil and protein are simultaneously extracted from soybeans [4, 5]. This water- and enzyme-based technology along with mechanical treatments, such as flaking and extruding (expanding), has achieved similar levels of oil extraction as conventional hexane extraction (>97%) [8]. Despite achieving high oil extraction yields (removal from solids), however, overall free oil recovery in EAEP of soybeans ranges from 79 to 83% due to emulsified oil remaining in the skim (primarily sugar- and protein-rich) and small residual amounts of unextracted oil in the insolubles (fiber-rich fraction) [9, 10]. The mild operating conditions used in EAEP of soybeans enables production of oil with good quality and proteins with similar nutritional compositions as proteins produced by conventional extraction procedures such as soy protein concentrate (SPC) or isolate (SPI) [11, 12].

Over the past decade, interest has been increasing in using subcritical water for extraction where hot water (100 °C < T < 374 °C) under moderate pressure to maintain water in the condensed phase has been used to extract protein, essential oils, and bioactive components from a wide variety of matrices [13-18]. At subcritical conditions, the density, dielectric constant, dissociation constant, viscosity, diffusivity, electrical conductance, and solvency change [19]. At subcritical conditions, water polarity decreases thereby favoring extraction of organic bioactive components. Water ionization constant (Kw) increases with increasing temperature, making subcritical water a suitable media to catalyze hydrolytic reactions [14, 16, 18]. In addition to extracting organic components, subcritical water has been used to hydrolyze triacylglycerols into free fatty acids [20, 21] and to convert waste into valuable products [19].

The use of subcritical water to simultaneously extract oil and protein from oilseeds has not been extensively evaluated. Most of the research conducted so far has mainly focused on extraction of oil and/or protein from rice bran and to a lesser extent on extracting protein from defatted soybean meal and full-fat soy flour [14-18]. Protein extraction yields from deoiled rice bran were greater when using subcritical water conditions compared with the alkali method [14]. The effects of temperature (200-220 °C), reaction time (10-30 min), and solids-to-liquid ratio (1:5 and 2:5) were evaluated when using subcritical water to extract protein from defatted soybean meal and full-fat soy flour [16]. About 50% protein recovery was achieved relative to both starting materials when extractions were performed at 200-210 °C and 1:5 solids-to-liquid ratio for 30 min. Although full-fat soy flour has been used, no oil extraction data were reported.

Oil and protein extraction yields from soybeans when using aqueous extraction systems are greatly affected by the extent of cell wall disruption, solids-to-liquid ratio, presence or lack of enzyme during extraction and extraction time and temperature [5, 22, 23, 25]. The present study was undertaken to gain a better understanding of how these parameters affect oil and protein extractions from soybeans under subcritical extraction conditions.

Materials and Methods

Soybeans

Full-fat soybean flakes were prepared from variety 92M91-N201 soybeans (Pioneer, a DuPont Business, Johnston, IA, USA) harvested in 2008.

Processing Methods

Soybean Flaking

The soybeans were cracked into 4-6 pieces by using a corrugated roller mill (model 10X12SGL, Ferrell-Ross, Oklahoma City, OK, USA) and the hulls were removed from the meats (cotyledons) by aspirating with a multi-aspirator (Kice, Wichita, KS, USA). The meats were conditioned at 60 °C to make them plastic for flaking by using a triple-deck seed conditioner (French Oil Mill Machinery Co., Piqua, OH, USA) and were flaked to approximately 0.25 mm thickness by using a smooth-surface roller mill (Roskamp Mfg, Inc., Waterloo, IA, USA). The soybean flakes contained 20.3% oil (as is), 35.9% protein (as is), and 7.6% moisture (as is).

Extruding Full-fat Soybean Flakes

The moisture content of the flakes was increased to 15% by spraying water onto the flakes while mixing in a Gilson mixer (model 59016A, St. Joseph, MO, USA). The moistened full-fat soybean flakes were extruded/expanded by using a twin-screw extruder (ZSE 27-mm diameter; American Leistritz Extruders, Somerville, NJ, USA). High-shear geometry screws were used in co-rotational orientation at 90 rpm screw speed. The extruder barrel (1080 mm length) was composed of ten heating blocks that were set for the temperature profile 30-70-100-100-100-100-100-100-100-100 °C. The extruder was manually fed to achieve 10.5 kg/h output rate of extruded flakes. The collets were cooled to room temperature, placed in polyethylene bags, and stored in a cold room at 4 °C until extracted. The extruded soybean flakes contained 22.7% oil (as is), 88.7% solids (as is) and 35.3% protein (as is), and 11.3% moisture (as is).

Subcritical Water Extraction

Oil and protein extractions from flakes and extruded soybean flakes were carried out in a high-pressure 316 stainless-steel batch reactor as shown in Figure 47 (High-Pressure Equipment Co., Erie, PA, USA). The reactor, pressure rated for 35,000 psi, consisted of 1 L internal volume, heated by an electrical jacket, two J thermocouples (TC1 and TC2), an analog pressure gauge (Pa), digital pressure gauge (Pb), and a MagneDrive stirring assembly (Autoclave Engineers, Supercritical Fluid Technologies Inc., Newark, Delaware, USA).

Figure 47. High-pressure 316 stainless-steel batch reactor

Soybean flakes and extruded soybeans flakes were dispersed into deionized water to achieve solids-to-liquid ratios ranging from 1:3.3 to 1:11.7 (Table 10). The amount of slurry loaded into the reactor was determined based on the minimum amount needed to achieve adequate stirring (400 g) and the maximum amount that would fit into the reactor without plugging the vent lines located just above the slurry level. Slurries containing approximately 675 soybean flakes and 775 g extruded soybean flakes were loaded into the reactor at room temperature (extruded flakes are denser than flakes). A leak test was performed with helium at 100 psi. In order to degas the mixture prior to starting the experiments, the reactor was purged with helium at 100 psi and maintained for 6 min at 100 psi after which it was vented. The degassing cycle was repeated five times while stirring the slurry at 300 rpm. Extraction experiments were performed at temperatures ranging from 66 to 234 °C and extraction time ranging from 13.2 to 46.8 min (Table 10). The slurries were stirred at 300 rpm and the resulting pressure varied from 6 to 560 psi. The reactor heating cycle ranged from 40 min (66 °C) to 240 min (234 °C) while the cooling time from the target temperature to 70 °C ranged from 120 min (100 °C) to 480 min (234 °C). The system was cooled to 70 °C to ensure safe handling of the product before opening the reactor to remove the slurry.

Following extraction, the slurry was centrifuged at 3000 x *g* (20 min at 25 °C) to remove insolubles from the liquid phase (Fig. 48). Three phase layers were observed after centrifuging: an insoluble fraction (fiber-rich fraction), a skim fraction (protein- and sugar-rich fraction), and a cream fraction (oil-rich emulsion). After removing the insoluble fraction, the liquid phase was placed into a separatory funnel (2 L) and allowed to settle overnight at 4 °C. During settling, the liquid phase separated into two fractions (skim fraction and cream + free oil fraction). Since oil

and protein extractabilities were the focus of this study, only the insoluble fraction was analyzed to determine mass balances for oil and protein extraction from the solids.

Table 10. Variables and levels evaluated in the experimental design to model oil and protein extraction from extruded soybean flakes and soybean flakes

	Coded levels			Uncoded Levels		
Treatments	Solids-to-liquid ratio (X1)	Temperature (°C) – (X2)	Time (min) (X3)	Solids-to-liquid ratio (X1)	Temperature (°C) – (X2)	Time (min) (X3)
1	1	1	1	1:10	200	40
2	-1	1	1	1:5	200	40
3	1	-1	1	1:10	100	40
4	1	1	-1	1:10	200	20
5	-1	-1	1	1:5	100	40
6	-1	1	-1	1:5	200	20
7	1	-1	-1	1:10	100	20
8	-1	-1	-1	1:5	100	20
9	0	0	0	1:7.5	150	30
10	0	0	0	1:7.5	150	30
11	0	0	0	1:7.5	150	30
12	1.68	0	0	1:11.7	150	30
13	-1.68	0	0	1:3.3	150	30
14	0	1.68	0	1:7.5	234	30
15	0	-1.68	0	1:7.5	66	30
16	0	0	1.68	1:7.5	150	46.8
17	0	0	-1.68	1:7.5	150	13.2

Complete 2^3 factorial design parameters, with three independent variables in two levels, three repetitions in the central point and six repetitions in the axial points

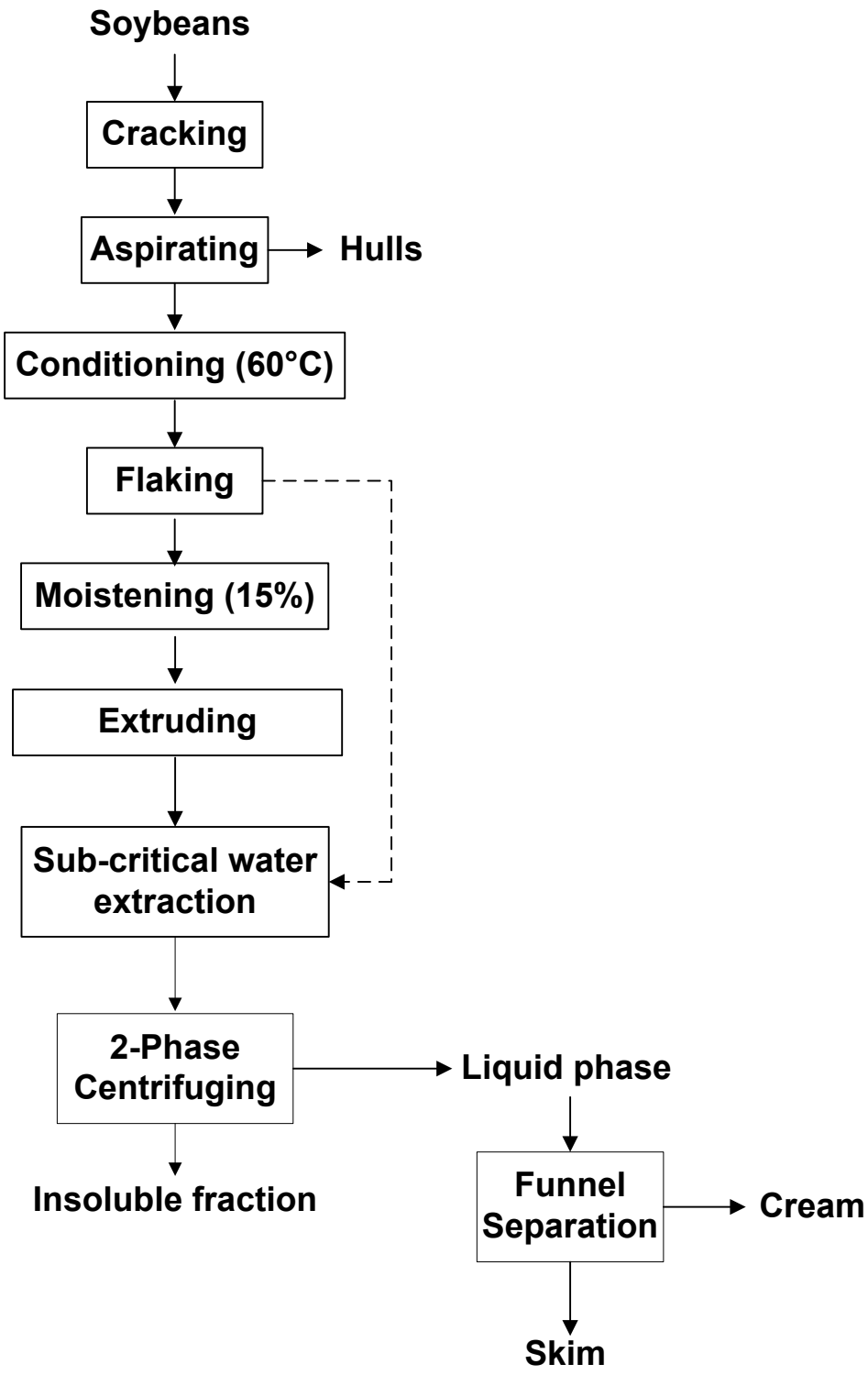

Figure 48. Process flow diagram for subcritical extraction from flaked and extruded soybeans

Oil, Protein, and Solids Recoveries

Analyses of oil and protein were carried out on the insoluble and starting materials (soybean flakes and extruded soybean flakes). Total oil content was determined by using the acid hydrolysis Mojonnier method (AOCS method 922.06) and protein content was determined by using the Dumas combustion method and the N conversion factor of 6.25 (vario MAXCN Elementary Analyses system Gmbh, Hanau, Germany). Extraction yields were expressed as percentages of each component in the insoluble fraction relative to the initial amount in the starting material. All chemical analyses were performed in duplicate.

Experimental Design and Statistical Analysis

In order to optimize for the best combination of solids-to-liquid ratio, temperature and reaction time for oil and protein extraction, a complete 2^3 factorial design of the central rotational type was established, with three central points and six axial points, based on Response Surface Methodology [24]. The effects of solids-to-liquid ratio (1:3.3 - 1:11.7), temperature (66 - 234 °C), and extraction time (13.2 - 46.8 min) on the extraction of oil and protein from soybean flakes and extruded soybeans flakes by using subcritical water treatment were evaluated. The independent variables (solids-to-liquid ratio, temperature, and extraction time) were evaluated according to coded levels ($-\alpha$, -1, 0, $+1$, $+\alpha$). Coded and uncoded levels and their corresponding independent variables are shown in Table 1. Dependent variables (i.e., evaluated responses) were oil and protein extraction yields for soybean flakes and extruded soybean flakes. Data were analyzed by using Statistica version 8.0 software. The significance of each model was tested by Analysis of Variance (ANOVA).

Results and Discussion

Oil and Protein Extraction Yields

Oil and protein extractabilities from soybeans are significantly affected by mechanical treatments such as grinding, flaking, extruding, and combination of these treatments [22, 23, 25]. The combination of flaking and extrusion is more effective in extracting oil when using aqueous extraction of soybeans due to more complete cell disruption that facilitates water penetration into the matrix, releasing soluble and insoluble components into the external environment [22, 23, 25]. In Table 11, the effects of extent of cell wall disruption on oil and protein extraction from soybeans flakes and extruded soybean flakes under different subcritical water extraction conditions are presented. Regardless of treatment applied, oil extraction yields were significantly improved when using extruded soybean flakes (38 - 84%) compared with soybean flakes (4 - 50%).

Campbell and Glatz [25] reported nearly complete cellular disruption of soybeans cotyledons was achieved when comminuted by extrusion, in relation to milling, flaking, and flaking followed by milling. Our results are in agreement with those of Lamsal at al. [21] in which oil extractability improved from 46 to 71% when combining flaking and extruding of soybeans compared to flaking alone. The highest oil extraction yields from soybean flakes (50%) and from extruded soybean flakes (84%) were achieved when extracting at 1:10 solids-to-liquid ratio and 100 °C for 20 min and at 1:11.7 solids-to-liquid ratio and 150 °C for 30 min, respectively. Lowest oil extraction yields for both soybean flakes (4%) and extruded soybean flakes (38%) were observed at 1:7.5 solids-to-liquid ratio and 234 °C for 30 min.

Temperature can affect extraction due to enhanced solute solubility and diffusion into the solvent bulk [26]. In some cases however, temperature has been associated with reductions in oil and protein extractions during aqueous extraction of soybeans [16]. Reduced extractability is likely a consequence of protein thermal denaturation [27], which affects both oil and protein extractions to different extents.

Table 11. Experimental design for optimizing oil and protein extraction from soybean flakes and extruded soybean flakes

Treatments	Solids-to-liquid ratio (X_1)	Temperature (°C) – (X_2)	Time (min) (X_3)	Oil extraction (%) EF	Oil extraction (%) F	Protein extraction (%) EF	Protein extraction (%) F
1	1:10	200	40	74.7	13.4	65.7	64.8
2	1:5	200	40	72.4	37.9	53.6	56.1
3	1:10	100	40	69.5	42.7	37.6	71.9
4	1:10	200	20	79.6	22.0	61.7	65.3
5	1:5	100	40	53.4	16.3	34.1	33.1
6	1:5	200	20	80.3	31.3	56.6	57.1
7	1:10	100	20	61.3	50.2	36.4	65.0
8	1:5	100	20	56.8	21.2	29.7	30.8
9	1:7.5	150	30	64.6	7.1	49.2	45.5
10	1:7.5	150	30	68.1	12.3	49.6	47.7
11	1:7.5	150	30	83.1	7.08	51.7	46.3
12	1:11.7	150	30	83.9	17.9	59.9	55.5
13	1:3.3	150	30	62.5	45.1	40.9	55.0
14	1:7.5	234	30	38.2	4.2	73.1	67.8
15	1:7.5	66	30	49.0	44.0	26.6	53.2
16	1:7.5	150	47	64.2	39.9	52.5	52.8
17	1:7.5	150	13	66.0	19.8	49.2	46.4

Heating favors protein-lipid interactions in which denatured protein is likely to sequester oil by exposing hydrophobic amino acids [23]. Since soybean flakes and extruded soybean flakes contain proteins with different solubilities [28] due to protein denaturation caused by the extrusion treatment, one would expect lower protein extractability when using extruded soybean flakes compared with soybean flakes. Protein extraction yields from soybean flakes and from extruded soybean flakes ranged from 33 to 72% and 27 to 73%, respectively. In general, extruded soybeans flakes had similar or slightly higher protein extractability when using water temperatures >150 °C. However, an opposite effect was observed when using temperatures <100 °C, where protein denaturation reduced protein solubility adversely affecting extraction yields. These results suggested that using temperatures >150 °C likely compensated for the reduced protein solubility due to extrusion treatment. High protein extraction yields of 68 and 73% were achieved when extracting soybean flakes and extruded soybean flakes, respectively, at 234 °C, which was the highest temperature evaluated and produced the lowest oil extraction yields for both soybean flakes and extruded soybean flakes. Although parameters that favor protein extractability also usually favor oil extraction, an opposite trend was observed at the highest temperature, which suggested some oil binding by unextracted protein. The use of subcritical water to extract protein from raw and deoiled soybean meal was previously reported by Watchararuji et al. [16]. In that study, 50% protein recovery was achieved when extracting at 210 °C, 1:5 solids-to-liquid ratio, and 30 min residence time although oil extractability was not reported.

Statistical Analysis

Estimated regression models and coefficients of determination for oil and protein extractions from soybean flakes and extruded soybean flakes are shown in Table 12. Only parameters significant at $p < 0.05$ were used in the regression models. Coefficients of determination (R^2) for models of oil extraction from soybean flakes and extruded soybean flakes were 0.27 and 0.38, respectively; while coefficients for models of protein extraction from soybean flakes and extruded soybean flakes were 0.63 and 0.96, respectively. While satisfactory coefficients of determination were achieved for the models predicting protein extraction, low coefficients for oil extraction suggested that other sources of variation were not accounted by the models.

The effects of soybean moisture content before flaking and storage time of the beans and flakes before extruding have been associated with phospholipase D activity [9, 29-31], which could increase emulsion stability and affect the separation of extracted material before and after centrifugation. Our material was prepared and used over a two- to three-month period, which might have allowed phospholipase D activity, a factor not accounted for by the models.

Another source of variation that may have impacted the oil extraction models was the heating/cooling system of the reactor. Typically, fast heating and fast cooling are preferred for these types of experiments under subcritical conditions to avoid thermal degradation of the reactants and for better evaluation of reaction time necessary to achieve the desired extraction yields. In order to follow our experimental design parameters (reaction time and temperature), heating the reactor required 0.67 h (25 to 66 °C) to 4 h (25 to 234 °C) followed by cooling 2 h (100 to 70 °C) to 8 h (234 to 70 °C), which could have confounded measuring effects of reaction time on extraction yields. In some cases, the long cooling times surpassed the time to conduct the extraction. These challenges with heating and cooling could be eliminated when transitioning from the current batch system to a continuous reactor. Although the real effect of

residence time was not determined, the remaining parameters (temperature and solids-to-liquid ratio) provided useful information on their effects on extraction yields.

Table 13, shows the analysis of variances of the models. For all cases, regression was significant ($F_{calculate}d/F_{table}$). Except for the models for oil and protein extraction from soybean flakes, the F-tests for the lack of fit were not statistically significant ($F_{calculated}/F_{table}$) indicating that the models do not show lack of fit and thus can be used for prediction in the range of the parameters evaluated. The F-test for lack of fit was statistically significant for oil and protein extraction from soybean flakes ($F_{calculated} > F_{table}$), which was associated with the pure error (extremely low) due to the low degrees of freedom (2).

Table 12. Estimated regression models and coefficient of determination (R^2) for oil and protein extraction yields from soybean flakes and extruded soybean flakes

Estimated Regression Models	R^2
% Estimated oil extraction from extruded soybean flakes = 73.18 – 8.54 X_2^2	0.38
% Estimated oil extraction from soybean flakes = 25.43 - 11.15 $X_1{}^*X_2$	0.27
% Estimated protein extraction from extruded soybean flakes = 48.70 + 4.33 X_1 +13.02 X_2	0.96
% Estimated protein extraction from soybean flakes = 53.78 + 6.65 X_1 + 4.91 X_2 – 7.01 $X_1{}^*X_2$	0.63

X_1 = coded level corresponding to SLR; X_2 = coded level corresponding to temperature, X_3 = coded level corresponding to time

Table 13. Analysis of variances of estimated regression models

Oil extraction from extruded soybean flakes

Source of variation	Sum of squares	Degrees of freedom	Mean squares	F-test
Regression	948	1	948	**9.30[a]**
Residual	1531	15	102	
Lack of fit	1337	13	103	1.06[b]
Pure error	193	2	97	
Total	2479			

Values in bold are statistically meaningful (P <0.05). Coefficient of determination: R^2=0.38; $F_{0.95\text{-}1,\ 15}$=4.54; $F_{0.95\text{-}13,2}$=19.42

Table 13 (Continued). Analysis of variances of estimated regression models

Oil extraction from soybean flakes

Source of variation	Sum of squares	Degrees of freedom	Mean squares	F-test
Regression	995	1	995	**5.55[a]**
Residual	2690	15	179	
Lack of fit	2672	13	206	**22.71[b]**
Pure error	18	2	9	
Total	3685			

Values in bold are statistically meaningful (P <0.05). Coefficient of determination: R^2=0.27; $F_{0.95\text{-}1,\ 15}$=4.54; $F_{0.95\text{-}13,2}$=19.42

Protein extraction from extruded soybean flakes

Source of variation	Sum of squares	Degrees of freedom	Mean squares	F-test
Regression	2573	2	1287	**162[a]**
Residual	111	14	7.90	
Lack of fit	107	12	8.90	4.73[b]
Pure error	3.77	2	1.88	
Total	2684			

Values in bold are statistically meaningful (P <0.05). Coefficient of determination: R^2=0.96; $F_{0.95\text{-}2,\ 14}$=3.74; $F_{0.95\text{-}12,2}$=19.41

Protein extraction from soybean flakes

Source of variation	Sum of squares	Degrees of freedom	Mean squares	F-test
Regression	1326	3	442	**7.44[a]**
Residual	773	13	59	
Lack of fit	770	11	70	**56.46[b]**

Pure error	2.48	2	1.24
Total	2099		

Values in bold are statistically meaningful (P <0.05). Coefficient of determination: R^2=0.63; $F_{0.95\text{-}3,13}$=3.26; $F_{0.95\text{-}11,2}$=19.405

[a] F-ratio (regression/residual), [b] F-ratio (lack of fit/pure error)

Based on the estimated regression models, response surfaces were built to express oil and protein extractions from soybean flakes and extruded soybean flakes (Figs. 48-51).

According to the estimated regression model and Figure 48 regardless the solids-to-liquid ratio used, oil extraction from extruded soybean flakes decreases when temperature gets further away from the center point (150 °C) with lower extraction values at the axial points (±1.68). According to the estimated regression model and Figure 49, highest oil extraction yields from soybean flakes are achieved at low temperature values (-1.68, 66 °C) and low solids-to-liquid ratio (+1.68, 1:11.7). Based on the estimated regression model and Figure 50, protein extraction from extruded soybean flakes is favored by increased temperature and low solids-to-liquid ratio, with higher extraction values at +1.68 for both variables (234 °C and 1:11.7 solids-to-liquid ratio). Although protein extraction yields increased at higher temperatures, the nutritional quality of the extracted protein might be adversely affected by thermal degradation. An opposite trend was observed for protein extraction from soybean flakes. According to the estimated regression model and Figure 51, highest protein extraction is achieved at low temperature (66 °C) and low solids-to-liquid ratio (1:11.7). The possibility of achieving high extractability of protein from soybean flakes at low temperature indicates the higher solubility of protein in soybean flakes compared with protein in extruded soybean flakes. Reaction time was not statistically significant, likely a consequence of the long residence time due to heating/cooling system that was used.

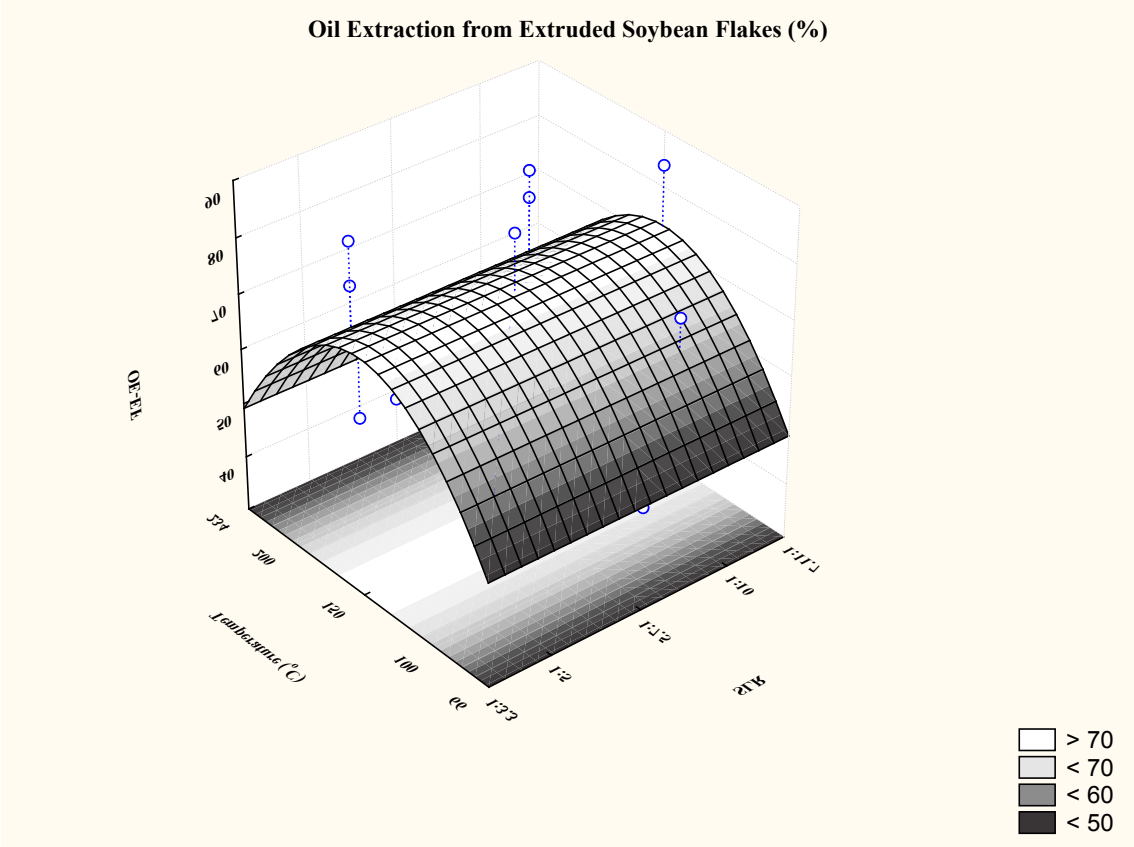

Figure 49. Effects of temperature and solids-to-liquid ratio on oil extraction from extruded soybean flakes

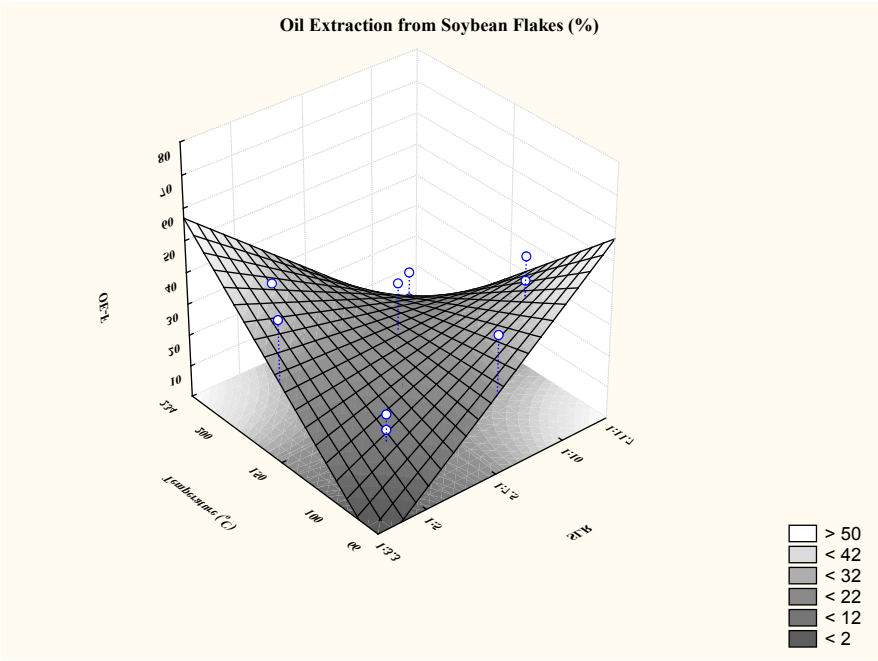

Figure 50. Effects of temperature and solids-to-liquid ratio on oil extraction from soybean flakes

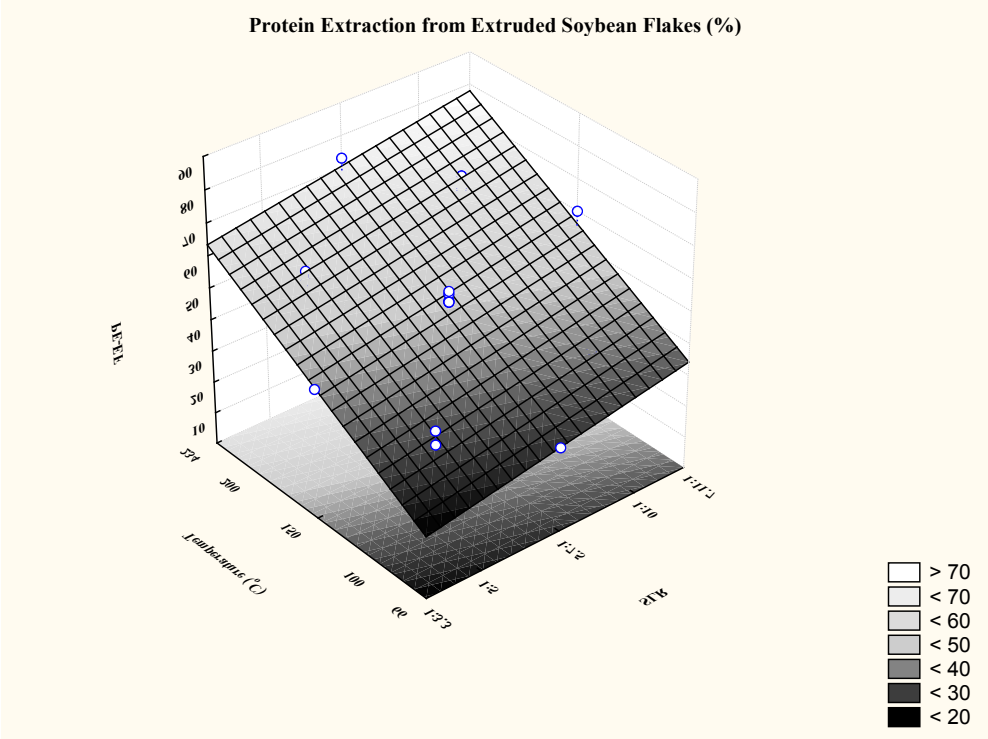

Figure 51. Effects of temperature and solids-to-liquid ratio on protein extraction from extruded soybean flakes

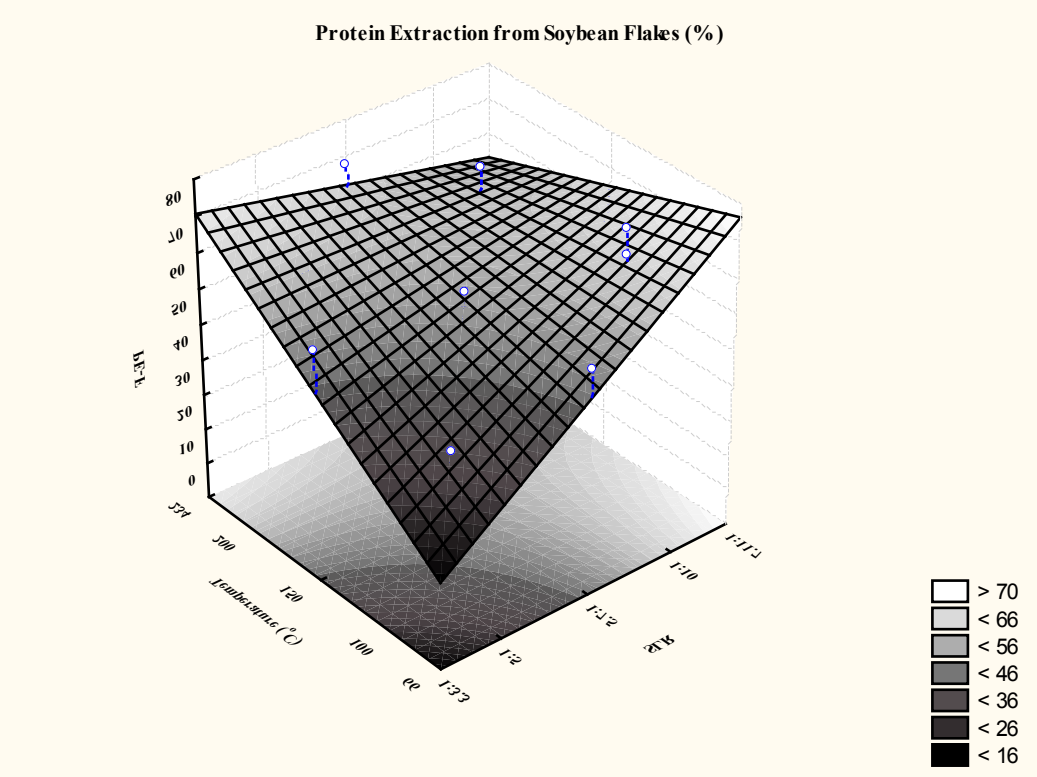

Figure 52. Effects of temperature and solids-to-liquid ratio on protein extraction from soybean flakes

Conclusions

Temperature and solids-to-liquid ratio significantly affected oil and protein extraction yields from soybean flakes and extruded soybean flakes. The economical viability of aqueous extraction of soybeans depends on both oil and protein extractabilities, therefore, conditions that favor both oil and protein extractions must be considered. Although oil extraction yields from extruded soybean flakes was not significantly affected by solids-to-liquid ratio, conditions that favor both oil and protein extraction yields are temperature around 150 °C and low solids-to-liquid ratio (1:11.7). For soybean flakes, low temperature (66 °C) and low solids-to-liquid ratio (1:11.7) favored both oil and protein extraction yields.

References

1. USDA-FAS (2007) Oilseeds: World Markets and Trade. Circular Series FOP 8-07, FOP 10-07 http://www.fas.usda.gov/oilseeds/circular/2007/October/oilseedsfull1007.pdf, http://www.fas.usda.gov/oilseeds/circular/2007/August/oilseedsfinal0807.pdf
2. Johnson LA (2008) Oil recovery from soybeans. In: Johnson LA, White PJ, Galloway R (eds) Soybeans: Chemistry, Production Processing, and Utilization. AOCS Press, Urbana, IL, pp 331-375

3. Galvin JB (1997) Toxicity data for commercial hexane and hexane isomers. In: Wan PJ, Wakelyn P J (eds) Technology and Solvents for Extracting Oilseeds and Nonpetroleum Oils. AOCS Press, Champaign, IL, pp 75-85
4. de Moura JMLN, Campbell K, Mahfuz A, Jung S, Glatz CE, Johnson LA (2008) Enzyme-assisted aqueous extraction of oil and protein from soybeans and cream de-emulsification. J Am Oil Chem Soc 85:985-995
5. de Moura JMLN, Johnson LA (2009) Two-stage countercurrent enzyme-assisted aqueous extraction processing of oil and protein from soybeans. J Am Oil Chem Soc 86:283-289
6. Stahl E, Quirin KW, Blagrove RJ (1984) Extraction of seed oils with supercritical carbon dioxide: Effect on residual proteins. J Agric Food Chem 32:938-940
7. King JW, Srinivas K (2009) Multiple unit processing using sub- and supercritical fluids. J Supercritical Fluids 47:598:610
8. de Moura JMLN, Almeida NM de, Johnson LA (2009) Scale-up of enzyme-assisted aqueous extraction processing of soybeans. J Am Oil Chem Soc 86:809-815
9. de Moura JMLN, Almeida NM de, Jung S, Johnson LA (2010) Flaking as a pretreatment for enzyme-assisted aqueous extraction processing of soybeans. J Am Oil Chem Soc 87:1507-1515
10. de Moura JMLN, Maurer D, Jung S, Johnson LA. Proof-of-concept of countercurrent two-stage enzyme-assisted aqueous extraction processing of soybeans. Submitted to J Am Oil Chem Soc
11. Maurer D, Mahfuz A, Johnson LA, Jung S (2008) Enzymatic destabilization of natural occurring soy emulsion and oil quality. 99th AOCS Annual Meeting & Expo, Seattle, Washington, USA, pp 124
12. de Almeida, NM, de Moura JMLN, and Johnson LA (2010) Functional properties of protein produced by two-stage aqueous countercurrent enzyme-assisted aqueous extraction. Abstracts pp 130. 101st Annual Meeting and Exposition of the American Oil Chemists Society, May 16-19, Phoenix, AZ
13. Teo CC, Tan SN, Yong JWH, Hew CS, Ong ES (2010) Pressurized hot water extraction (PHWE). J Chromatography A 1217:2484-2494
14. Sereewatthanawut I, Prapintip S, Watchiraruji K, Goto M, Sasaki M, Shotipruk A (2008) Extraction of protein and amino acids from deoiled rice bran by subcritical water hydrolysis. Bioresource Tech 99:555-561
15. Pourali O, Asghri FS, Yoshida H (2009) Simultaneous rice bran oil stabilitization and extraction using sub-critical water medium. J Food Eng 95:510-516
16. Watchararuji K, Goto M, Sasaki M, Shotipruck A (2008) Value-added subcritical water hydrolyate from rice bran and soybean meal. Bioresource Tech 99:6207-6213
17. Pourali O, Asghari FS, Yoshida H (2009) Sub-critical water treatment of rice bran to produce valuable materials. Food Chem 115:1-7
18. Basile A, Jimenez-Carmona MM, Clifford AA (1998) Extraction of Rosemary by superheated water. J Agric Food Chem 46:5205-5209
19. Goto M, Obuchi R, Hirose T, Sakaki T, Shibata M (2004) Hydrothermal conversion of municipal organic waste into resources. Bioresource Tech 93:279-284
20. Holliday RL, King JW, List GR (1997) Hydrolysis of vegetable oils in sub- and supercritical water. Ind Eng Chem Res 36:932-935
21. King JW, Holliday RL, List GR (1997) Hydrolysis of soybean oil in subcritical water flow reactor. Green Chem, December 261-264
22. Rosenthal A, Pyle DL, Niranjan K (1996) Aqueous and enzymatic process for edible oil extraction. Enz Microb Tech 19:402-420

23. Lamsal BP, Murphy PA, Johnson LA (2006) Flaking and extrusion as mechanical treatments for enzyme-assisted aqueous extraction of oil from soybeans. J Am Oil Chem Soc 83:973-979
24. Rodrigues MI, Iemma AF (2005) Planejamento de experimentos e otimizacao de processos: uma estrategia sequencial de planejamentos. Casa do Pao, Campinas, Brazil, pp 95-123
25. Campbell KA, Glatz CE, Johnson LA, Jung S, de Moura JMLN, Kapchie V, Murphy P (2011) Advances in aqueous extraction processing of soybeans. J Am Oil Chem Soc 88:449-465
26. Takeuchi TM, Pereira CG, Braga MEM, Marostica MR, Leal PF, Meireles MAA (2009) Low-pressure solvent extraction (solid-liquid extraction, microwave assisted, and ultrasound assisted) from condimentary plants. In: Meireles MAA (ed) Extracting Bioactive Compounds for Food Products: Theory and Applications. Boca Raton: CRC Press.
27. Kinsella JE (1979) Functional properties of soy proteins. J Am Oil Chem Soc 56:242-258
28. de Almeida NM, JMLN Moura, L Johnson (2010) Functional properties of protein produced by two-stage aqueous countercurrent enzyme-assisted aqueous extraction. Abstracts pp 130. 101st Annual Meeting and Exposition of the American Oil Chemists Society, May 16-19, Phoenix, AZ
29. Yao L, Jung S (2010) 31P NMR phospholipids profiling of soybean emulsion recovered from aqueous extraction. J Agric Food Chem 58:4866-4872
30. List RG, Mounts TL, Lanser AC, Holloway RK (1990) Effect of moisture, microwave heating, and live steam treatment on phospholipase D activity in soybeans and soy flakes. J Am Oil Chem Soc 67:867-871
31. Jung S, Maurer D, Johnson LA (2009) Factors affecting emulsion stability and quality of oil recovered from enzyme-assisted aqueous extraction of soybeans. Bioresource Tech 100:5340-5534
32. Campbell KA, CE Glatz (2009) Mechanisms of aqueous extraction of soybean oil. J Ag Food Chem 57:10904-10912

Algae analysis and hydrolysis

In Table 14 are analytical results evaluating the composition of macro marine algae species. As indicated in the table, the oil and total nitrogen content (protein content) estimate was by solvent extraction and a high temperature protein analyzer. All samples were dried to 5 to 10% moisture content prior to analysis with the exception of the wet focus sample, which presented challenges during the analysis such that its oil and protein content was indeterminable. As noted in the table, the oil content (3 to 6%) and protein content (as N_2 content: 0 to 4%) were very low. However, the biomass content was much higher (70 to 79%) compared to oil and protein. Knowing the composition and concentration prompted our research to then focus on simultaneously extracting oil, in the presence of water-CO_2, while converting the biomass portion to sugars. Using an LCMS electron spray method EI^-, initial analysis of a sample from such experiments suggested that levoglucosan was one of the dominant species present.

Table 14. Macro marine algae species composition

	Oil (%)	Solid (%)	Nitrogen (%)
Fucus(a)	4.41	78.38	2.00

Irish moss	0.91	70.39	3.39
Fucus(b)	4.89	76.31	1.60
Ulva	5.78	71.69	4.47
Wet Fucus	-	-	2.38
Laminaria	3.22	72.65	0.41

The % are "as is" values on the weight basis.
One replicate was done for each sample.

Flash Column Chromatography

In previous reports, separation using a TLC and flash chromatography assisted in providing less complex spectra from a GCMS analysis. Currently, the TLC was run using a 20% hexane to 80% ethyl acetate solvent and then followed by passing through a silica column. Two samples were collected (A and B) and then analyzed using GCMS. Spectra comparing these systems are shown in Figure 53. The top spectrum represents methanol-sulfolane-cellulose, the middle spectrum is the first collection (A) (yellow in color) from a silica column, and the bottom spectrum is the clear portion collected (B). As observed in these spectra, this method was able to remove sulfolane as indicated by spectra for collection B. Sample B suggested the presence of sugars, toluene, aldehydes and organic ester derivatives. Details of these analyses associated with each peak are depicted in Table 15, comparing the three systems as shown in Figure 53. Spectra for collection A had a major peak at 9.75 associated with sulfolane, whereas a peak at 14.99 for collection B is associated with two different organic acid methyl esters $C_{17}H_{34}O_2$ and $C_{16}H_{22}O_4$. Additionally, in Figure 53, these compounds appear as minor peaks for collection A. Peak 19.08 was the minor peak for collection B, which is associated with larger molecular weight organic acid methyl esters $C_{24}H_{38}O_4$ and $C_{26}H_{42}O_4$. At the lower end of the peaks 1.67 to 3.8, there are some overlaps between the two systems as suggested in Table 3. Compounds in that range include smaller molecular weight methyl ester derivatives (formic acid propyl esters, acetic acid ethyl esters), propylene glycol, toluene, and aldehyde derivatives.

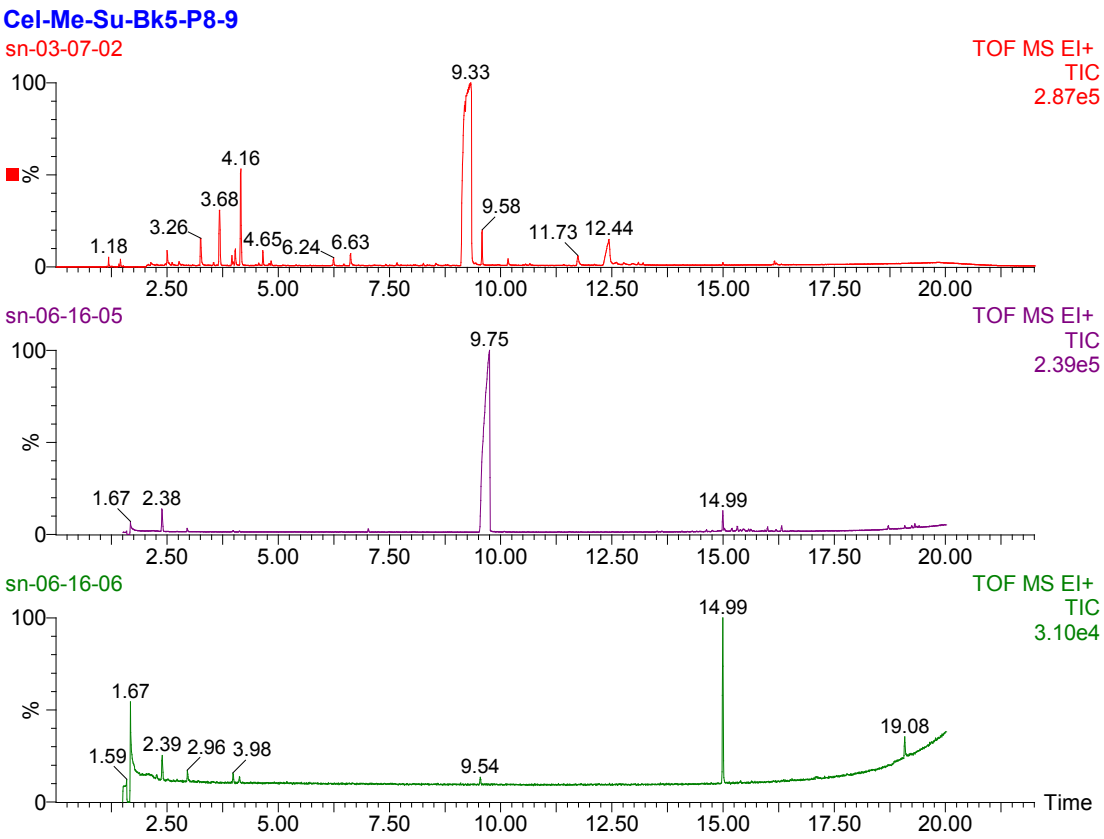

Figure 53. GCMS Chromatogram for Cellulose/MeOH/Sulfolane (top) at 300°C, Collection A (middle), and Collection B (bottom) from flash chromatography

Table 15. GCMS Chromatogram for Cellulose/MeOH/Sulfolane (top) at 300°C, Collection A, and Collection B from flash chromatography

Cellulose-MeOH-Sulfolane 300C				Cellulose-MeOH-Sulfolane Flash Col. A 300C				Cellulose-MeOH-Sulfolane Flash Col. B 300C			
GC peaks from EI, CH4-CI, and NH3-CI data	**Compound m/z based on EI and CI data**	**Compound Structural Formula**	**Corresponding Compound from GCMS database**	**GC peaks from EI, CH4-CI, and NH3-CI data**	**Compound m/z based on EI and CI data**	**Compound Structural Formula**	**Corresponding Compound from GCMS database**	**GC peaks from EI, CH4-CI, and NH3-CI data**	**Compound m/z based on EI and CI data**	**Compound Structural Formula**	**Corresponding Compound from GCMS database**
2.5; 2.916	72; 154	C_4H_8O;$C_8H_{10}OS$	Propanal, 2-Methyl-,Benzene, [methylsulfinyl)methyl]	2.916	154	$C_8H_{10}OS$	Benzene, [methylsulfinyl)methyl]	2.916	154	$C_8H_{10}OS$	Benzene, [methylsulfinyl)methyl]
3.259	104; 76	$C_4H_8O_3$; $C_3H_8O_2$	Propanoic acid, hydroxy-methy; ester, (+-); 1,2-propanediol (propylene glycol)	3.259	104; 76	$C_4H_8O_3$; $C_3H_8O_2$	Propanoic acid, hydroxy-methy; ester, (+-); 1,2-propanediol (propylene glycol)	3.259	104; 76	$C_4H_8O_3$; $C_3H_8O_2$	Propanoic acid, hydroxy-methy; ester, (+-); 1,2-propanediol (propylene glycol)
3.684	92	C_7H_8	Toluene	3.684	92	C_7H_8	Toluene	3.684	92	C_7H_8	Toluene
4	118	$C_6H_{14}O_2$	2,2-dimethoxybutane	4	118	$C_6H_{14}O_2$	2,2-dimethoxybutane	4	118	$C_6H_{14}O_2$	2,2-dimethoxybutane
4.034	106	$C_4H_{10}O_3$	Glycolaldehyde dimethyl acetal	4.034	106	$C_4H_{10}O_3$	Glycolaldehyde dimethyl acetal	4.034	106	$C_4H_{10}O_3$	Glycolaldehyde dimethyl acetal
4.159	120	$C_5H_{12}O_3$	Ethane, 1,1,2-trimethoxy-	4.159	120	$C_5H_{12}O_3$	Ethane, 1,1,2-trimethoxy-	4.159	120	$C_5H_{12}O_3$	Ethane, 1,1,2-trimethoxy-
6.242	142	$C_7H_{10}O_3$	2-Furanethanol, Beta-methoxy-(S)-	1.67	150, 158	$C_{12}H_{14}$; $C_6H_{14}O_2S$	Propane, 1,1-sulfonylbis-; Tricycl[3.2.1.0(2,4)]oct-6-ene,3-(2-mthyl-1-propenylliden e)	1.67	150, 158	$C_{12}H_{14}$; $C_6H_{14}O_2S$	Propane, 1,1-sulfonylbis-; Tricycl[3.2.1.0(2,4)]oct-6-ene,3-(2-mthyl-1-propenylliden e)
6.626	130	$C_6H_{10}O_3$	Pentanoic acid, (Methyl levulinate)	2.96	88	$C_4H_8O_2$	Formic acid, propyl ester	2.96	88	$C_4H_8O_2$	Formic acid, propyl ester

Table 15 (continued). GCMS Chromatogram for Cellulose/MeOH/Sulfolaneat 300°C, Collection A, and Collection B from flash chromatography

Cellulose-MeOH-Sulfolane 300C				Cellulose-MeOH-Sulfolane Flash Col. A 300C				Cellulose-MeOH-Sulfolane Flash Col. B 300C			
GC peaks from EI, CH4-CI, and NH3-CI data	**Compound m/z based on EI and CI data**	**Compound Structural Formula**	**Corresponding Compound from GCMS database**	**GC peaks from EI, CH4-CI, and NH3-CI data**	**Compound m/z based on EI and CI data**	**Compound Structural Formula**	**Corresponding Compound from GCMS database**	**GC peaks from EI, CH4-CI, and NH3-CI data**	**Compound m/z based on EI and CI data**	**Compound Structural Formula**	**Corresponding Compound from GCMS database**
9.326	120	$C_4H_8O_2S$	Sulfolane(2,3,4,5-tetrahydrothiophene-1,1-dioxide	3.8	88	$C_4H_8O_2$	acetic acid, ethyl ester	3.8	88	$C_4H_8O_2$	acetic acid, ethyl ester
9.58	156	$C_6H_4O_3S$	Thiophene-2-carboxylic acid, 5-formyl-	9.54	128	$C_7H_{12}O_2$	2(2H)-Furanone, 5-Ethyldihydro-5-methyl-	9.54	128	$C_7H_{12}O_2$	2(2H)-Furanone, 5-Ethyldihydro-5-methyl-
10.17	160	$C_6H_8O_3S$	2(5H)-Furanone,4-(mercaptomethyl)-3-methoxy-	10.17	160	$C_6H_8O_3S$	2(5H)-Furanone,4-(mercaptomethyl)-3-methoxy-	10.17	160	$C_6H_8O_3S$	2(5H)-Furanone,4-(mercaptomethyl)-3-methoxy-
11.73	180; 162	$C_6H_{12}O_6$;$C_6H_{10}O_5$	D-Allose; Levoglucosan	11.73	180; 162	$C_6H_{12}O_6$;$C_6H_{10}O_5$	D-Allose; Levoglucosan	11.73	180; 162	$C_6H_{12}O_6$;$C_6H_{10}O_5$	D-Allose; Levoglucosan
11.82;.13.15	370 – 592	$C_{16}H_{30}O_4Si_3$, $C_{16}H_{48}O_8Si_8$	Benzoic acid, 2,6-bis[(trimethylsilyl)oxy]-trimethyl ester; Cyclooactasiloxane, hexadecamethyl-	11.82;.13.15	370 – 592	$C_{16}H_{30}O_4Si_3$, $C_{16}H_{48}O_8Si_8$	Benzoic acid, 2,6-bis[(trimethylsilyl)oxy]-trimethyl ester; Cyclooactasiloxane, hexadecamethyl-	11.82;.13.15	370 – 592	$C_{16}H_{30}O_4Si_3$, $C_{16}H_{48}O_8Si_8$	Benzoic acid, 2,6-bis[(trimethylsilyl)oxy]-trimethyl ester; Cyclooactasiloxane, hexadecamethyl-
12.435	194	$C_{11}H_{22}O_2$	alpha-D-Glucopyranoside, methyl (or Beta-D Glucopyranoside)	14.994	270; 278	$C_{17}H_{34}O_2$; $C_{16}H_{22}O_4$	Hexadecanoic acid, methyl ester (Palmitic acid, methyl ester), 1,2-Benzedicarboxylic acid, butyl 2-methylpropyl ester	14.994	270; 278	$C_{17}H_{34}O_2$; $C_{16}H_{22}O_4$	Hexadecanoic acid, methyl ester (Palmitic acid, methyl ester), 1,2-Benzedicarboxylic acid, butyl 2-methylpropyl ester
12.427	194	$C_7H_{14}O_6$	alpha-D-Glucopyranoside, methyl (or Beta-D Glucopyranoside)	16.31, 16.32	298	$C_{19}H_{36}O_2$	Heptadecanoic acid, 10 methyl-, methyl ester				
11.82;.13.15,17.211	356 – 592	$C_{16}H_{30}O_4Si_3$, $C_{16}H_{48}O_8Si_8$	Benzoic acid, 2,6-bis[(trimethylsilyl)oxy]-trimethyl ester; Cyclooactasiloxane, hexadecamethyl-	18.72	356	$C_{23}H_{36}OSi$ $C_{26}H_{42}O_4$	Silane, trimethyl-[[(17alpha)-19-norpregn-4-20-yn-17-yl]oxy]-				
14.994	270; 278	$C_{17}H_{34}O_2$; $C_{16}H_{22}O_4$	Hexadecanoic acid, methyl ester (Palmitic acid, methyl ester), 1,2-Benzedicarboxylic acid, butyl 2-methylpropyl ester	19.085	390, 418	$C_{24}H_{38}O_4$; $C_{26}H_{42}O_4$	1,2-Benzenedicarboxylic acid, diisooctyl ester; [Phthalic acid, Bis(2-ethylhexyl) phthalate];6-ethyl-3-yl 2-ethylhexyl ester	19.085	390; 418	$C_{24}H_{38}O_4$; $C_{26}H_{42}O_4$	1,2-Benzenedicarboxylic acid, diisooctyl ester; [Phthalic acid, Bis(2-ethylhexyl) phthalate];6-ethyl-3-yl 2-ethylhexyl ester
16.31,16.152	298; 296	$C_{19}H_{36}O_2$; $C_{19}H_{36}O_2$	Heptadecanoic acid, 10 methyl-, methyl ester;11-Octadecenoic acid, methyl ester, (oleic acid, methyl ester or 9-Octadecenoic acid, methyl ester),	19.31 & 19.24	274; 316	$C_{22}H_{20}S$; $C_{21}H_{22}$	1-Propene, 3-(2-cyclopentenyl);Benzene, 1,1'-[2-methy-2-(phenylthio) cyclopropylidene]bis]				

3. **Explanation of Variance**: This part of the overall effort is now finished according to planned schedule. All milestones completed.

4. **Plans for Next Quarter**: None. Project has reached termination per Grant Agreement.

Patents: None

Publications: None

Presentations:

Ndlela Sipho C., Olson Norman, K., "Evaluating biomass reactions with cosolvents/CO_2 under subcritical and supercritical conditions.", Iowa State University, Iowa Energy Center, BECON, Nevada, IA, USA, Salt Lake City, Utah, November 2010.

Ndlela Sipho C., Olson Norman K., "Catalyst-free biodiesel reactions and post treatment using commercial polymeric resins.", Iowa State University, Iowa Energy Center, BECON, Nevada, IA, USA, Salt Lake City, Utah, November 2010.

Ndlela Sipho C., Nobrega de Moura Maria Leite [2], Johnson Lawrence A.[2], Olson Norman K.[1] "Aqueous Extraction of Oil and Protein from Soybean**s** *by Subcritical Water* Treatment." [1]Iowa State University, Iowa Energy Center, BECON, Nevada, IA, USA, [2]Iowa State University, Center for Crops Utilization Research, Food Science Department, Ames, IA, USA, *101st AOCS conference*, Phoenix, AZ May 2010

Project Schedule

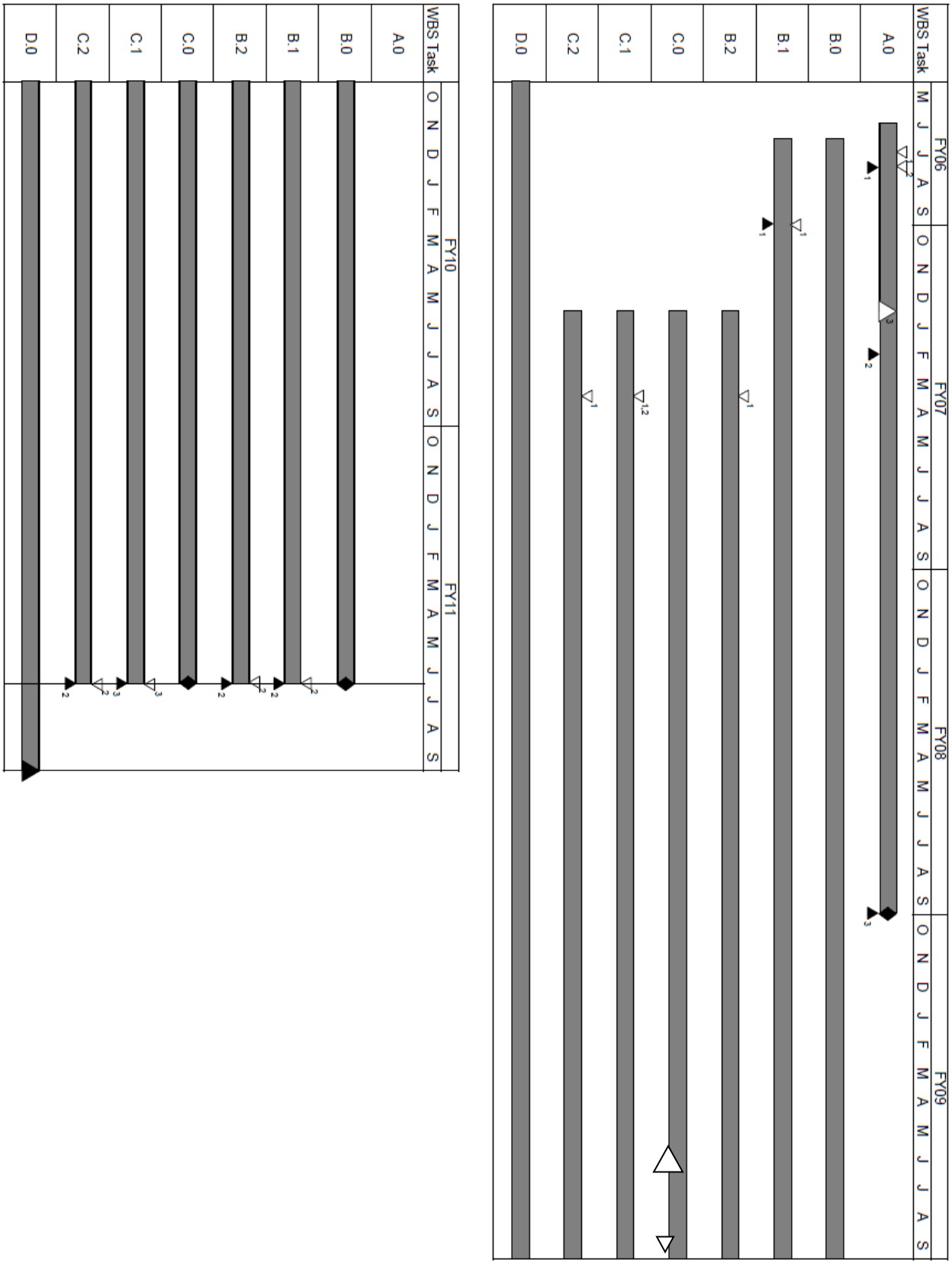

A.ML.3 Equipment purchased and installed

B.0 Supercritical Reaction Systems Research
- B.1 Liquid-Liquid Reactions
  - B.1.ML.1 Candidate liquids and reactions screened and prioritized
  - B.1.ML.2 Determine initial reaction conditions and identify key parameters for follow-on optimization
- B.2 Solid-Liquid Reactions
  - B.2.ML.1 Candidate solids, liquids and reactions screened and prioritized
  - B.2.ML.2 Determine initial reaction conditions and identify key parameters for follow-on optimization

C.0 Supercritical Extraction/Separation Systems Research
- C.1 Extractions from Liquid Feedstocks
  - C.1.ML.1 Conversion processes that create liquid mixtures of products screened and prioritized
  - C.1.ML.2 Candidate extractants, liquids and desired extraction products screened and prioritized
  - C.1.ML.3 Determine initial extraction conditions and identify key parameters for follow-on optimization
- C.2 Extractions from Solid Feedstocks
  - C.2.ML.1 Candidate extractants, solids and desired extraction products screened and prioritized
  - C.2.ML.2 Determine initial extraction conditions and identify key parameters for follow-on optimization

D.0 Project Management and Reporting
- D.DL.1 Complete final report

▲ Completed milestone

△ Late milestone

 Activity timeline

 Schedule slippage